NASA
CR
72650
c.1

TECH LIBRARY KAFB, NM
0062523

NASA CR-72650
TE 4068-168-69

FINAL REPORT

PERFORMANCE STABILITY OF PREFERRED-ORIENTED VAPOR-DEPOSITED TUNGSTEN EMITTERS FOR THERMIONIC CONVERTERS

LOAN COPY: RETURN TO
AFWL (WLOL)
KIRTLAND AFB, N MEX

by

C. C. Wang, F. Rufeh, D. P. Lieb, and T. O. P. Speidel

Thermo Electron Corporation
85 First Avenue
Waltham, Massachusetts 02154

prepared for

NATIONAL AERONAUTICS AND SPACE ADMINISTRATION

April 25, 1969

CONTRACT NAS 3-9424

NASA Lewis Research Center
Cleveland, Ohio
James J. Ward, Project Manager
Direct Energy Conversion Division

RECEIVED
8 MAY 1969

NOTICE

This report was prepared as an account of Government-sponsored work. Neither the United States, nor the National Aeronautics and Space Administration (NASA), nor any person acting on behalf of NASA:

A.) Makes any warranty or representation, expressed or implied, with respect to the accuracy, completeness, or usefulness of the information contained in this report, or that the use of any information, apparatus, method, or process disclosed in this report may not infringe privately-owned rights; or

B.) Assumes any liabilities with respect to the use of, or for damages resulting from the use of, any information, apparatus, method or process disclosed in this report.

As used above, "person acting on behalf of NASA" includes any employee or contractor of NASA, or employee of such contractor, to the extent that such employee or contractor of NASA or employee of such contractor prepares, disseminates, or provides access to any information pursuant to his employment or contract with NASA, or his employment with such contractor.

Requests for copies of this report should be referred to:

National Aeronautics and Space Administration
Scientific and Technical Information Facility
P. O. Box 33
College Park, Md. 20740

TECH LIBRARY KAFB, NM
0062523

NASA CR-72650
Report No. TE4068-168-69

FINAL REPORT

PERFORMANCE STABILITY OF PREFERRED-ORIENTED VAPOR-DEPOSITED TUNGSTEN EMITTERS FOR THERMIONIC CONVERTERS

1. Thermionic Generators
2. Tungsten — Electron Emission

by

C. C. Wang, F. Rufeh, D. Lieb, and T. O. P. Speidel

Thermo Electron Corporation
85 First Avenue
Waltham, Massachusetts 02154

Prepared for

National Aeronautics and Space Administration

April 25, 1969

Contract NAS 3-9424

NASA Lewis Research Center
Cleveland, Ohio
James J. Ward, Project Manager
Direct Energy Conversion Division

FOREWORD

The work reported herein was done at Thermo Electron Corporation under NASA Contract NAS3-9424, with Mr. James J. Ward, Direct Energy Conversion Division, NASA-Lewis Research Center, as Project Manager.

TABLE OF CONTENTS

TABLE OF CONTENTS (continued)

ABSTRACT

The performance of tungsten, deposited from its halides by hydrogen reduction of hexafluoride (fluoride tungsten) and hexachloride (chloride tungsten), as emitters of thermionic converters was studied in seven planar geometry converters with niobium collectors and inter-electrode spacings of 8 ± 1/2 mils. The parametric data are presented in the form of variable cesium temperature families and cover an emitter temperature range of 1600 to 2000 °K. The results show that the maximum power achieved with chloride tungsten emitters at a given emitter temperature is higher than that achieved with fluoride tungsten emitters throughout the temperature range studied. For example, at an emitter temperature of 2000 °K, the maximum power achieved with chloride tungsten emitters is about twice that achieved with fluoride tungsten emitters. The performance of fluoride tungsten emitters was considerably improved by chemical etching and by the additional deposition of a thin layer of chloride tungsten on the surface of the fluoride tungsten (duplex tungsten). Performance stability was examined by life-testing, which indicated that performance is stable with respect to time for test periods up to 4000 hours at emitter temperatures up to 2030 °K.

SUMMARY

A series of thermionic converters having tungsten, deposited from its halides by the hydrogen reduction of hexafluoride (fluoride tungsten) and hexachloride (chloride tungsten), as emitters was fabricated and tested. Specifically, the emitter materials used were chloride tungsten (in three converters), fluoride tungsten (in two converters), chemically-etched fluoride tungsten (in one converter), and duplex (chloride on fluoride) tungsten (in one converter). The parametric data cover the emitter temperature range of 1600 to 2000°K, and the performance comparisons presented are based on variable cesium temperature current-voltage families. The results show that the maximum power achieved with chloride tungsten emitters at a given emitter temperature is higher than that achieved with fluoride tungsten emitters throughout the temperature range studied. Chemical etching and the additional deposition of a thin layer of chloride tungsten on the surface of the fluoride tungsten (duplex tungsten) result in a considerable improvement in performance. Correlation among the degree of crystal orientation, the cesiated and bare work functions, and the performance of the emitters was observed. Performance stability was evaluated by life-testing each converter. All of the life-tested converters with chloride emitters and the converter with a duplex emitter completed 4000 hours of stable performance; the converters with fluoride and etched fluoride emitters developed leaks after 2400 and 2190 hours, respectively.

I. INTRODUCTION

Tungsten deposited from its halides by hydrogen reduction of hexafluoride (fluoride tungsten) and hexachloride (chloride tungsten) has been shown to exhibit (100) and (110) preferred crystal orientation, respectively. This technique of emitter production is of practical interest since it readily allows fabrication of emitters in various configurations. Previous investigation (reference 1) has shown bare work functions as high as 4.5 eV for the fluoride tungsten and 5.0 eV for the chloride tungsten. However, there is no systemic documentation of their performance characteristics.

The performance of vapor-deposited tungsten as a thermionic emitter has been investigated (reference 2) in two cylindrical converters with niobium collectors and 10-mil spacing. The emitter of one converter was chloride tungsten which had a partial (110) crystal orientation; the other converter had a fluoride tungsten emitter, which had a high degree of (100) crystal orientation. At an emitter temperature of 2070°K and an output current density of 12 A/cm^2, the former converter gave about 20 percent higher power density. Hence, there is an indication that chloride tungsten emitters offer a higher power density than fluoride tungsten emitters. From structural considerations, however, chloride tungsten emitters may be less favorable because of their high rate of grain growth.

Chemical etching as a means of developing a surface with a high bare work function, and thus with improved performance, was previously applied to rhenium emitters with satisfactory results (reference 3). Its application to a tungsten emitter was first studied

by Wilson and Lawrence (reference 4); the emitter prepared in this manner showed an unusually good initial performance, but it degraded as the emitter was aged at 2150°K.

The objective of the program reported herein was to provide a more complete documentation of performance and performance stability of vapor-deposited tungsten as the emitter material. A series of converters having vapor-deposited tungsten emitters and niobium collectors was fabricated and tested for the NASA-Lewis Research Laboratory under the program, "Performance Stability of Preferred-Oriented Vapor-Deposited Tungsten Emitters for Thermionic Converters." The emitter materials used in this series of converters were chloride tungsten (in three converters), fluoride tungsten (in two converters), chemically-etched fluoride tungsten (in one converter), and duplex tungsten, a thin layer of chloride tungsten on the surface of fluoride tungsten (in one converter). The performance comparisons presented are based on variable cesium temperature families of voltage-ampere characteristics taken over the emitter temperature range of 1600 to 2000°K, with collector temperatures optimized for maximum power output. In addition, the relationship among the degree of crystal orientation, the cesiated work function, and the performance of the emitters was examined. Performance stability was evaluated by life-testing each converter.

II. EMITTER PREPARATION

The emitter material was supplied by San Fernando Laboratories and the emitter structures were prepared by Gulf General Atomic, Inc. (references 5 and 6). The fabrication procedures discussed below are summarized in Table II-1.

A. EMITTER B_2-2

Emitter B_2-2 was machined from a fluoride vapor-deposited tungsten disk. The surface of the 0.63 inch diameter disk was ground to the required 44-mil thickness with a water-cooled alundum wheel; it was then outgassed for 200 hours at 2070°K in a 10^{-6} torr environment. After outgassing, the tungsten disk was diffusion-bonded to a Ta-10% W backup plate and a hohlraum was machined into the plate by means of a flat-bottom drill. The emitter was then heated for 200 hours at 2070°K, machined to the final dimensions, and given an additional 100-hour heat treatment.

B. EMITTER B_6-2

The preparation of emitter B_6-2 was similar to that of B_2-2 except that, before the final heat treatment, the surface was mechanically polished with 1-micron diamond paste and then electropolished in a 10% NaOH solution.

C. EMITTERS C_1-2, C_1-4 and C_1-5

Emitter structures C_1-2, C_1-4 and C_1-5 were fabricated from a single disk of chloride vapor-deposited tungsten. The emitters were ground to the required thickness with a water-cooled alundum

wheel, heat-treated for 4 hours at 2070°K, and machined to the final dimensions. The emitting surface was then polished with 1-micron diamond paste and electropolished in a 10% NaOH solution. A heat treatment at 2070°K for 100 hours completed the preparation.

D. EMITTER C_3-3

Emitter C_3-3 employed a composite structure; a substrate of fluoride vapor-deposited tungsten coated with nominally 10 mils of chloride vapor-deposited tungsten. The preparation of this emitter was the same as that of the other C-series of emitters.

E. EMITTER D_1-1

Preparation of emitter D_1-1 was similar to that of the B_6-2 emitter, with the addition of a chemical etch for 2 hours in a solution of 100 parts saturated $K_3Fe(CN)_6$, 5 parts saturated KOH, and 95 parts H_2O before the final heat treatment.

TABLE II-I

PROCEDURES USED IN EMITTER STRUCTURE PREPARATION

Emitter Structure Designation	Material		Heat Treatment Before Machining		Emitter Surface Finish	Chemical Treatment
			Temp., °K	Time, Hrs.		
B_2-2	Emitter	Fluoride Vapor Deposited Tungsten	2073	200	Ground with water cooled alundum wheels	
	Back-up Plate	Ta-10% wt W				
B_6-2	Emitter	Fluoride Vapor Deposited Tungsten	2073	200	Ground with water cooled alundum wheel, polished with 1 micron diamond paste and then electro-polished with 10% Na OH	
	Back-up Plate	Ta-10% wt W				
D_1-1	Emitter	Fluoride Vapor Deposited Tungsten	2073	200	Same as emitter B_6-2	Etched for 2 hours in 100 pts. $K_3Fe(N)_6$, 5 pts KOH and 95 pts. H_2O solution
	Back-up Plate	Ta-10% wt W				
C_1-2 C_1-4 C_1-5	Emitter	Chloride Vapor Deposited Tungsten	2073	4	Same as emitter B_6-2	
	Back-up Plate	Ta-10% wt W				
C_3-3	Emitter	Duplex Tungsten	2073	4	Same as emitter B_6-2	
	Back-up Plate	Ta-10% wt W				

III. EMITTER CHARACTERIZATION

Because of the correlation between crystal plane orientation and thermionic emission, it is important to determine the fraction of the particular crystal planes lying within a given angle of the bulk surface. Such measurement of the degree of preferred orientation is useful in comparing and ranking samples.

Measurement of the degree of preferred orientation can be made conveniently using a conventional pole figure accessory for an x-ray diffractometer. The sample is located so that the x-ray detector receives the beam diffracted from the particular plane under investigation. The sample surface is then tilted so that the surface normal moves out of the plane formed by two x-ray beams while it continues to bisect the angle between them. The resulting intensity of reflected x-rays vs tilt angle α is then integrated cumulatively to give a curve which represents the total intensity originating from a crystal plane within the angle α of the surface. This curve is the so-called "pole figure."

The pole figures of all emitters used in this program were obtained by Gulf General Atomic, Inc. (references 6 and 10). Figure III-1 shows the pole figures of chloride vapor-deposited tungsten emitters. Note that emitter C_1-2 has the highest degree of (110) crystal plane orientation. The pole figures of emitter D_1-1 and B_6-2 are shown in Figure III-2. It is difficult, however, to compare these pole figures, since the treatments of the two surfaces are quite different.

The vacuum work functions of the emitters were not measured prior to the initiation of testing due to difficulties encountered in welding the tantalum sleeve to a heat treated Ta-10% W backup plate. Gulf General Atomic Inc. carried out the post life test investigation of the emitter surfaces, and reported the bare work functions (reference 7) shown in Table III-1.

TABLE III-1

EMITTER BARE WORK FUNCTION MEASUREMENTS

Emitter	ϕ Bare, eV
C_1-2	5.0
C_1-4	4.91
C_1-5	4.91
C_3-3	4.84
D_1-1	4.77

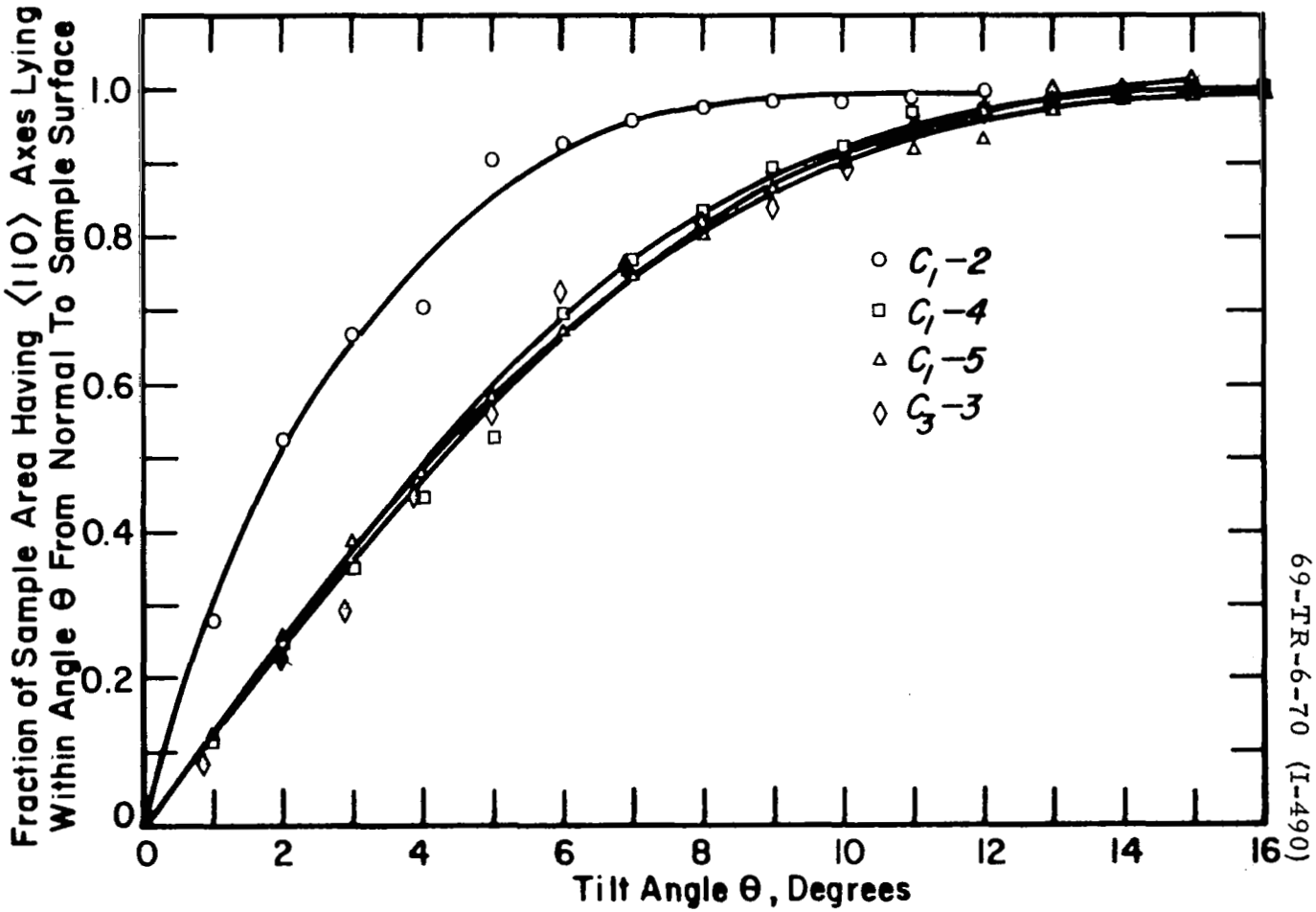

Figure III-1. Pole Figure of Spatial Distribution of the ⟨110⟩ Axes in Emitters C_1-2, C_1-4, C_1-5 and C_3-3.

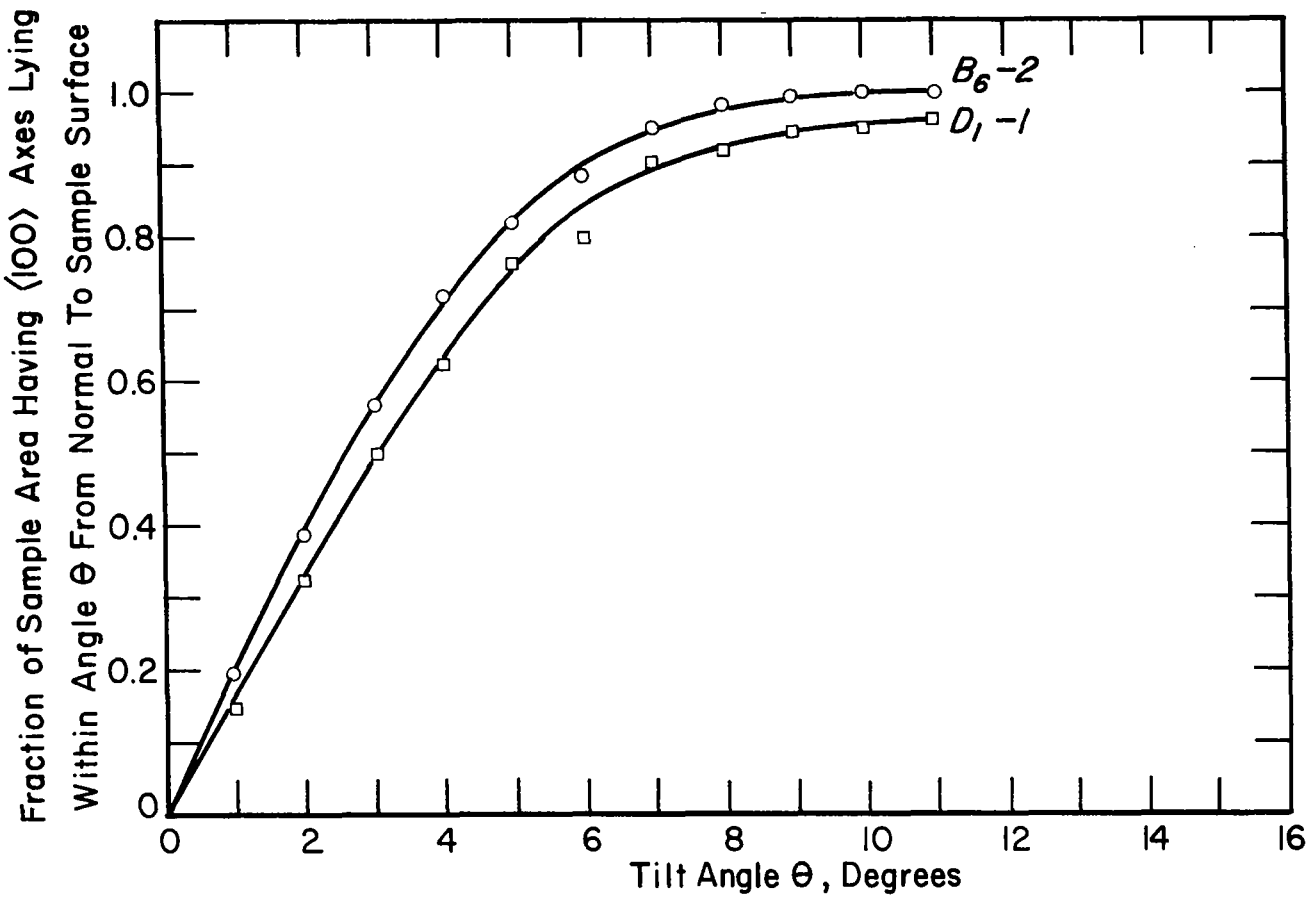

68-TR-10-4 (I-489)

Figure III-2. Pole Figure of Spatial Distribution of the ⟨100⟩ Axes in Emitters B_6-2 and D_1-1.

THERMO ELECTRON CORPORATION

IV. EXPERIMENTAL APPARATUS

A. CONVERTER

The converters used in this program were designed primarily for life-testing purposes. The converter and associated components are shown in Figures IV-1 through IV-3. The emitter structure consisted of a vapor-deposited tungsten disk diffusion-bonded to a Ta-10% W backup plate. The emitter structure was electron-beam welded to a tantalum sleeve, which in turn was welded to the niobium flange of the insulating seal assembly.

The collector section was machined from a single piece of niobium and could be considered in three sections: an upper section, which contained the collector surface and support; a heater section, which contained the brazed-on sheathed tantalum heaters; and the lower or heat flux section, in which the capability for heat flux measurement was provided. To establish the desired 8-mil interelectrode spacing, the upper section of the collector was selectively machined to match the emitter and seal assembly. The emitter assembly was then brazed to the collector section to complete the converter. The actual interelectrode spacing and alignment could be measured from indicating surfaces on the emitter and collector body. The cesium reservoir tubulation was brazed to the lower section of the collector structure, but is thermally isolated from the heat flux section by an annular cavity.

The emitter was heated by electron bombardment from a filament positioned above the backup plate. A hohlraum with a diameter of 0.040 inch and depth-to-diameter ratio of 7 was drilled into the backup

plate to provide for optical pyrometer temperature measurements. Collector temperature was controlled by balancing the heater input against the losses through the heat choke section to the water-cooled heat sink. A chromel-alumel thermocouple, positioned 0.12 inch below the collector surface, and two additional thermocouples in the heat flux section were provided for collector temperature and heat flux measurements, respectively. Cesium reservoir temperature was controlled by balancing the heat input from the tubulation against the heat losses through the cold strap to the heat sink.

The weld between the weld lip on the back-up plate of the emitter structure and the sleeve caused considerable difficulty during the course of this program. To minimize thermal stresses, the thickness of the weld lip on both the back-up plate and sleeve was originally set at 0.007". In order to establish the feasibility of this design, two sets of Ta-10% W dummy emitters and tantalum sleeves were prepared for electron-beam welding tests. In the first weld attempt, the sleeve was burned through in several places, and the second weld was not leaktight. The sleeve weld lip thickness was then increased to 0.015 inches and the length of the weld lip was increased from 0.05 to 0.1 inch. A third set of dummy parts was fabricated and, in this case, the beam weld was leaktight.

Following the successful welding of dummy parts, emitters A-1 and A-2 were electron-beam welded to the thicker tantalum sleeves and subjected to thermal soak and thermal cycle testing. These emitters consisted of vapor-deposited tungsten diffusion-bonded to Ta-10% W. After a 100-hour soak at 2173 °K and 100 thermal cycles from room temperature to 2173 °K, the emitter sleeve assemblies

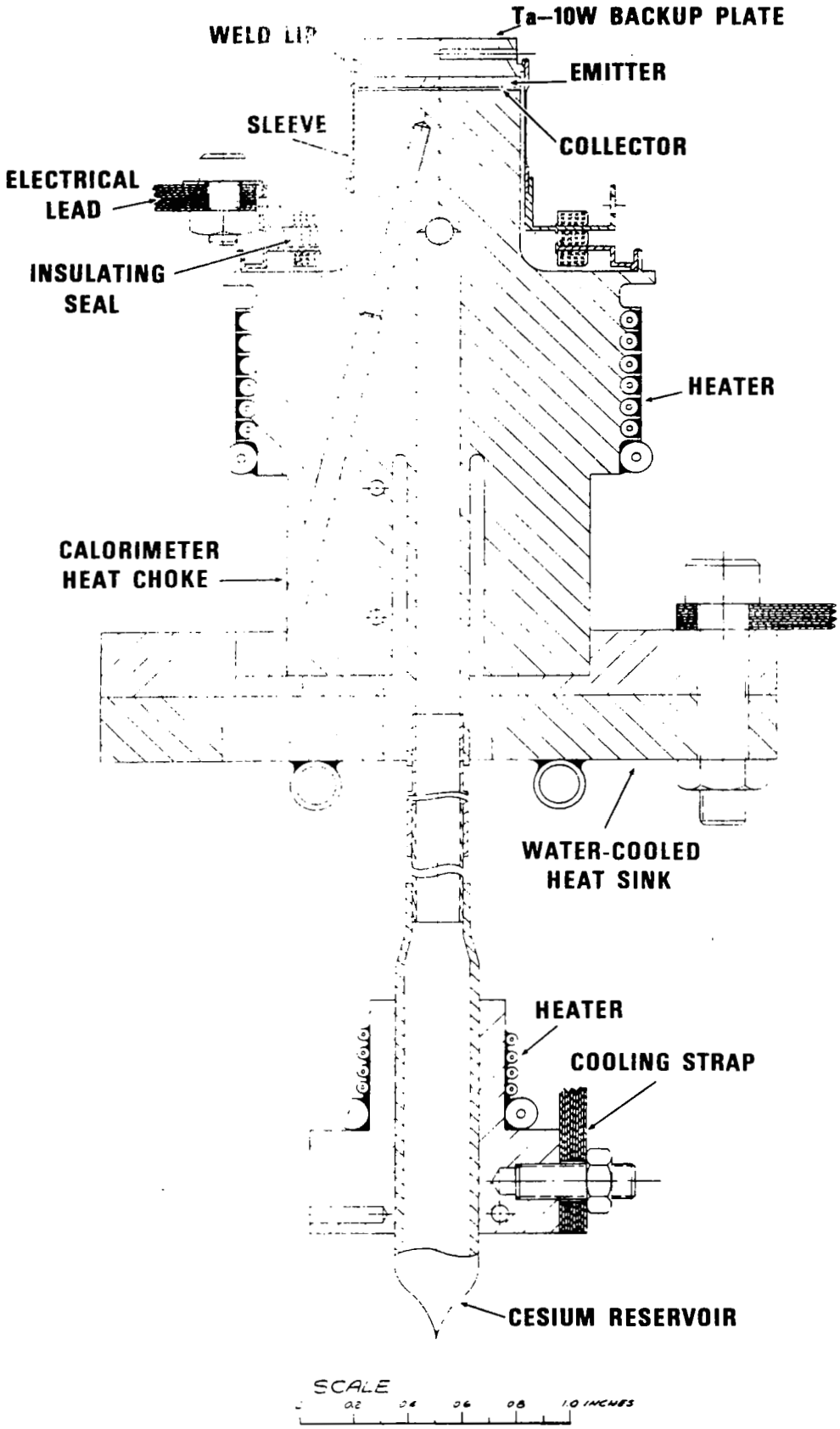

Figure IV-I. Schematic of the Converter.

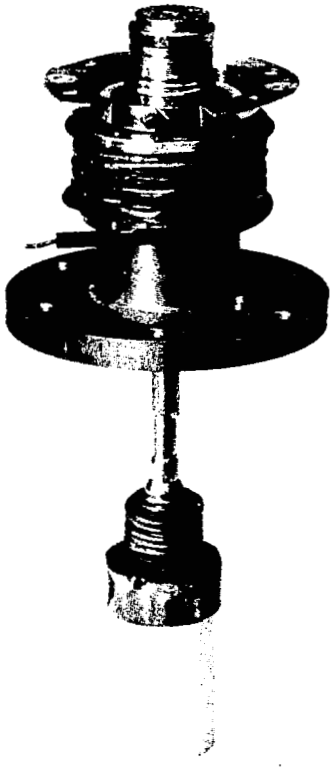

Figure IV-2 Converter Assembly.

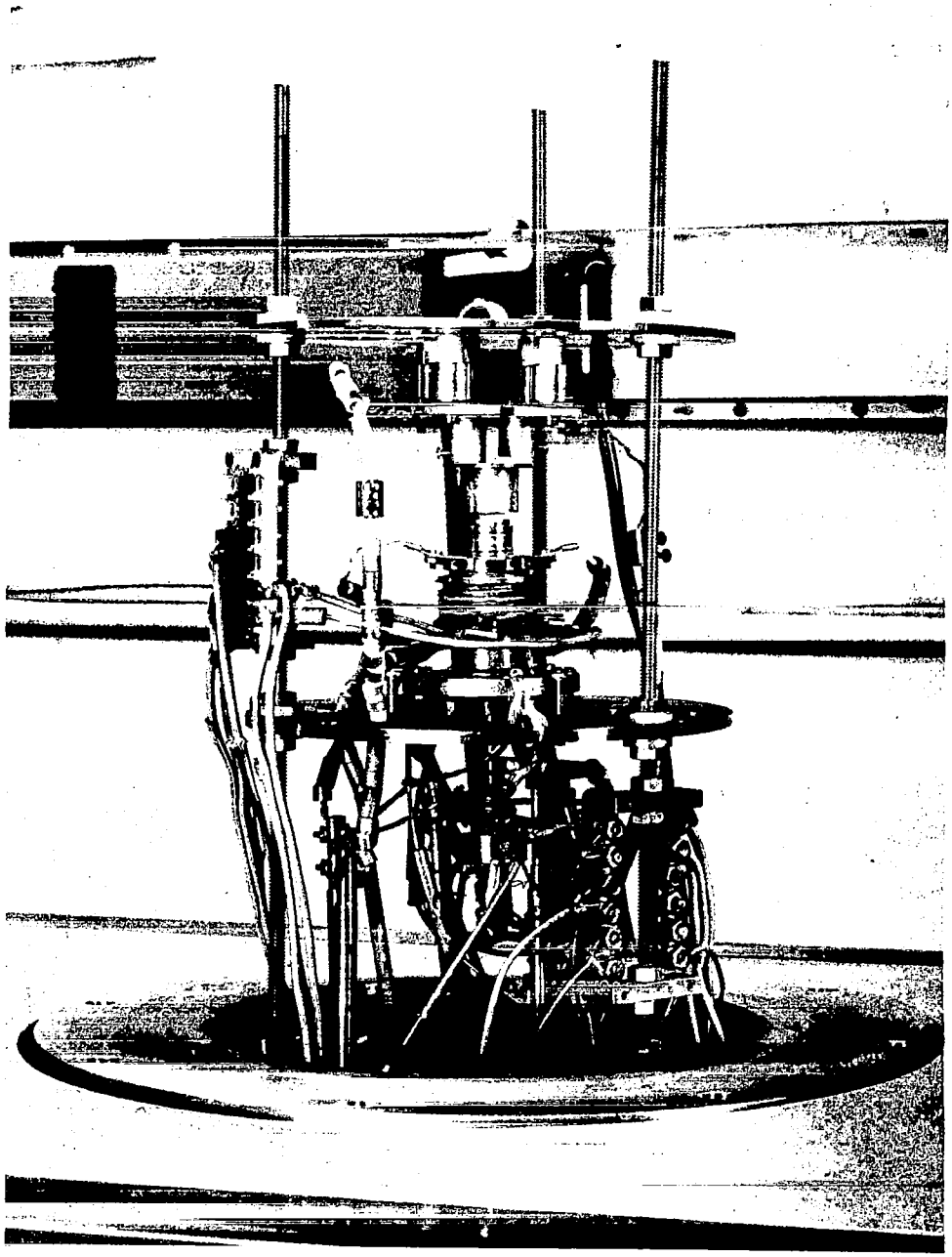

Figure IV-3 Converter Mounted on Test Station.

were leak-tight. It should be noted that neither of these emitters underwent heat treatment as recommended by Gulf General Atomic (200 hours at 2073 °K) prior to welding.

Having apparently established an adequate weld lip design and adequate welding procedures, General Atomic emitter B_1-4 was welded to a sleeve, and this structure was assembled into the prototype converter. Prior to welding, emitter B_1-4 had been heat-treated at Gulf General Atomic for 200 hours at 2073 °K. During the final stage of outgassing the converter, a leak developed near the bottom of the weld lip on the emitter structure below the sleeve-to-emitter weld. At that time, it was decided to rebuild the prototype converter with heat-treated emitter B_1-3. The structure was leak-tight after the emitter-to-sleeve weld; however, the converter again developed a leak during the final outgassing stage.

The emitter weld lip design was then changed by increasing the lip thickness from 0.007 inch to 0.015 inch. Emitter B_2-2, which had the thicker lip, was welded to a sleeve and assembled into the prototype converter. Again, this emitter had been heat-treated for 200 hours at 2073 °K prior to welding. The converter was successfully outgassed and put on test. After 273 hours of operation in a liquid nitrogen-trapped, oil diffusion-pumped vacuum system at a pressure on the order of 4×10^{-6} mm Hg, the converter developed a leak and lost cesium. Examination showed cracks in the emitter back-up plate and at the emitter-to-sleeve weld. Photomicrographs showed impurities precipitated along grain boundaries in the back-up plate and grain boundary separation. Also, slight amounts of impurities were apparent in the tantalum sleeve near the weld area.

In an effort to establish the source of contamination, further studies were conducted with emitter B_3-1. This emitter was heat-treated for 200 hours at 2173 °K and then cut in half. Both halves were electron-beam welded to tantalum sleeves; one half was maintained in the as-welded condition, and the other half was soaked for 100 hours at 2000 °K in a liquid nitrogen-trapped, oil diffusion-pumped vacuum system. During this period, pressure was maintained between 9×10^{-6} to 6×10^{-6} mm Hg. These tests were inconclusive; metallographic examination of both the as-welded and the welded and heat-treated sections showed no contamination of either the Ta-10% W or tantalum sections. However, there was again evidence of grain boundary separation in the Ta-10% W in the heat-treated emitter section.

Based on repeated observations of grain boundary separation due to thermal treatment and the possibility that this resulted in poor welds, pre-weld heat treatment of the emitter structures was discontinued and the sleeve-emitter structure was heat-treated after welding for 100 hours at 2073 °K in a vac-ion pumped system. This change in procedure resulted in 6 of the next 7 emitter-to-sleeve welds being leaktight.

B. VACUUM CHAMBER

The converters were tested in stainless steel vacuum chambers, 7.75 inches in inner diameter and 9 inches high. The chambers were enclosed with a stainless steel water jacket to absorb the heat radiated from the converter and electron-bombardment gun. The cooling water system contained a pressure-sensitive switch which opened upon sensing insufficient water pressure. This switch was interlocked

with the electron-bombardment gun and heater power supplies. When it opened, all power was automatically cut off, thus providing a fail-safe arrangement with respect to the cooling of the unit.

A replaceable one-inch Pyrex window was used for pyrometry observations. The window was protected against deposition by a nickel gate, which was pivoted out of the line of sight during observations with the aid of a small magnet.

The base plate was made of stainless steel pipe 10 inches in diameter and 7 inches high, and had provisions for all necessary electrical and water leadthroughs and the rough-down valve port. All leadthroughs were of metal-ceramic construction and were welded to the base plate.

The chamber was initially mechanically pumped to a pressure level below 10 microns and a 100 liter/sec (Ultek) ion pump was then used to maintain the nominal 10^{-7} mm Hg vacuum required for the experiment.

C. ELECTRON BOMBARDMENT GUN

The heat source for the emitter was an electron bombardment gun, supported from the same structure as the diode. The electron gun incorporated a tungsten filament fabricated from 0.030-inch diameter wire. The electron gun power supply was a self-contained unit and provided a maximum of 50 amperes at 10 volts ac to the filament; this current was regulated by a control circuit. A 1-kilovolt, dc, 750-milliampere Sorensen MD power supply provided the accelerating voltage. It was regulated at ±1% for line voltage variations, and the output had less than 1% ripple.

D. CESIUM RESERVOIR POWER SUPPLY AND TEMPERATURE CONTROLLER

The power supply for the cesium reservoir heater consisted of an 18-volt, 10-ampere ac supply with a variable-voltage transformer and a stepdown isolation transformer. The cesium reservoir temperature was controlled by a Minneapolis Honeywell thermocouple-operated controller, which provided time-portioned on-off switching. The controller was equipped with a temperature-indicating dial from which the cesium reservoir temperature was read directly. A voltmeter and ammeter were provided so that the power input to the heater could be determined.

E. COLLECTOR TEMPERATURE CONTROLLER AND POWER SUPPLY

The power supply for the collector heater consisted of a 36-volt, 10-ampere ac supply with a variable-voltage transformer and a stepdown isolation transformer. The collector temperature was controlled in the same manner as the cesium reservoir temperature.

F ELAPSED-TIME METER

An elapsed-time meter which recorded the time during which a converter in the life-test unit operated was also provided.

G. CONVERTER LOADING FOR LIFE TESTING

The converter was loaded by means of a power transistor which dissipated the electrical output. The circuit allowed a continuous variation of converter load resistance from 0.003 ohm to 50 ohms. The load could be programmed to maintain either constant output current or constant output voltage during life-testing.

H. LOADING AND DATA COLLECTION EQUIPMENT FOR DYNAMIC DATA

The converter output was obtained in the form of current density-voltage plots on an x-y recorder. The entire I-V characteristic was swept at a rate greater than the thermal time constant of the electrodes. This was accomplished by using a transformer-isolated, half-wave, rectified line frequency, sweeping load source so that the characteristics were swept in a series of 60 Hz pulses. Because of the limited response time of the x-y recorder, the effective sweeping of the converter characteristic had to be slowed to about one second. A sample-and-hold circuit driven at a rate differing only slightly from 60 Hz sampled the current and voltage pulses from the converter and slowed their effective rate of change. An oscilloscope continually monitored the actual characteristics and provided a continuous display of the behavior of the converter.

I. OUTGASSING SYSTEM

The outgassing system consisted of a glass bell jar, evacuated by a 100 liter per second ion pump. An 8 liter per second ion pump and a mass spectrometer outlet for evacuation and gas analysis of the converter volume were also provided. The mass spectrometer (CEC Model 21-613-1) employed a cycloidal-focussing mass analyzer to separate high molecular weight compounds. An auxiliary 180° controller was used to detect masses from 2 to 4. It had a sensitivity sufficient to detect 10^{-11} torr of nitrogen. Unit resolution was achieved up to a mass number of 150. The entire assembly, including the mass spectrometer chamber, was made of metal and was bakable up to 250°C.

V. PROCEDURE

A. CONVERTER OUTGASSING AND GAS ANALYSIS

After fabrication, the converters were mounted on a special test stand which allowed mass-spectrometric gas analysis during the outgassing. The converter assembly was placed in a bell jar which was maintained at a vacuum of 10^{-6} torr or lower by a 100 liter/second ion pump. For evacuation and gas analyses, an 8 liter/second ion pump and a mass spectrometer were connected to the cesium tubulation. The converter was evacuated to 5.0×10^{-8} torr before heating was begun.

The mass spectrometer was calibrated with a mixture of known quantities of carbon dioxide, hydrogen, and nitrogen. The analyses of other gases were based upon the calibrated nitrogen sensitivity. Figure V-1 shows a schematic diagram of the calibration system, which was designed to produce accurate results without employing intricate units such as the micromanometer. Based upon successive expansions of minute quantities of gases, it was capable of delivering any desired gas quantity in the range of 10^{-4} to 10^{-8} cc (STP) with an accuracy of 1 percent.

Needle valves S_1 and S_2 were used to produce the desired pressure in chambers C_A and C_B. The pressure was read accurately from the manometer by a cathetometer. The quantity of gas present in chamber C_B was expanded into C_M and C_D, and chamber C_D was then isolated by closing valve S_5. Since the volumes of chambers C_B, C_M, and C_D had been measured accurately, the pressure in C_D could easily be calculated. Knowing the pressure, volume, and temperature of chamber C_D, the quantity of gas present was specified.

Outgassing of the converter was performed by heating each component of the converter and monitoring the gases that were evolved from the surfaces. Appendix A shows typical raw data obtained during the various stages of outgassing of converter D_1-1. The reduced data of converter C_1-2 and D_1-1 are presented in Figures V-2 to V-5 and the temperature history of the converter is presented in Figure V-6 and V-7. As the temperature is increased, a sharp rise, followed by a subsequent decrease, in the partial pressure of various gases is observed. The dominant gases are hydrogen, carbon monoxide, nitrogen, and argon. Methane, water vapor, and carbon dioxide are also present but in much lower quantities. The mass spectrometric analysis of the other converters showed similar results.

After the outgassing was completed, the converters were cesiated and transferred to the life test stations; thermionic testing was then started.

B. EMITTER TEMPERATURE DETERMINATION

Since the emitter hohlraum was located 130 mils above the emitter surface, the temperature observed from the hohlraum must be corrected for the temperature drop through the emitter disk to obtain the true surface temperature required for performance comparisons. To calculate this temperature difference, the thermal conductivity of the emitter structure materials and the magnitude of the heat flux through the emitter must be known. The thermal conductivities were obtained from recently published data (reference 7); the magnitude of the heat flux through the emitter was determined

experimentally by calorimetric measurements in the heat flux section of the collector. The procedure for this evaluation is outlined below.

1. First, the temperature difference in the calorimeter section at different power inputs to the collector heater was measured. In this measurement, an attempt was made to maintain the emitter at about the same temperature as the collector surface to avoid heat flows from collector to emitter.

2. From the information obtained in step 1, the heat flux (Q_H) flowing through the calorimeter was determined as a function of collector heater power (Q_C).

3. The emitter was then heated to the predetermined operating temperature. The temperature differences in the calorimeter due to electron bombardment power (Q_B) and collector heater power (Q_C) were measured.

4. From the information obtained in step 3, the heat flux (Q_T) flowing through the calorimeter due to both electron bombardment and the collector heater was obtained. The quantity $Q_K = Q_T - Q_H$ is the heat flux flowing through the emitter structure due to the bombardment. The quantity $Q_R = Q_B - Q_K$ is the heat loss at the observed hohlraum temperature, assuming that Q_R depends only on the emitter temperature and not on the bombardment power.

5. From the information obtained in step 4, the heat flux through the emitter at a particular hohlraum temperature and bombardment power can be calculated. Then the required correction for the surface temperature of the emitter can be obtained.

At the initiation of testing of the converters using emitters C_1-2 and C_1-4, bright and dark rings were observed at the bottom of the hohlraums. These rings were not observed in the case of previously tested emitters B_2-2 and B_6-2. From a comparison of surface brightness and hohlraum temperatures, it was concluded that the observed hohlraum temperatures of emitters C_1-2 and C_1-4 were significantly lower than the actual temperatures. In order to correct this deficiency, rolled, sand-blasted tantalum foils were inserted into the hohlraums of these converters; further testing showed that the bright and dark rings disappeared, and the observed temperature was in good agreement with the temperature determined from surface brightness measurements. For the sake of uniformity, tantalum foils were then inserted into other converters operating at the time (D_1-1 and C_1-5). No difference in temperature was observed between measurements made before and after the insertion of the tantalum foil into the hohlraum of these converters.

C. PERFORMANCE DATA

The parametric data obtained were in the form of cesium families, i.e., electrode temperatures were held constant and the volt-ampere characteristics were recorded for several cesium reservoir temperatures. The output voltage was measured between the emitter seal and the collector body, and was not corrected for the voltage drop in the emitter sleeve; 1.8 mV per amp/cm^2 should be added to the output voltage to convert to electrode voltage. A typical family is shown in Figure V-8. This family of I-V curves forms an envelope, shown by the dashed line, representing the optimized performance with respect to cesium temperature. The

remaining variable, the collector temperature, was optimized by selecting the temperature giving the highest output power. After the initial set of parametric data was obtained, the converters were life-tested at the maximum power point. During the life test, the emitter, collector and cesium reservoir temperatures and the output current were held constant. The emitter, collector, and cesium reservoir temperature and input and output power of the converter were checked and recorded daily.

In order to more thoroughly evaluate the overall performance stability, another set of parametric data was obtained after 3000 hours of life testing.

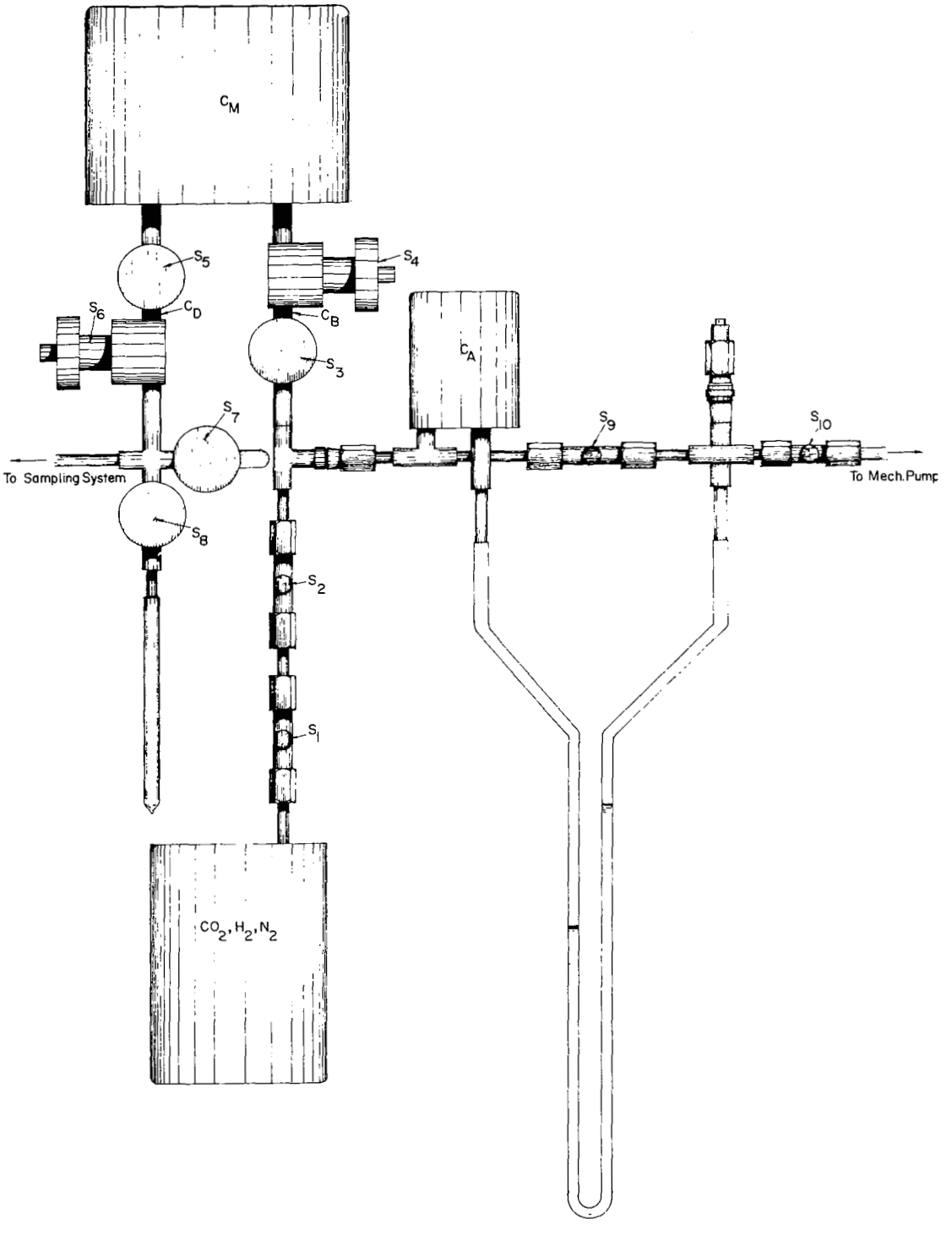

Figure V-1. Schematic of Calibration System

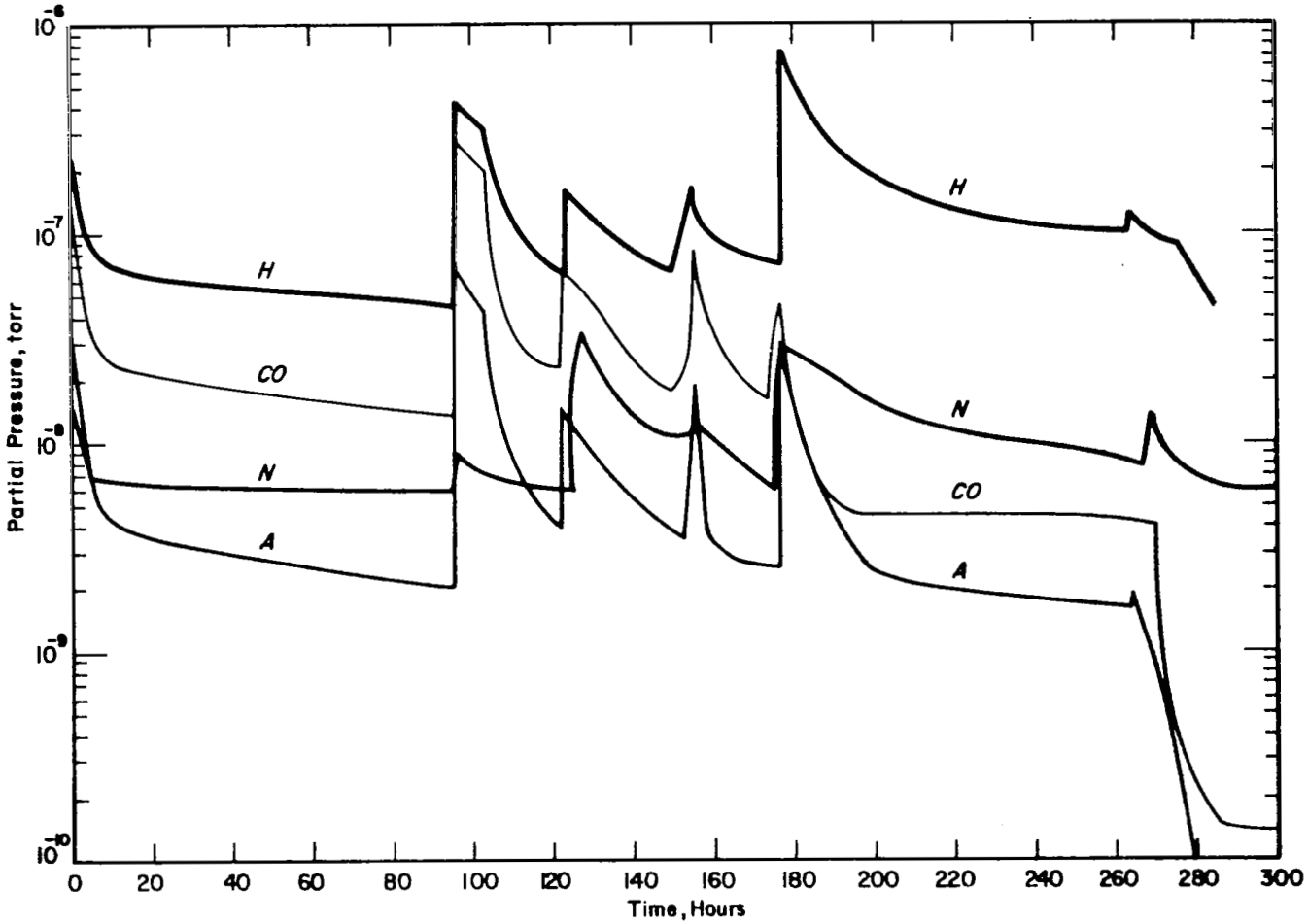

Figure V-2. Partial Pressure of Residual Gases of Converter D_1-1 During Outgassing.

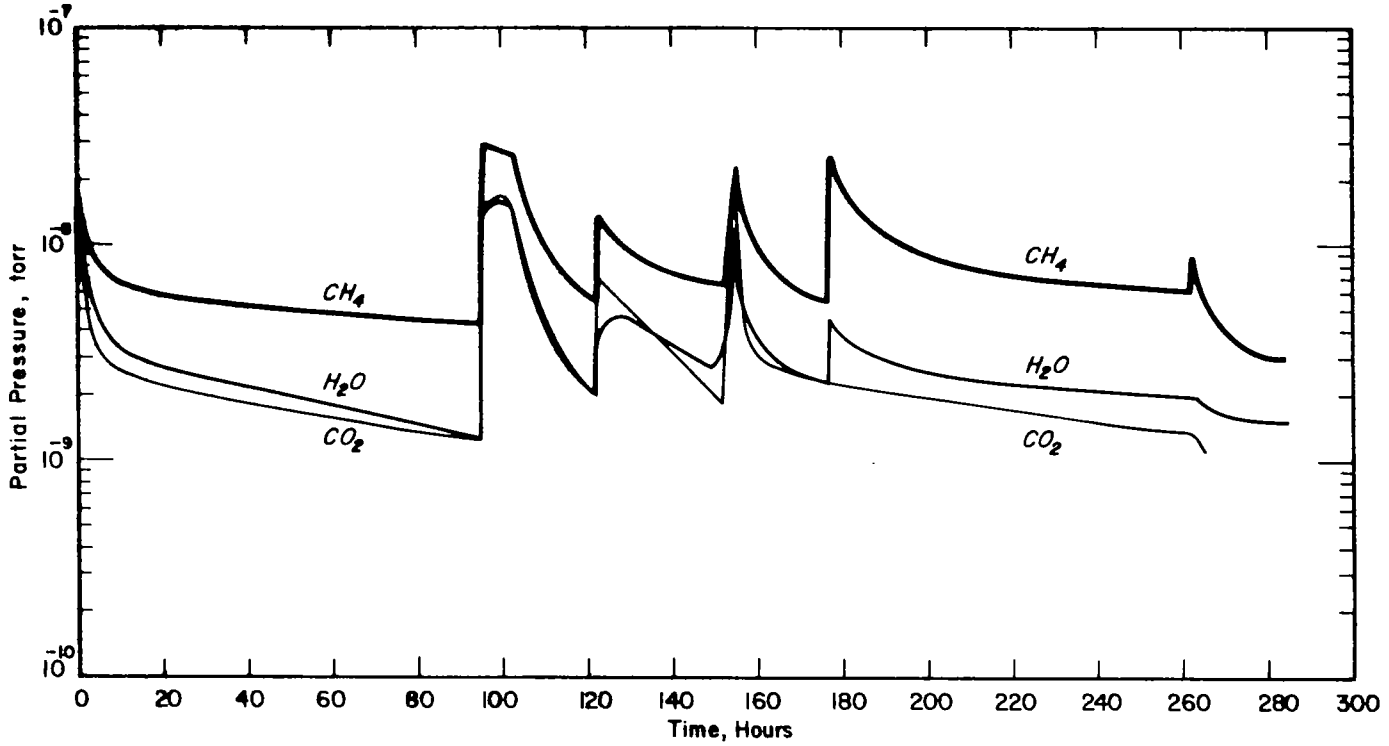

Figure V-3. Partial Pressure of Residual Gases of Converter D_1-1 During Outgassing.

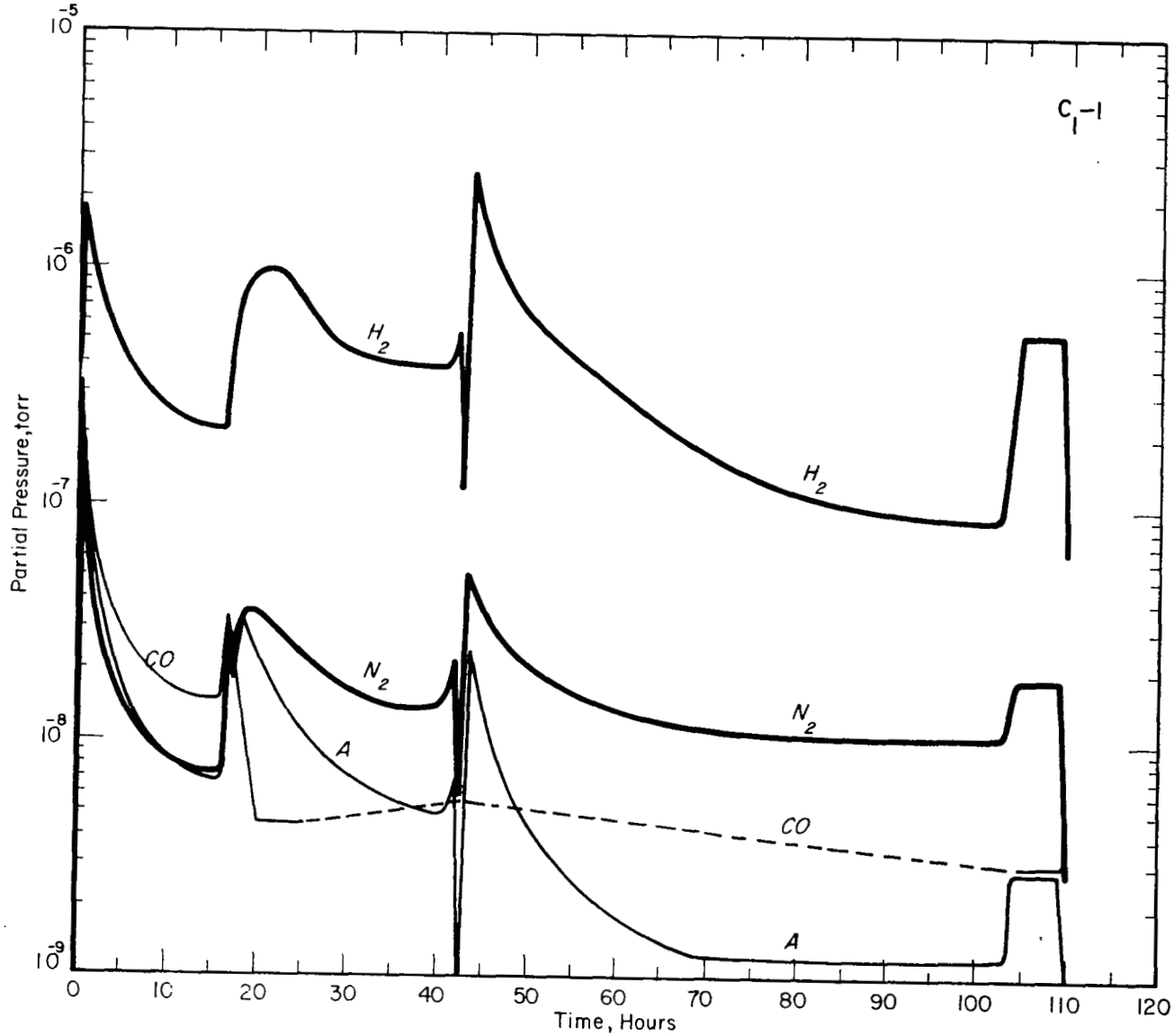

Figure V-4. Partial Pressure of Residual Gases of Converter C_1-1 During Outgassing.

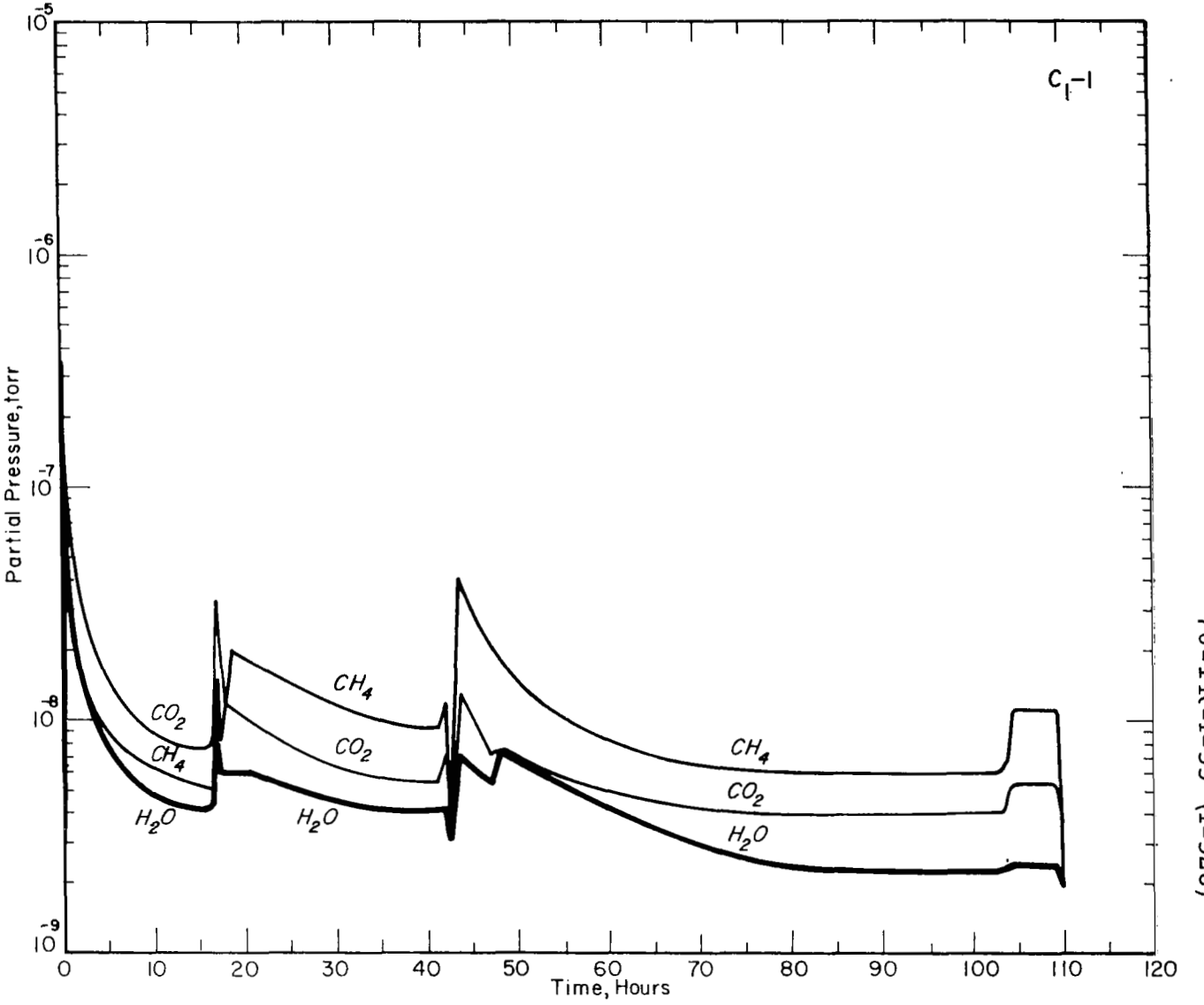

70-TR-1-33 (I-526)

Figure V-5. Partial Pressure of Residual Gases of Converter C_1-1 During Outgassing.

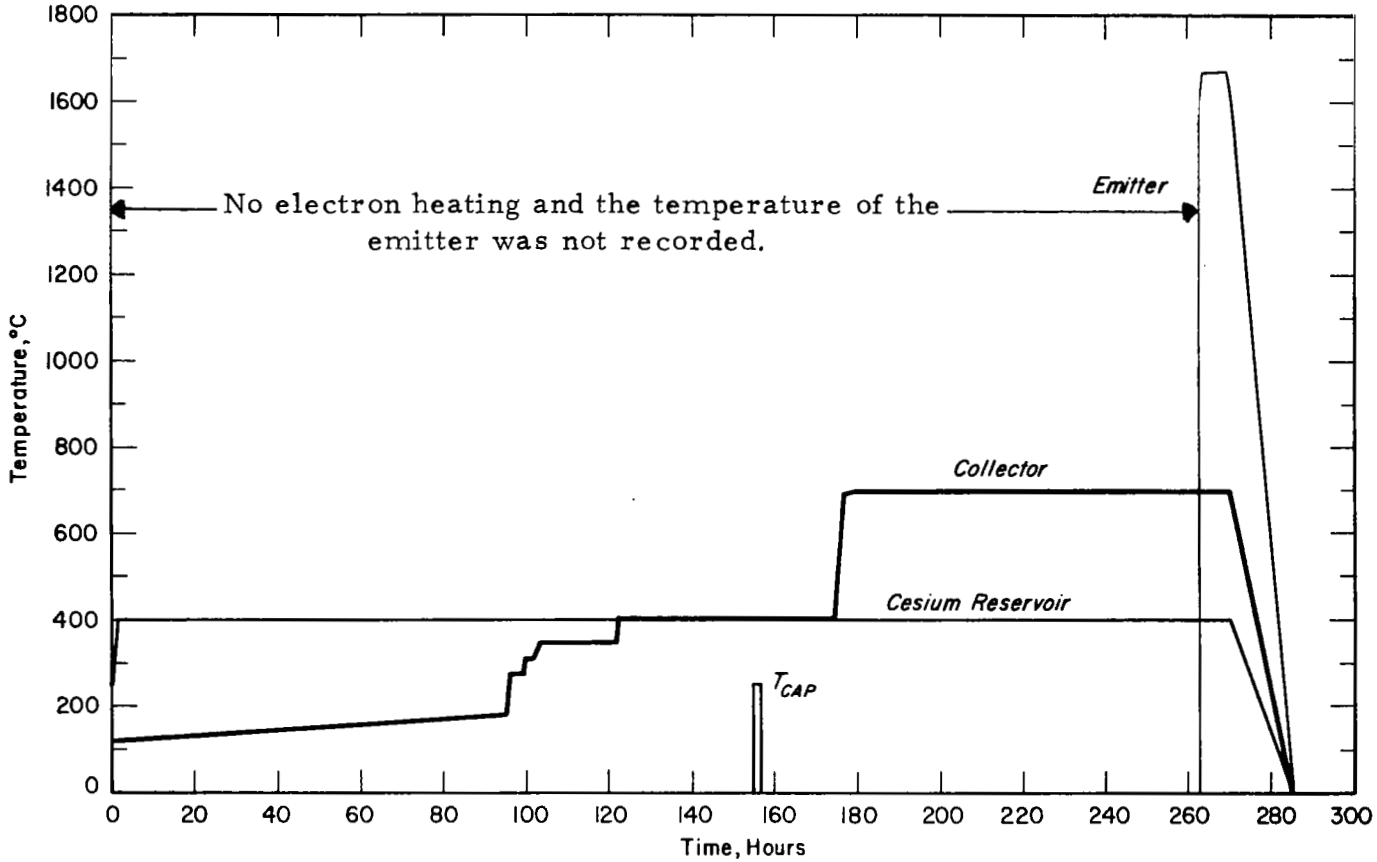

Figure V-6. Temperature History of Converter D_1-1 during Outgassing.

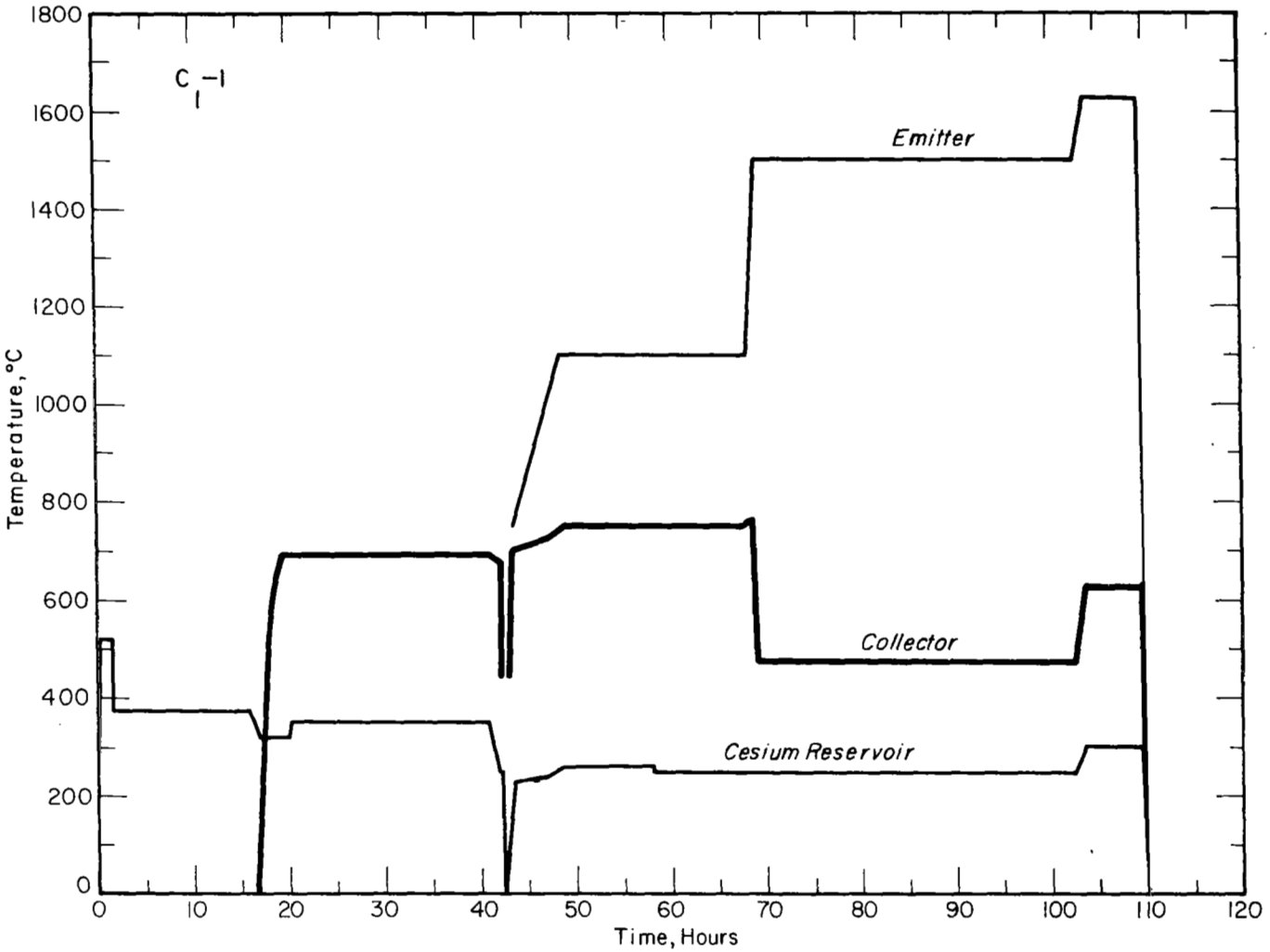

Figure V-7. Temperature History of Converter C_1-1 During Outgassing.

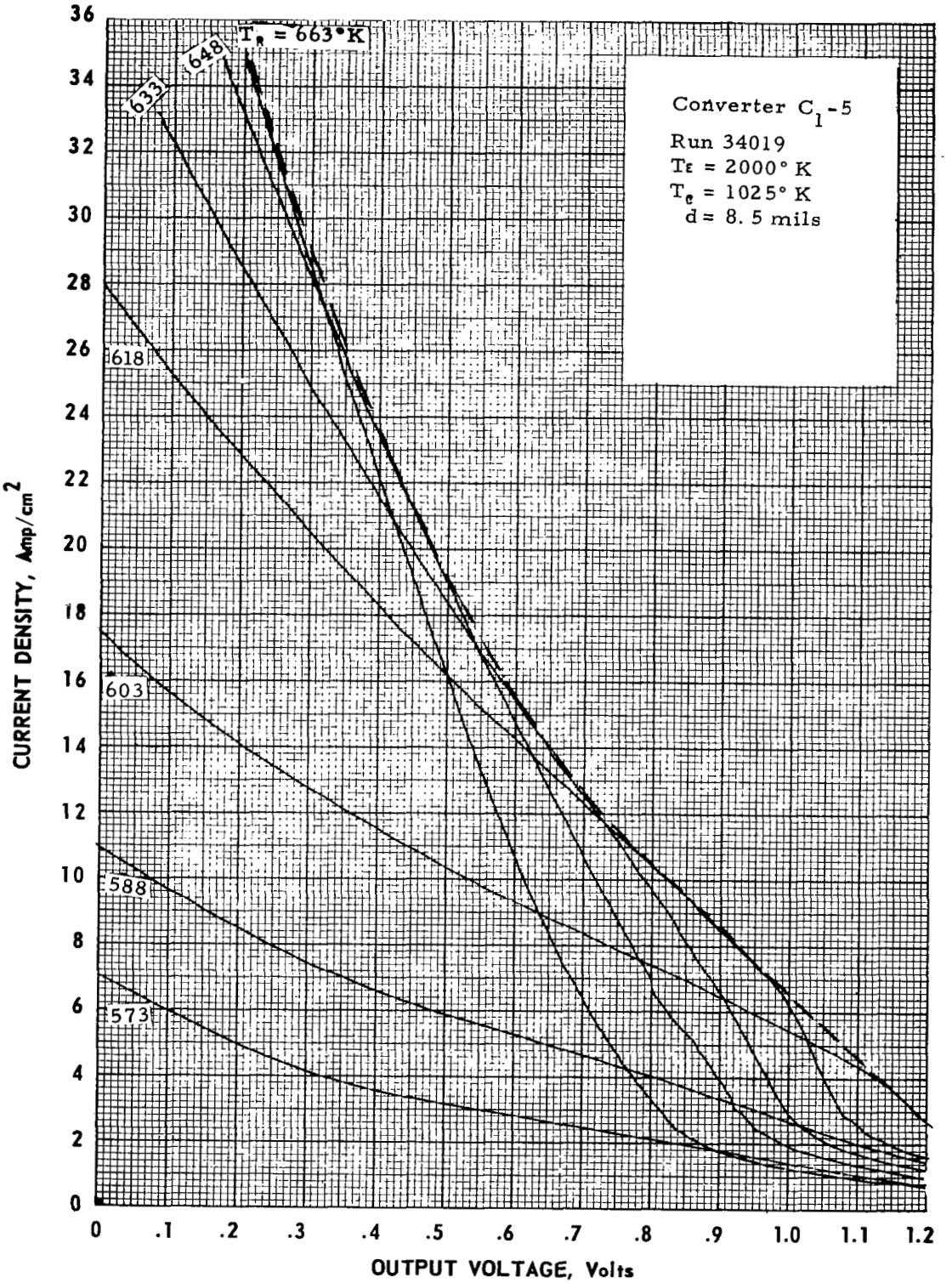

Figure V-8 Typical Cesium Family and Envelope.

VI. EXPERIMENTAL RESULTS AND DISCUSSION

A. PARAMETRIC DATA

Cesium families were obtained for the converters near optimum collector temperature, over the emitter temperature range of 1600 to 2000°K. These families are shown in Appendices B and C, and their envelopes are shown in Figures VI-1 through VI-7. Each figure shows the optimized performance of the converter with respect to cesium and collector temperatures for several emitter temperatures. Data were not available at all emitter temperatures for all of the converters. The dashed curves, obtained by interpolation at constant current density, represent the performance of the converter at the emitter temperatures to be used for comparison among other converters.

The optimized performances of all converters are compared at emitter temperatures of 1600, 1700, 1800, 1900 and 2000°K in Figures VI-8 through VI-12. As shown in Figures VI-10 to VI-12, the performance of chloride tungsten emitters (C_1-2, C_1-4, C_1-5) is higher than that of the fluoride tungsten emitters (B_2-2, B_6-2) over the temperature range of 1800 to 2000°K. For example, at an emitter temperature of 2000°K, the maximum power achieved with chloride tungsten emitters is about twice that obtained with fluoride tungsten emitter B_2-2.

The relative merit of emitters can be evaluated from the slopes of their cesium envelopes. Generally, a steep envelope is associated with an emitter which is highly uniform or which requires a low cesium pressure for a given emission. Based on the slopes of the envelopes,

the emitters can be classified into two major groups. The envelopes of the Group 1 emitters, consisting of the chloride tungsten, chemically-etched fluoride tungsten, and duplex tungsten emitters (C_1-2, C_1-4, C_1-5, D_1-1, and C_3-3), show steeper slopes than those of the Group 2 emitters, consisting of the fluoride tungsten emitters (B_2-2 and B_6-2). Group 1 emitters are considered to be superior to Group 2 emitters, even though under some particular conditions Group 2 emitters show higher output. For example, at T_E = 1600 °K and at high voltages, the output of emitter C_1-2 is less than that of B_6-2 (Figure VI-8. Under these conditions, the interelectrode spacing of converter C_1-2 (8.5 mils) is less than the optimum value, and the capabilities of the surface are not fully realized. At T_E > 1700 °K, where the cesium pressures are higher and the optimum spacing is smaller, emitter C_1-2 shows higher performance than emitter B_6-2 throughout the voltage range of practical interest. At an emitter temperature of 2000 °K, the maximum power achieved with chloride tungsten (emitters C_1-2, C_1-4 and C_1-5) is about twice that obtained with fluoride emitter B_2-2.

The higher performance of the chloride vapor-deposited tungsten emitters (C_1-2, C_1-4 and C_1-5), as compared with the fluoride vapor-deposited tungsten emitter (B_2-2) and the electropolished fluoride vapor-deposited tungsten emitter (B_6-2), is reasonable, since the former have a (110) and the latter a (100) preferred orientation. It is interesting to note that chemical etching improves the performance of fluoride vapor-deposited tungsten emitters almost to the level of chloride vapor-deposited tungsten emitters. On the other hand, electropolishing reduces the performance of fluoride vapor-deposited tungsten emitters, as shown by comparing the performances of

emitters B_2-2 and B_6-2 (Figures VI-10 and VI-11). Independent experiments carried out at Thermo Electron (references 8 and 9) have shown that when the surface of a piece of tungsten, such as this fluoride material, is ground and heat-treated at temperatures of about 2600 °K, it recrystallizes and a nearly randomly oriented surface is obtained which contains considerable areas which do not have (100) orientation but which are superior to (100) oriented areas for thermionic emission. The surface of emitter B_2-2 is presumably this type of recrystallized material. On the other hand, electropolishing the surface removes the randomly oriented material and exposes material with a fairly strong (100) orientation. In removing the non-(100) material, the thermionic performance is reduced. Another interesting point indicated by this data is that the performance of the duplex vapor-deposited tungsten emitter (C_3-3) is not as good as the performance of the chloride tungsten emitters. This result is rather surprising, since the surface layer of the duplex emitter was deposited by the chloride process. The difference between the chloride emitters and the duplex emitters is that the thickness of the chloride layer in the former was 40 mils, as compared to a thickness of about 10 mils in the latter. It is possible that the difference in the thickness of the chloride layer is responsible for their difference in performance, and the difference in performance is consistent with the difference in bare work function. The technique of vapor deposition has not yet reached a high degree of reproducibility, and the above difference in performance can possibly be explained by sample-to-sample variations in orientation.

The cesiated work functions estimated from cesium families are shown in Figure VI-13. Emitter C_1-2, with the highest degree of (110) orientation, shows the steepest envelopes and the lowest cesiated work functions. Emitter B_6-2, with a (100) preferred orientation, shows the flattest envelopes and the highest cesiated work functions. These characteristics are plausible, since the slope of the envelopes and the cesiated work functions depend on the cesium pressure required for a given level of emission, which in turn is influenced by the crystallographic orientation.

B. LIFE-TEST RESULTS

The converters were life-tested at the maximum power point after the initial set of parametric data was taken. The emitter, collector and cesium reservoir temperatures and output power of the converter were checked and recorded daily. The life test data for these converters in terms of power density versus time are shown in Figure VI-14 through VI-19. The test results for each converter are described below.

1. Converter B_2-2

This was the first converter which was successfully outgassed and put on test; however, it developed a leak and lost cesium after 273 hours of operation. Examination showed cracks in the Ta-10% W emitter back-up plate and at the emitter-to-sleeve weld. Photomicrographs showed impurities precipitated along grain boundaries in the back-up plate and grain boundary separation. Also, slight amounts of impurities were apparent in the tantalum sleeve. Attempts to establish the source of contamination are discussed in Section III.

2. Converter B_6-2

Following the acquisition of preliminary performance data, converter B_6-2 was life-tested at an emitter temperature of 1910 °K, a collector temperature of 930 °K, a cesium reservoir temperature of 620 °K and an output power density of 3.94 watts/cm^2. The converter failed after 2400 hours of life testing. During the course of life testing, the maximum deviation of power output was about 4.7 percent from the average value. The life test data are shown in Figure VI-14.

3. Converter C_1-2

This converter was life-tested after a complete set of parametric data was taken. The life test was interrupted after 3000 hours and a second set of parametric data was taken. These two sets of data were in good agreement. The life-testing conditions were: emitter temperature of 2030 °K; collector temperature of 970 °K; cesium temperature of 610 °K; and output power density of 9.0 watts/cm^2. The life test data are shown in Figure VI-15. The converter failed after 3480 hours of life test due to a cesium leak in the vicinity of the emitter-to-sleeve weld. The maximum deviation of power output during the life test was about 4 percent from the average value. The electron bombardment power supply unit used with this converter failed several times during the course of the life test, causing quick cool-down of the converter; however, the performance of the converter was apparently not affected.

4. Converter C_1-4

This converter was life-tested after a complete set of parametric performance data was taken. Another set of parametric data was also

taken after 3000 hours of life test. These two sets of data were in good agreement. The life-testing conditions were: emitter temperature of 1950 °K; collector temperature of 1070 °K; cesium reservoir temperature of 610 °K; and output power density of 8 watts/cm^2. The life test data are shown in Figure VI-16. The converter successfully achieved 4000 hours of life-testing, as designated in the contract. The maximum deviation of power output during the life test was about 4 percent from the average value.

5. Converter C_1-5

Parametric data for this converter were obtained prior to life-testing and after 3 000 hours of operation. These two sets of data were in good agreement The life test conditions were: emitter temperature of 2000 °K; collector temperature of 1070 °K; cesium reservoir temperature of 650 °K; and output power density of 8.5 watts/cm^2. The converter successfully achieved 4000 hours of life testing. The maximum deviation of power output during the life test was about 5 percent from the average value. The life test data are shown in Figure VI-17.

6. Converter C_3-3

This converter was life-tested after a complete set of parametric data was taken. A set of parametric data was again taken after 3000 hours of life test. These two sets of data were in good agreement. The life test conditions were: emitter temperature of 2000 °K; collector temperature of 1070 °K; cesium reservoir temperature of 610 °K; and output power density of 7.58 watts/cm^2. The converter successfully achieved 4000 hours of life testing. The maximum

deviation of power output during the life test was about 9 percent from the average value. The life test data are shown in Figure VI-18.

7. Converter D_1-1

After parametric data were taken, at emitter temperatures of 1600 and 1700°K, the converter was put on static test at an emitter temperature of 1700°K and power output of 4.2 watts/cm^2 for 250 hours. The emitter temperature was then increased to 1800°K and parametric performance data were taken. The converter was then operated at this emitter temperature for 350 hours with a power output of 5.1 watts/cm^2. Finally, the converter was life-tested at the following operating conditions: emitter temperature of 1900°K; collector temperature of 970°K; cesium reservoir temperature of 600°K; and output power density of 6 watts/cm^2. The converter failed after 2190 hours of operation due to a cesium leak in the vicinity of the emitter-to-sleeve weld. The life test data are shown in Figure VI-19. As shown, the converter power output was stable for 1700 hours and then gradually dropped off.

The drop-off in performance after 1700 hours of operation could have been the result of either the leak which eventually caused the test to be terminated or a change in emitter performance. It is not possible to accurately establish the cause of degradation; however, post-test evaluation of the emitter by Gulf General Atomic (reference 10) showed that the work function was stable in vacuum for 300 hours at a temperature of 1900°K.

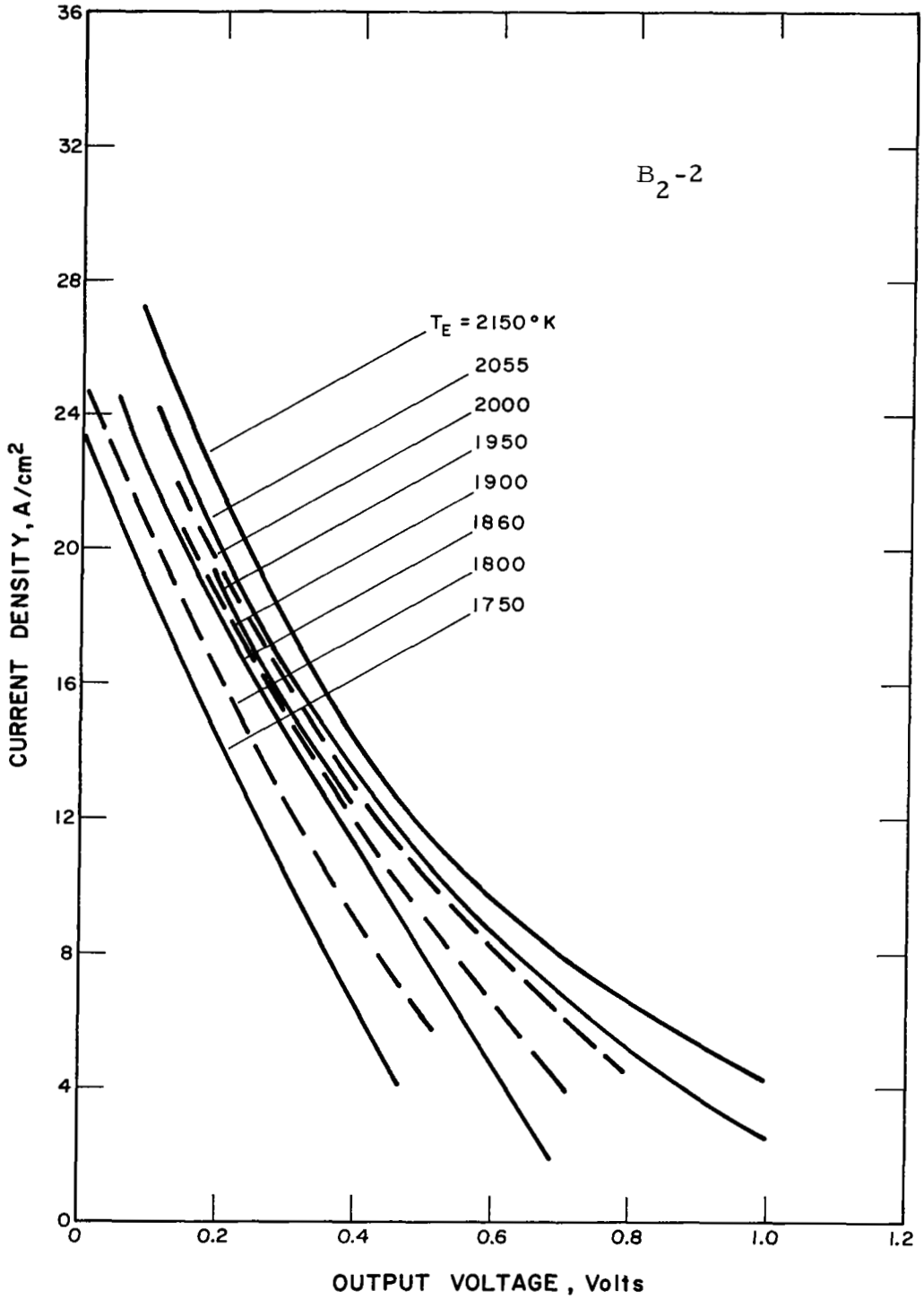

Figure VI-1 Optimized Cesium-Temperature Envelopes of Converter B_2-2.

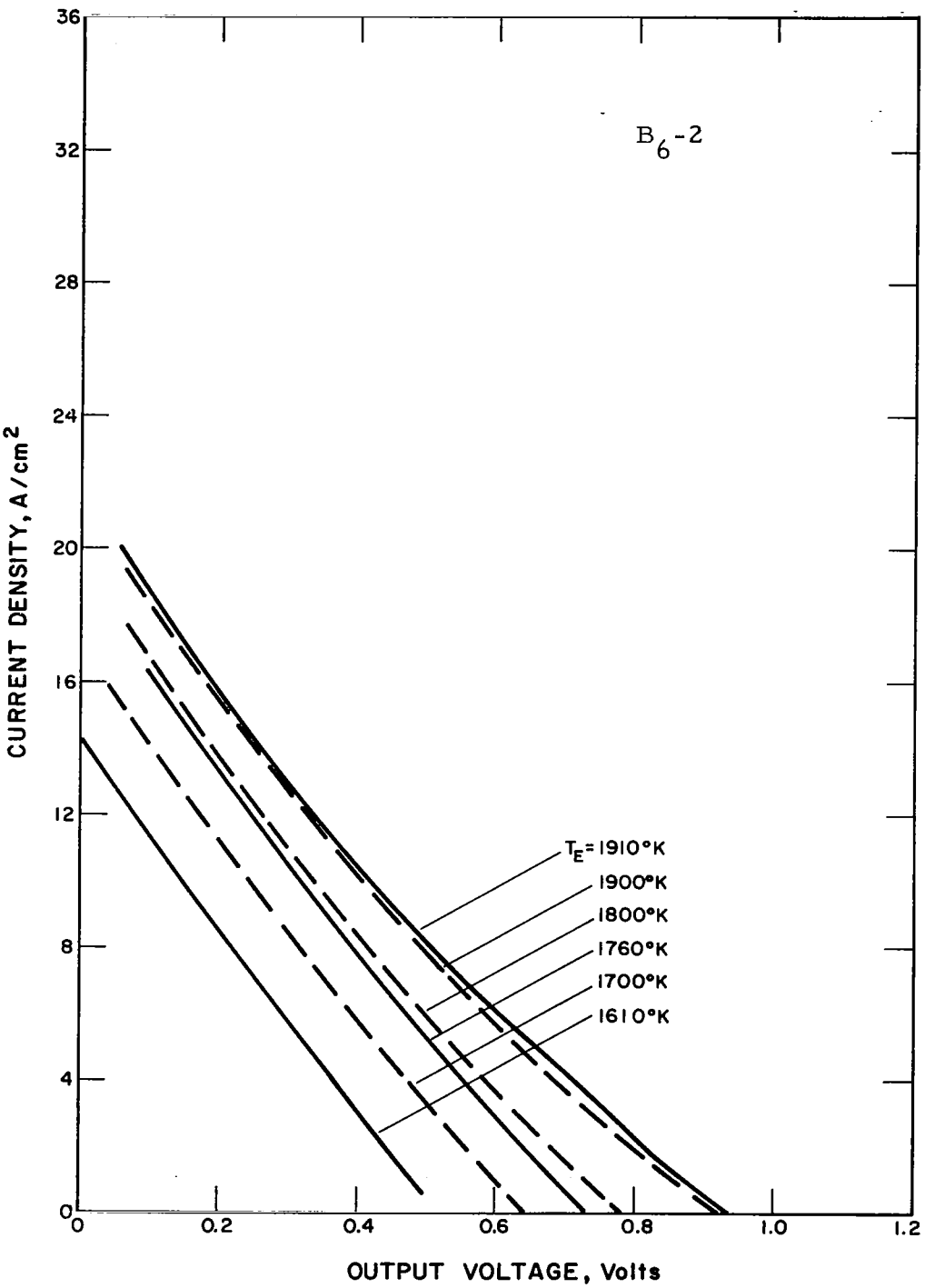

Figure VI-2 Optimized Cesium-Temperature Envelopes of Converter B_6-2.

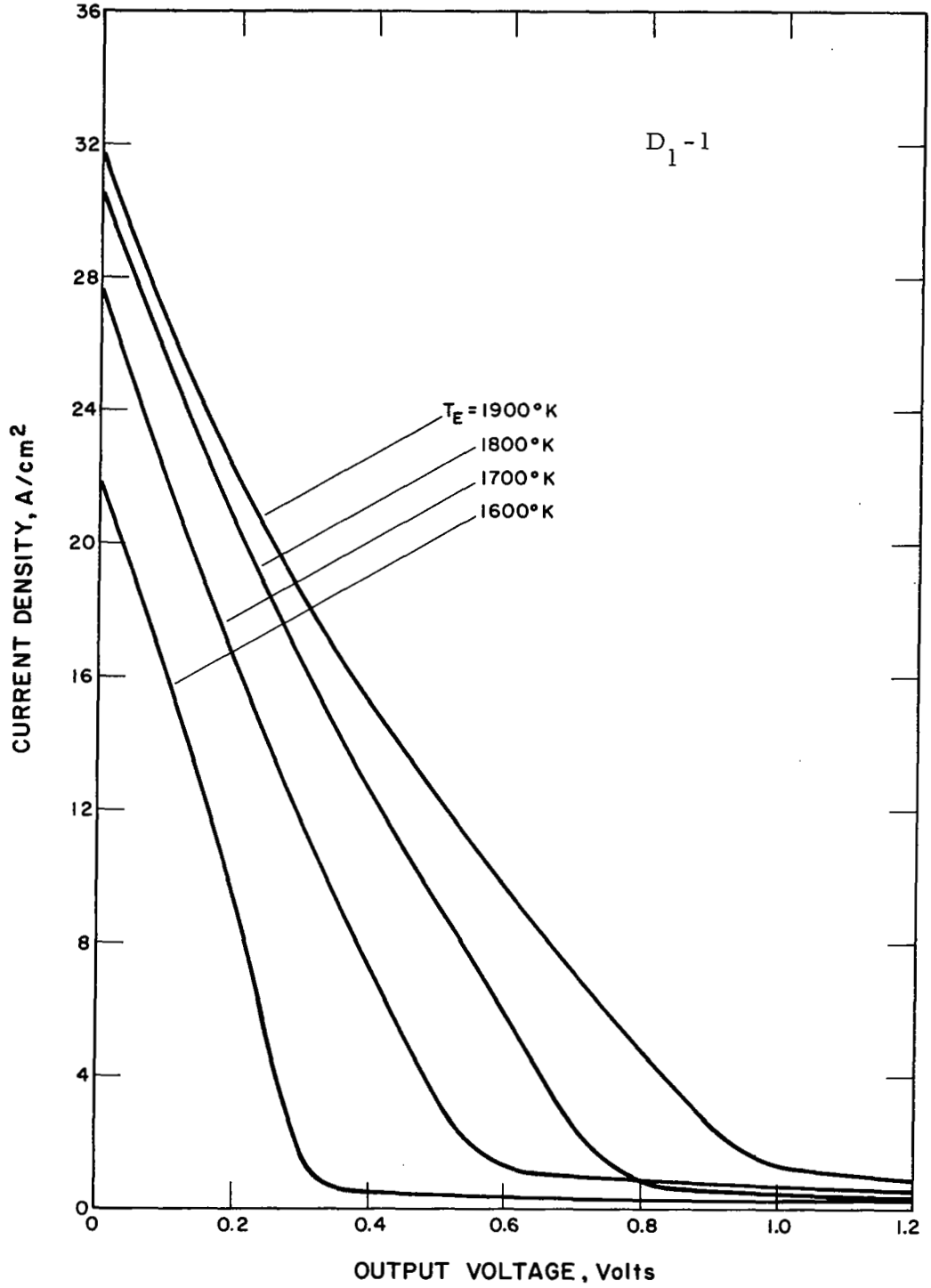

Figure VI-3 Optimized Cesium-Temperature Envelopes of Converter D_1-1.

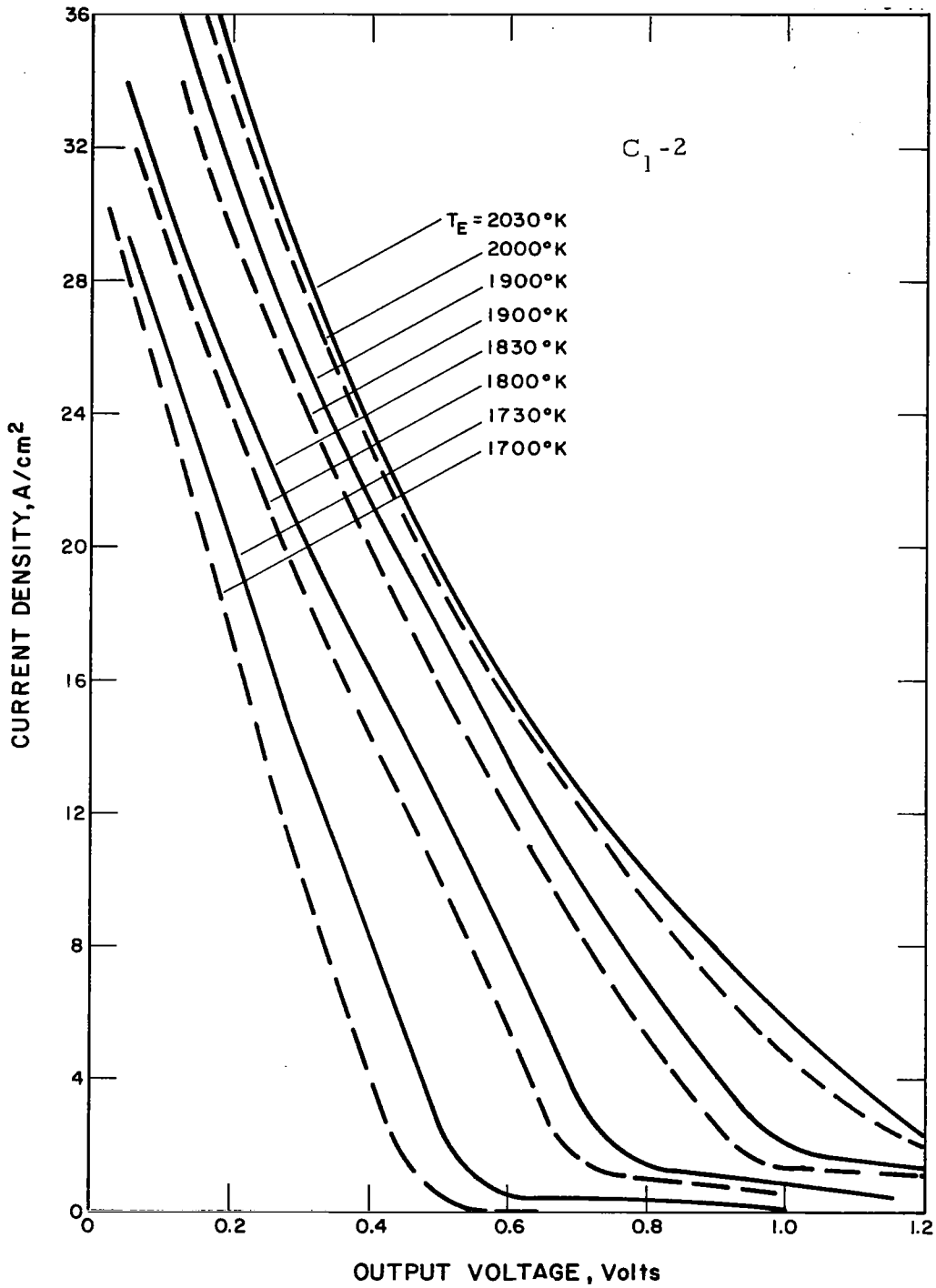

Figure VI-4 Optimized Cesium-Temperature Envelopes of Converter C_1-2.

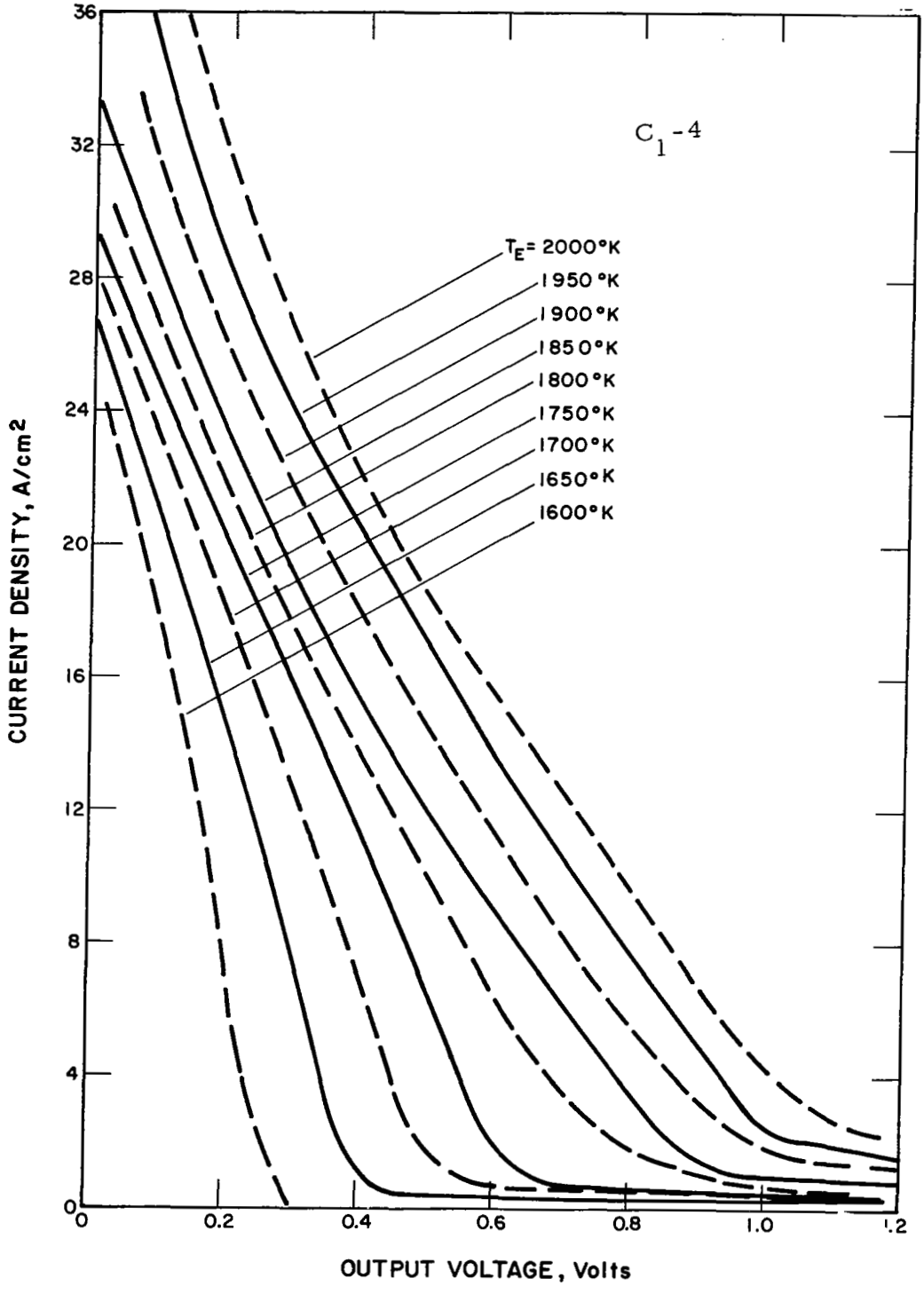

Figure VI-5 Optimized Cesium-Temperature Envelopes of Converter C_1-4.

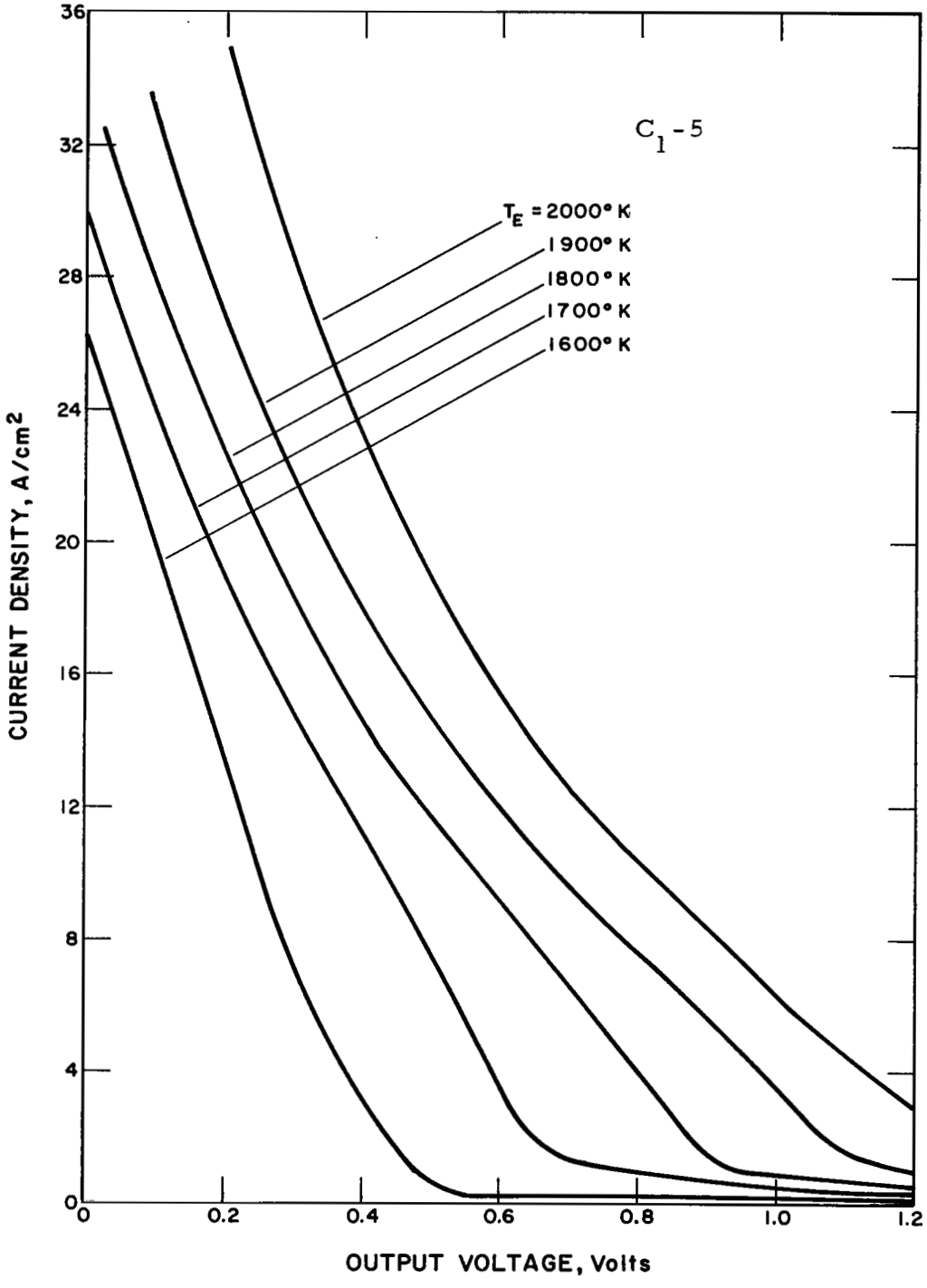

Figure VI-6 Optimized Cesium-Temperature Envelopes of Converter C_1-5.

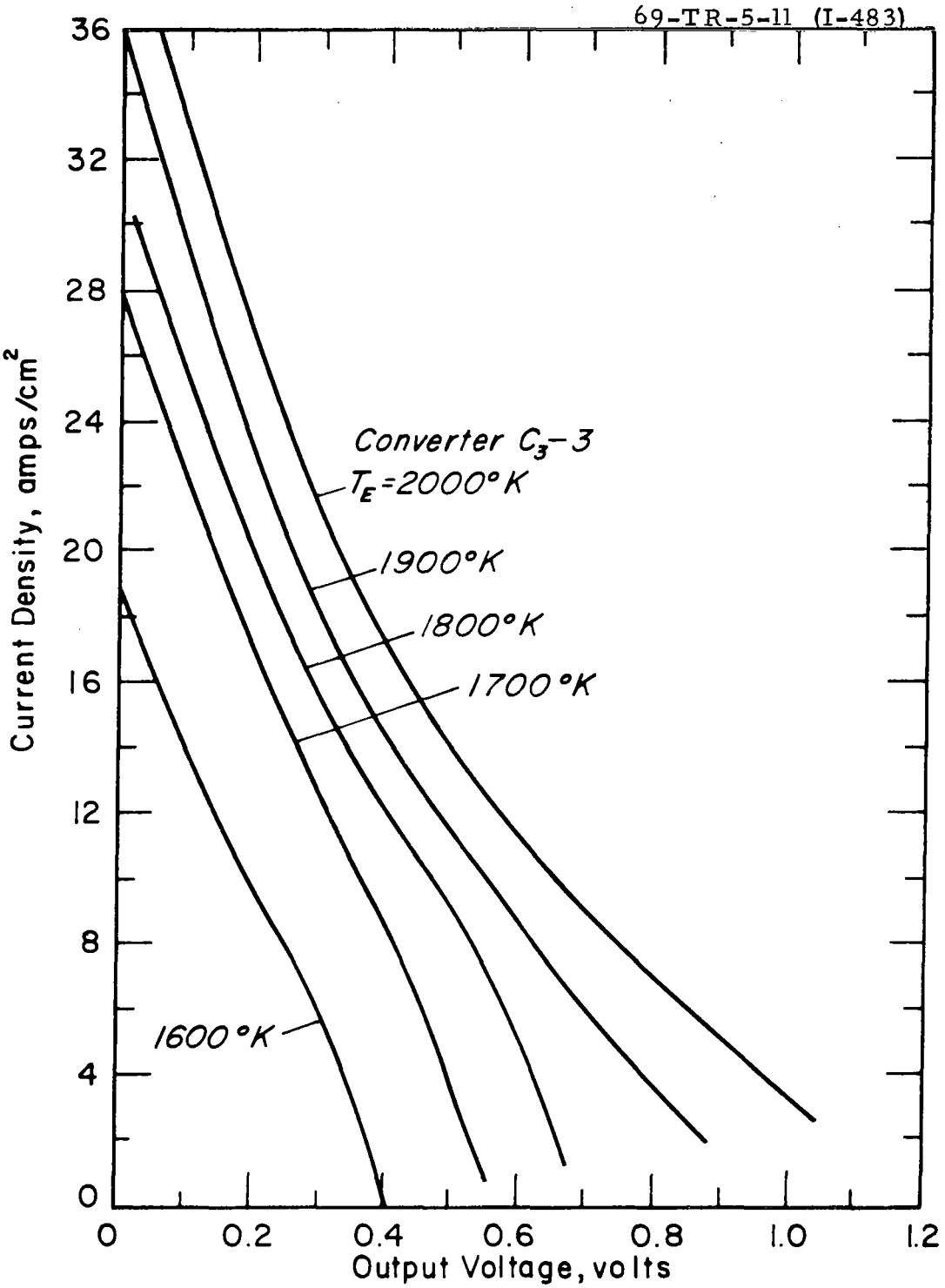

Figure VI-7. Optimized Cesium-Temperature Envelopes of Converter C_3-3.

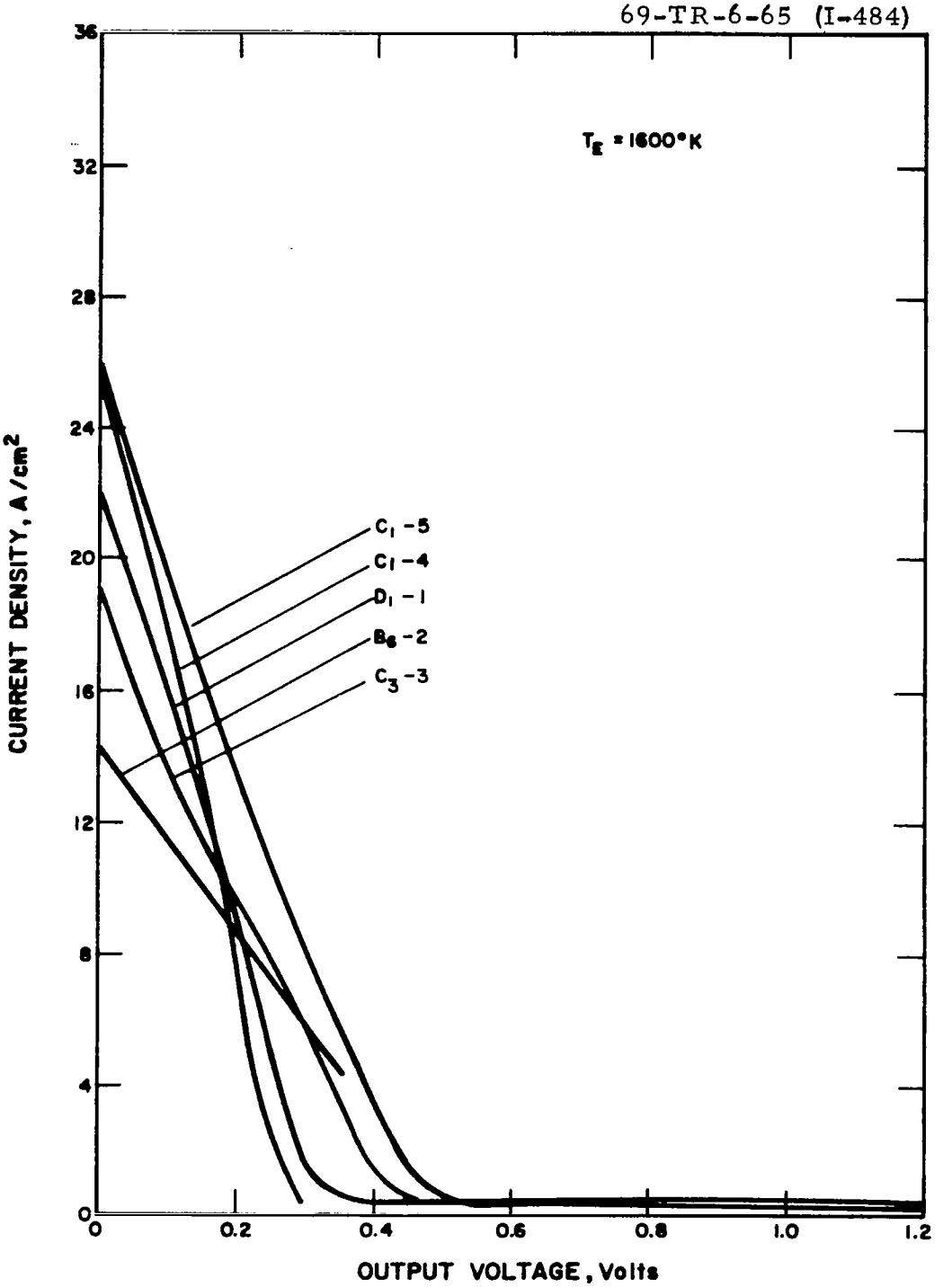

Figure VI-8. Comparison of Optimized Cesium-Temperature Envelopes at T_E = 1600°K.

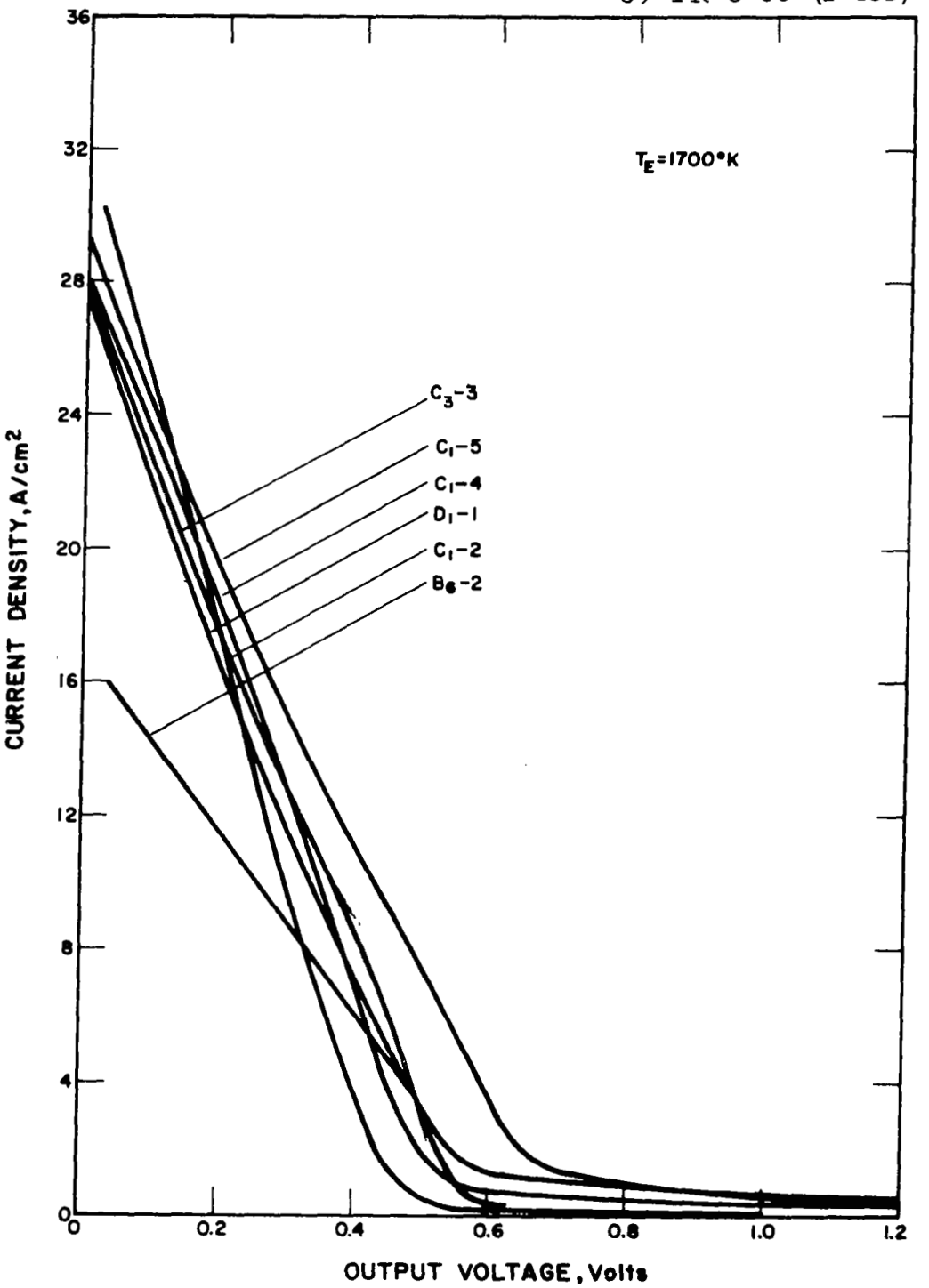

Figure VI-9. Comparison of Optimized Cesium-Temperature Envelopes at T_E = 1700°K.

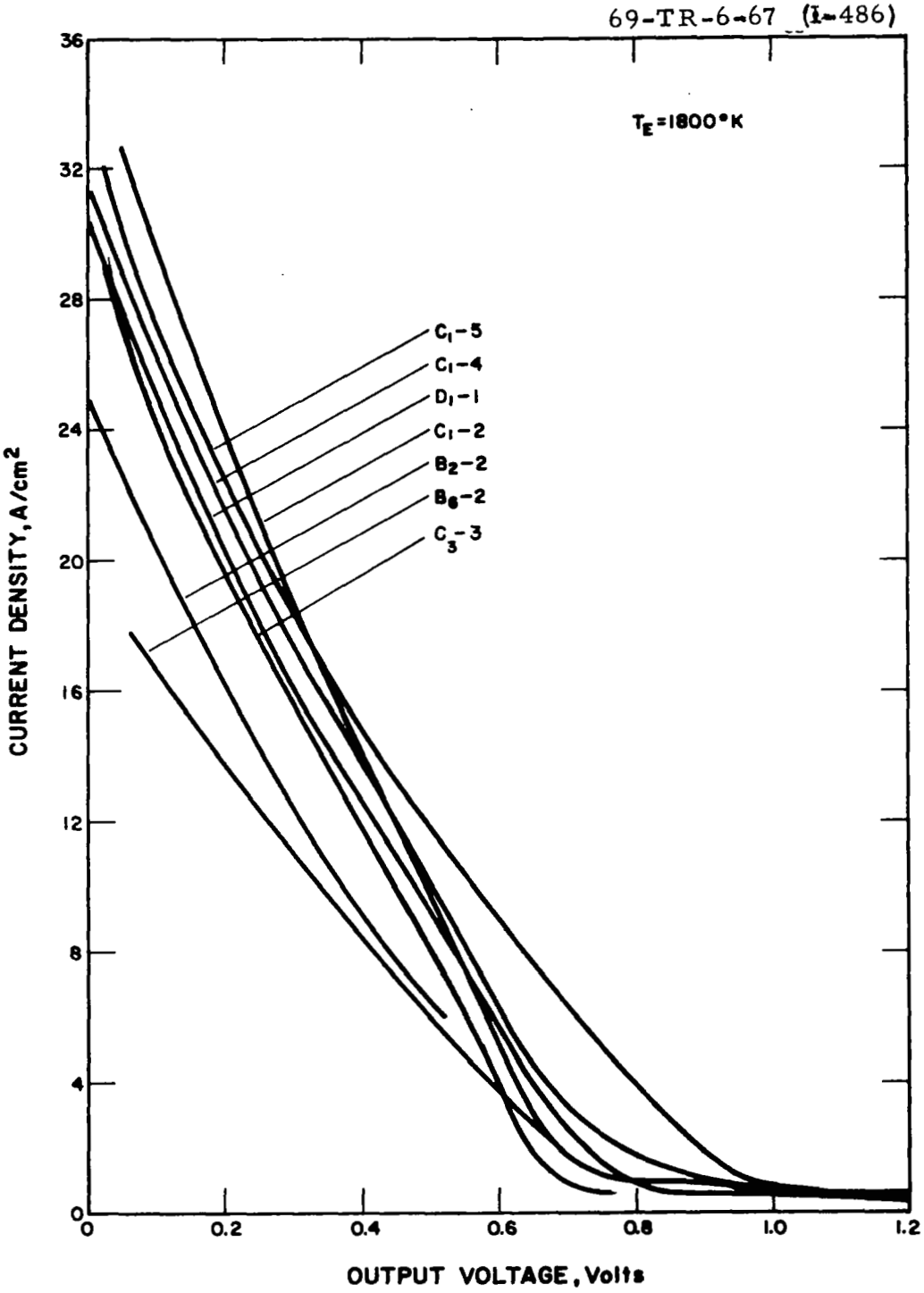

Figure VI-10 Comparison of Optimized Cesium-Temperature Envelopes at T_E = 1800°K.

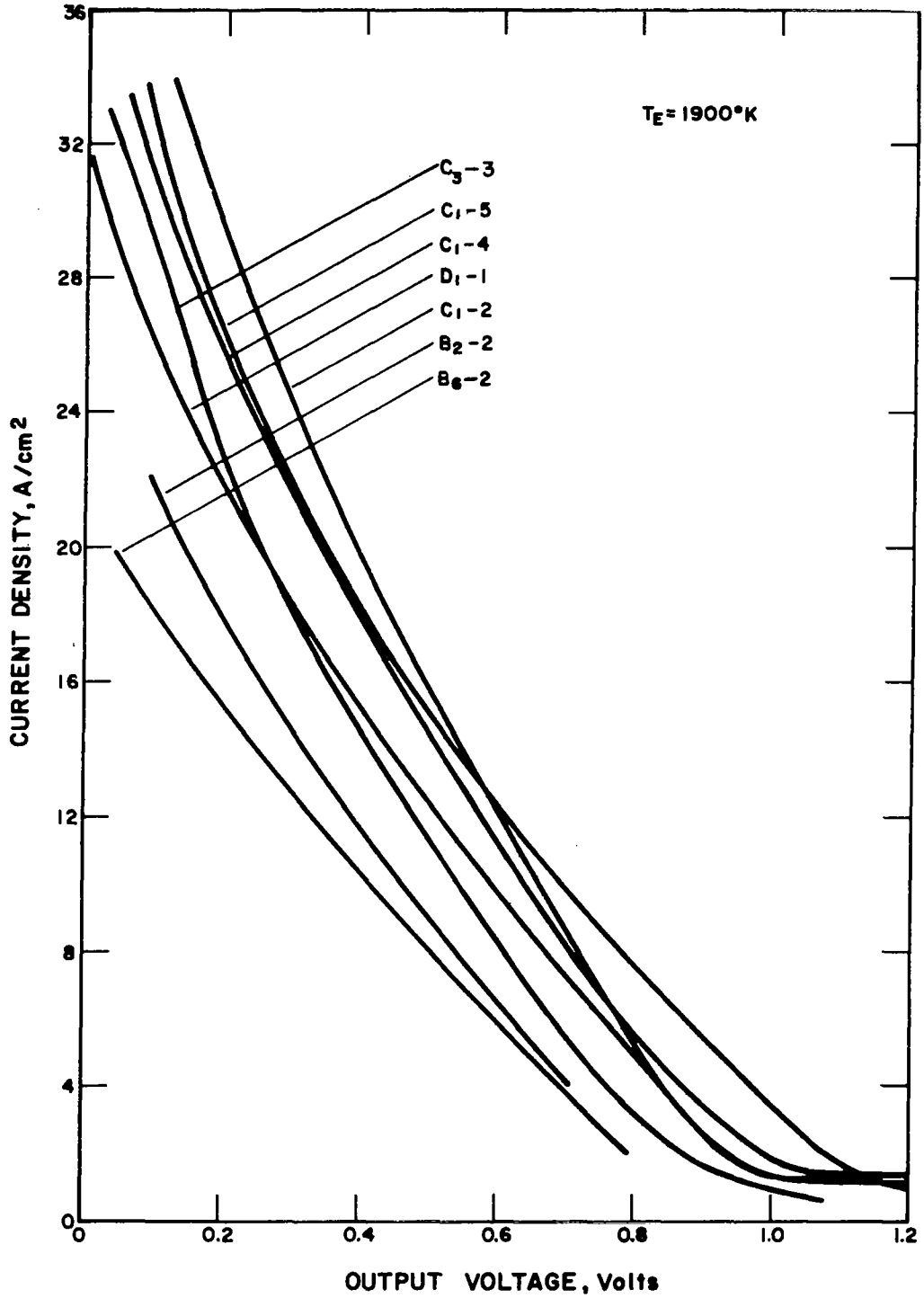

Figure VI-11. Comparison of Optimized Cesium-Temperature Envelopes at T_E = 1900°K.

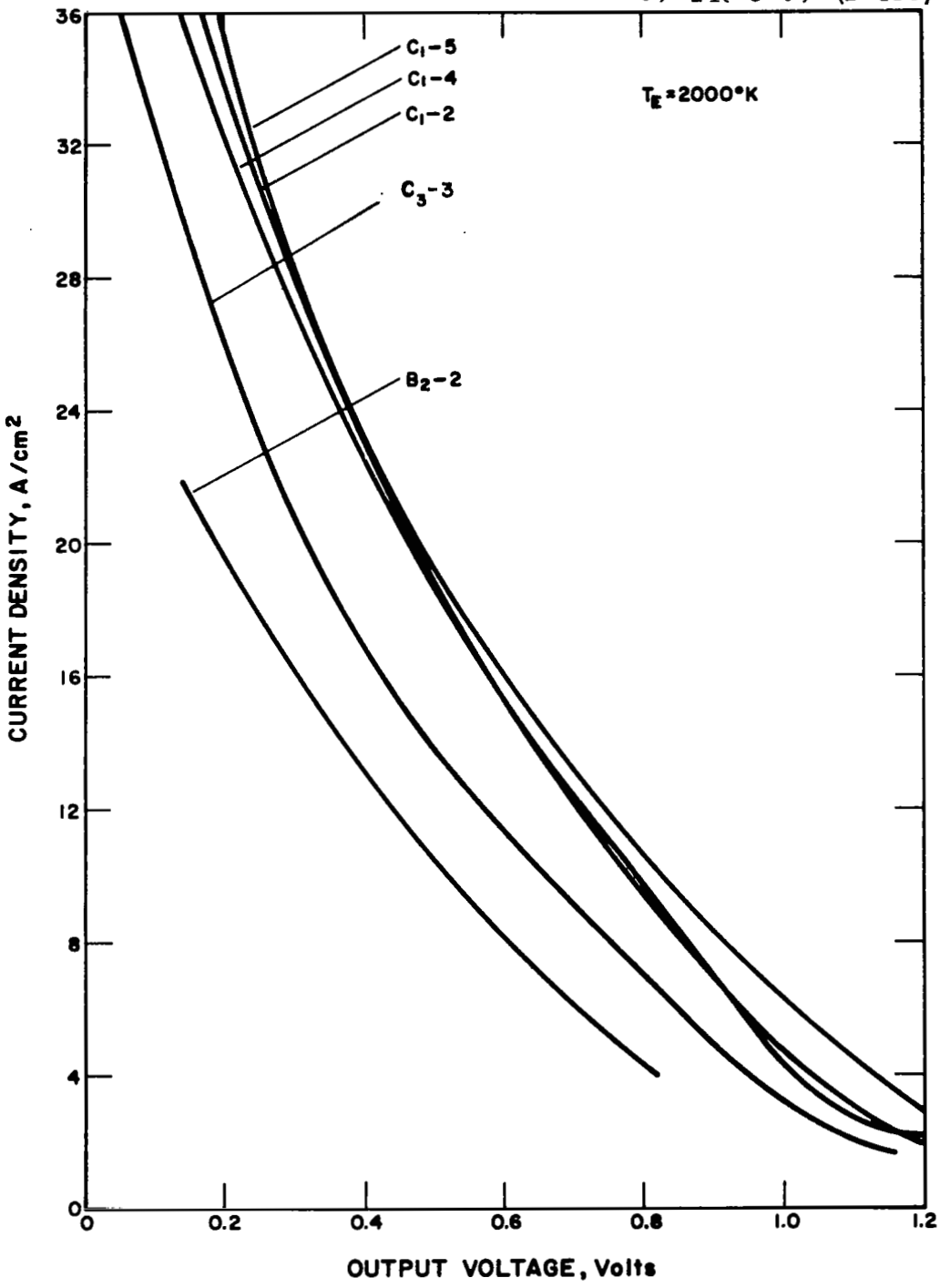

Figure VI-12. Comparison of Optimized Cesium-Temperature Envelopes at $T_E = 2000°K$.

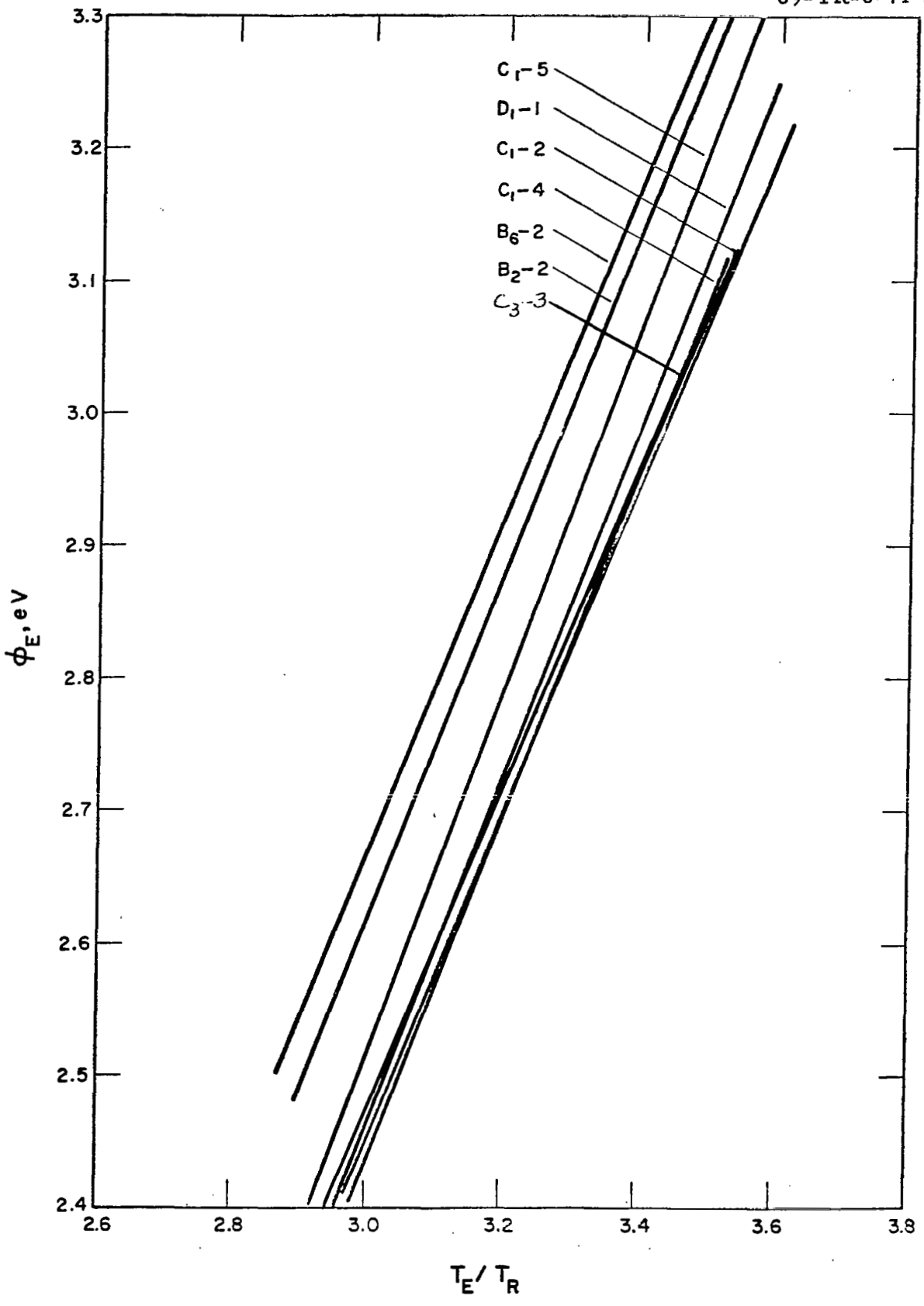

Figure VI-13. Apparent Emitter Work Functions of Converters C_1-2, C_1-4, C_1-5, C_3-3, D_1-1, B_6-2 and B_2-2.

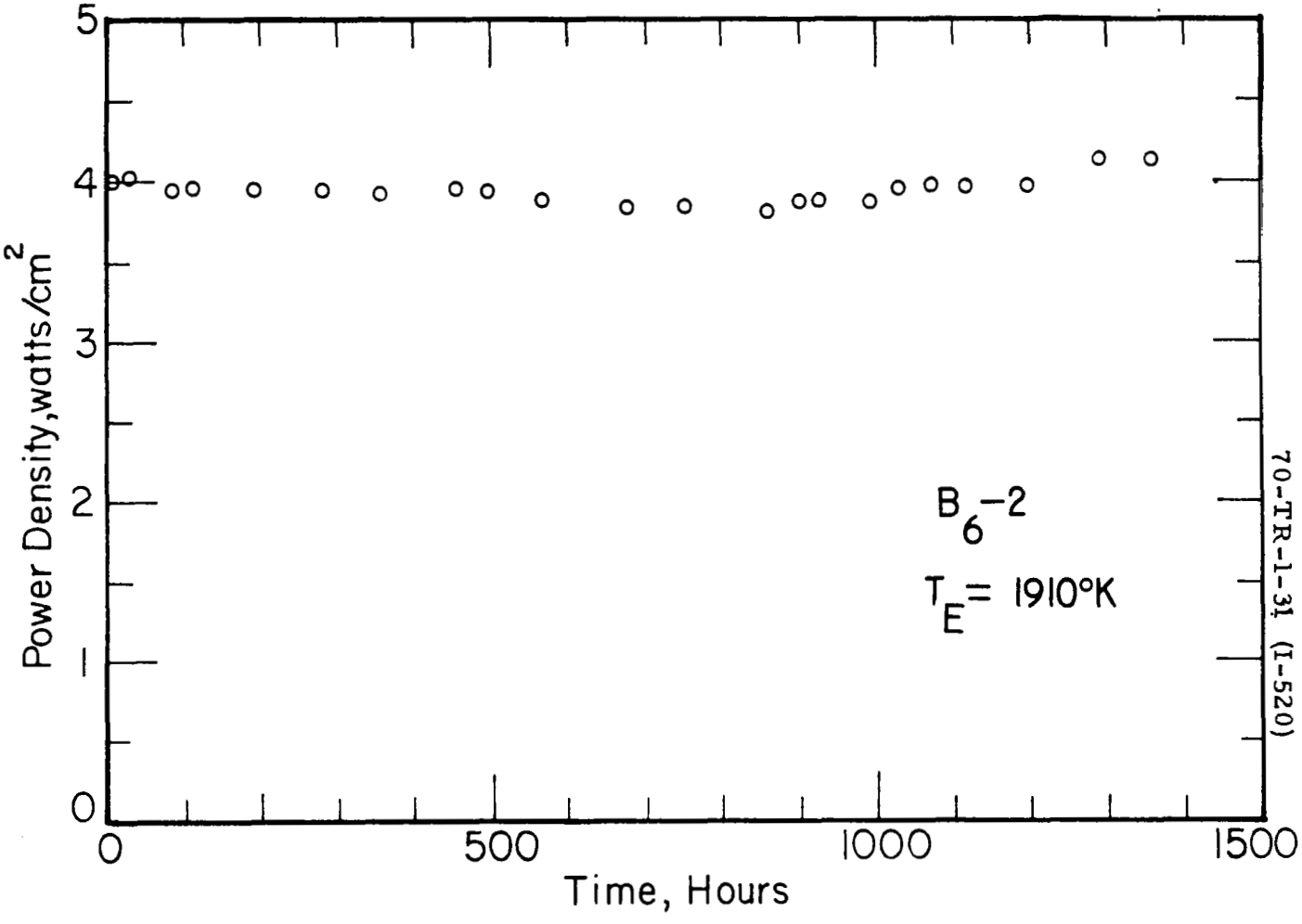

Figure VI-14. Life Test Data for Converter B_6-2 at T_E = 1910°K.

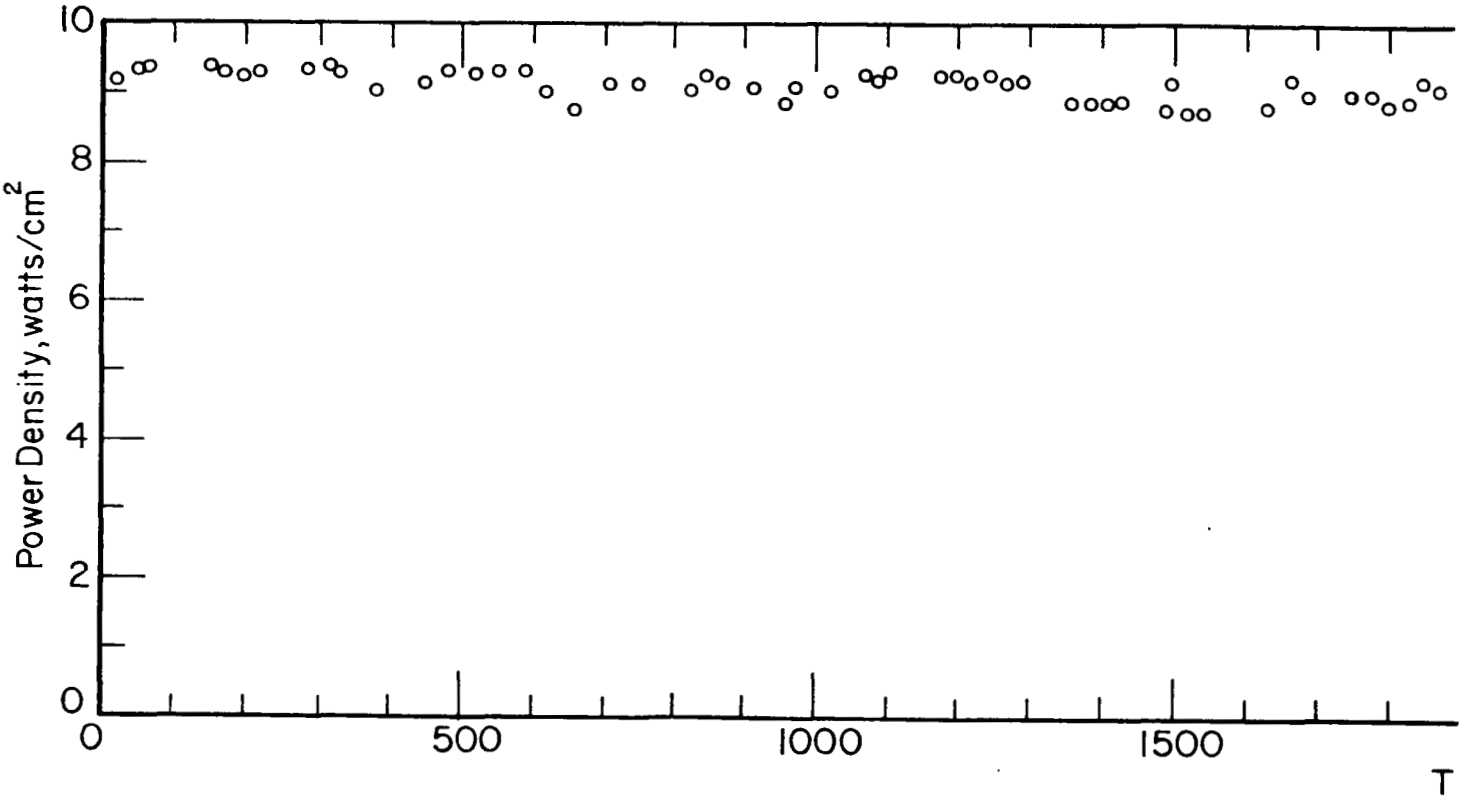

Figure VI-15. Life Test D

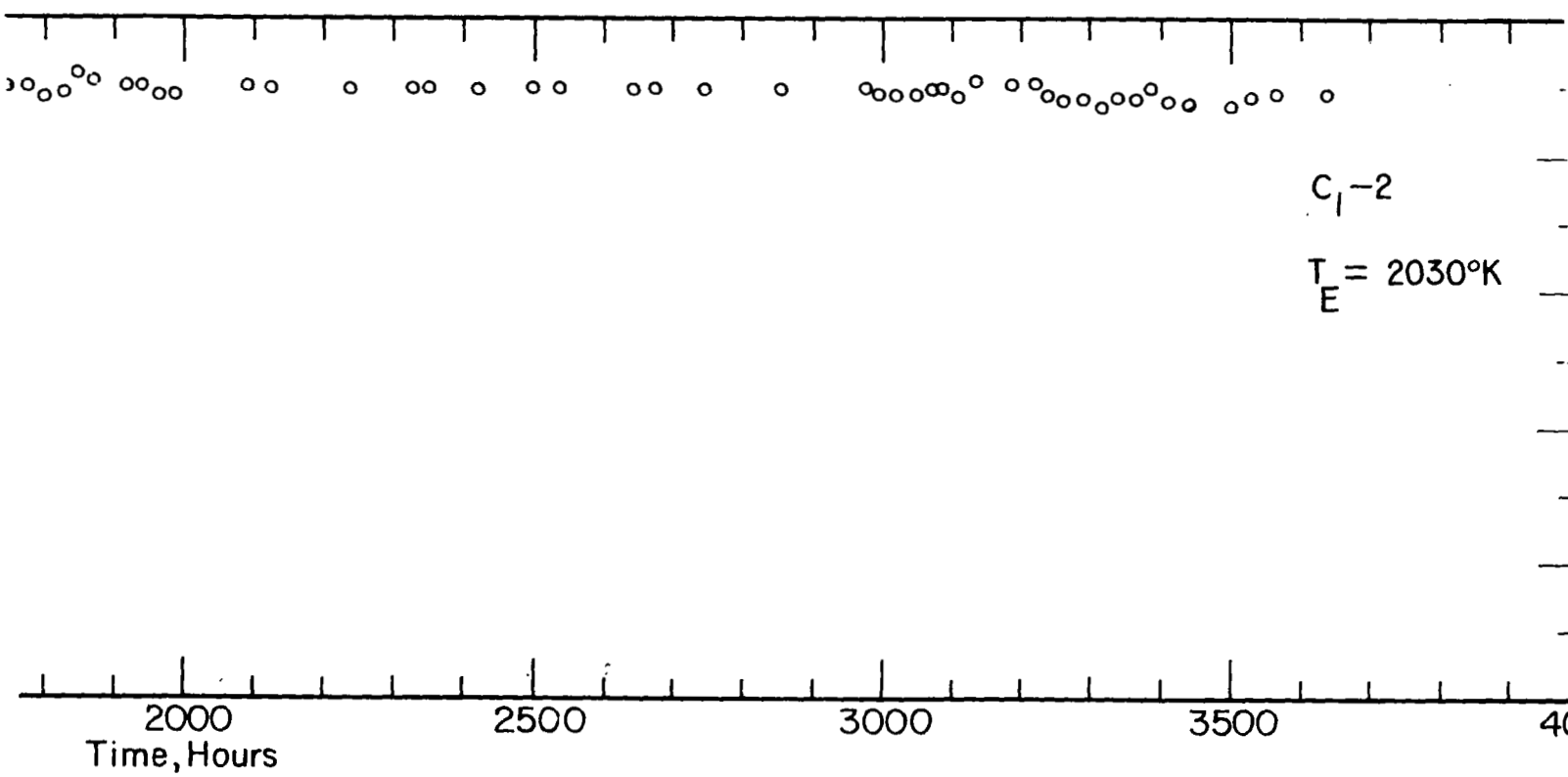

'est Data for Converter C_1-2 at T_E = 2030°K.

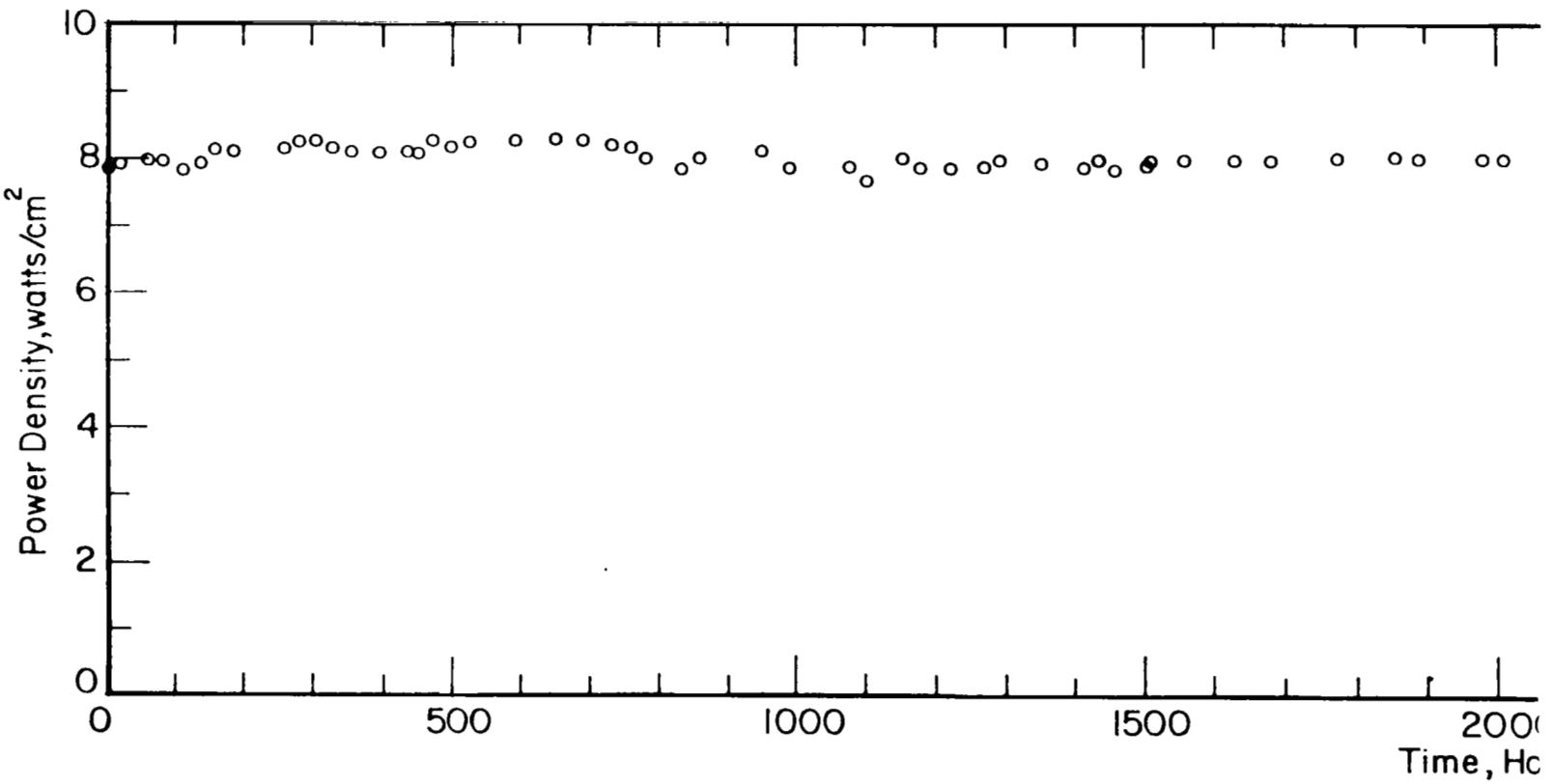

Figure VI-16. Life Test Data for

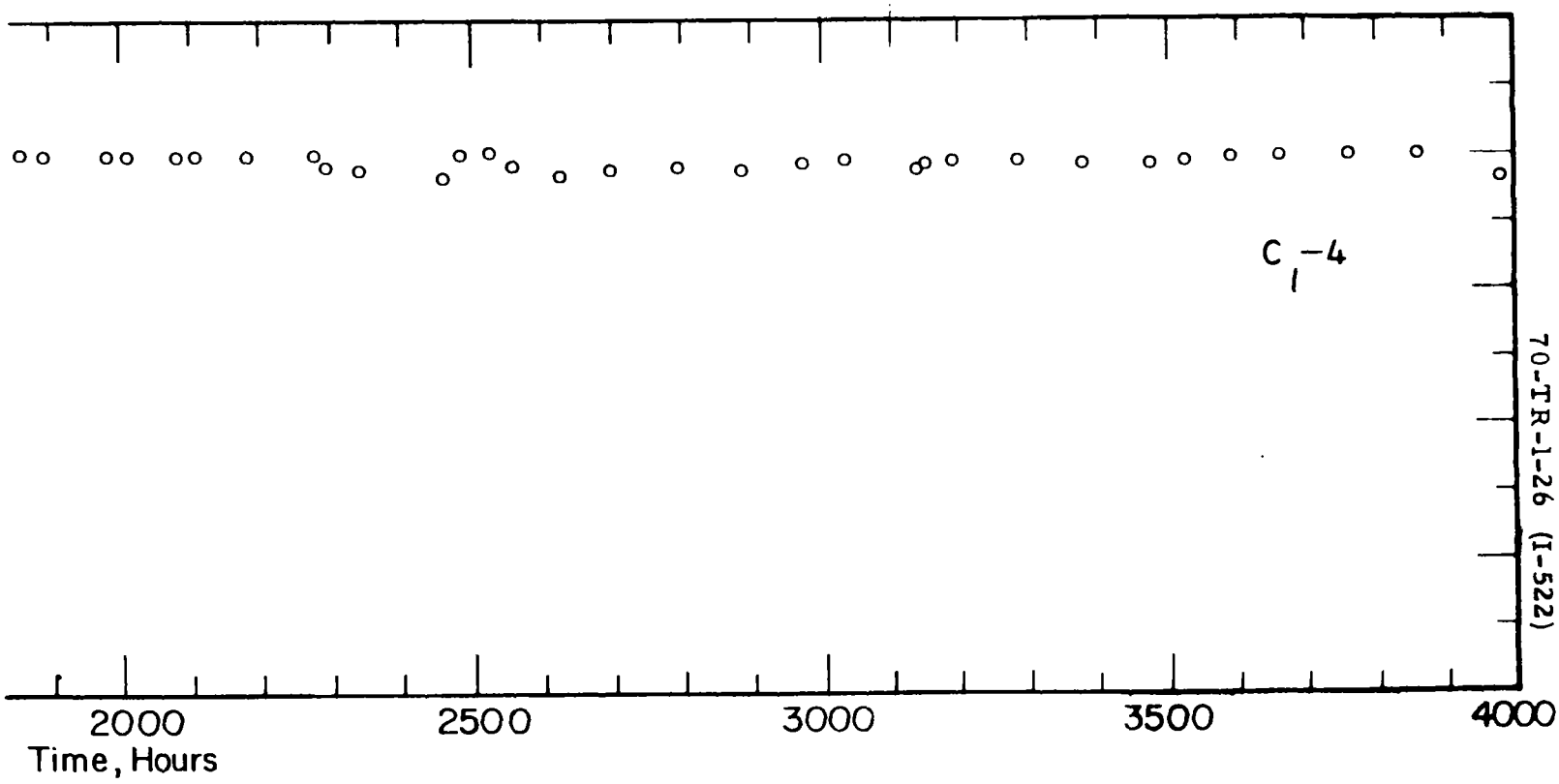

t Data for Converter C_1-4 at T_ε = 1950°K.

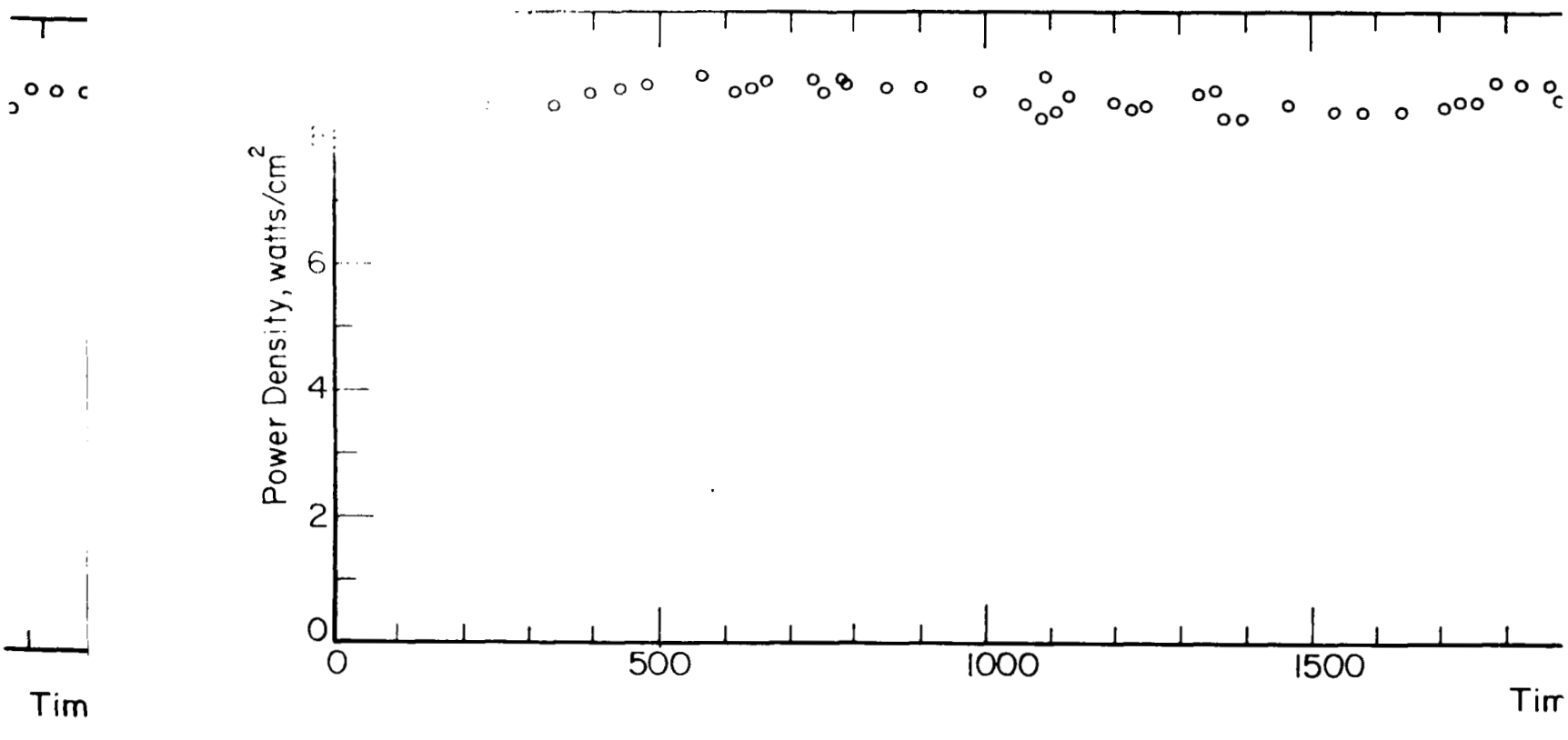

Figure VI-17. Life Test D

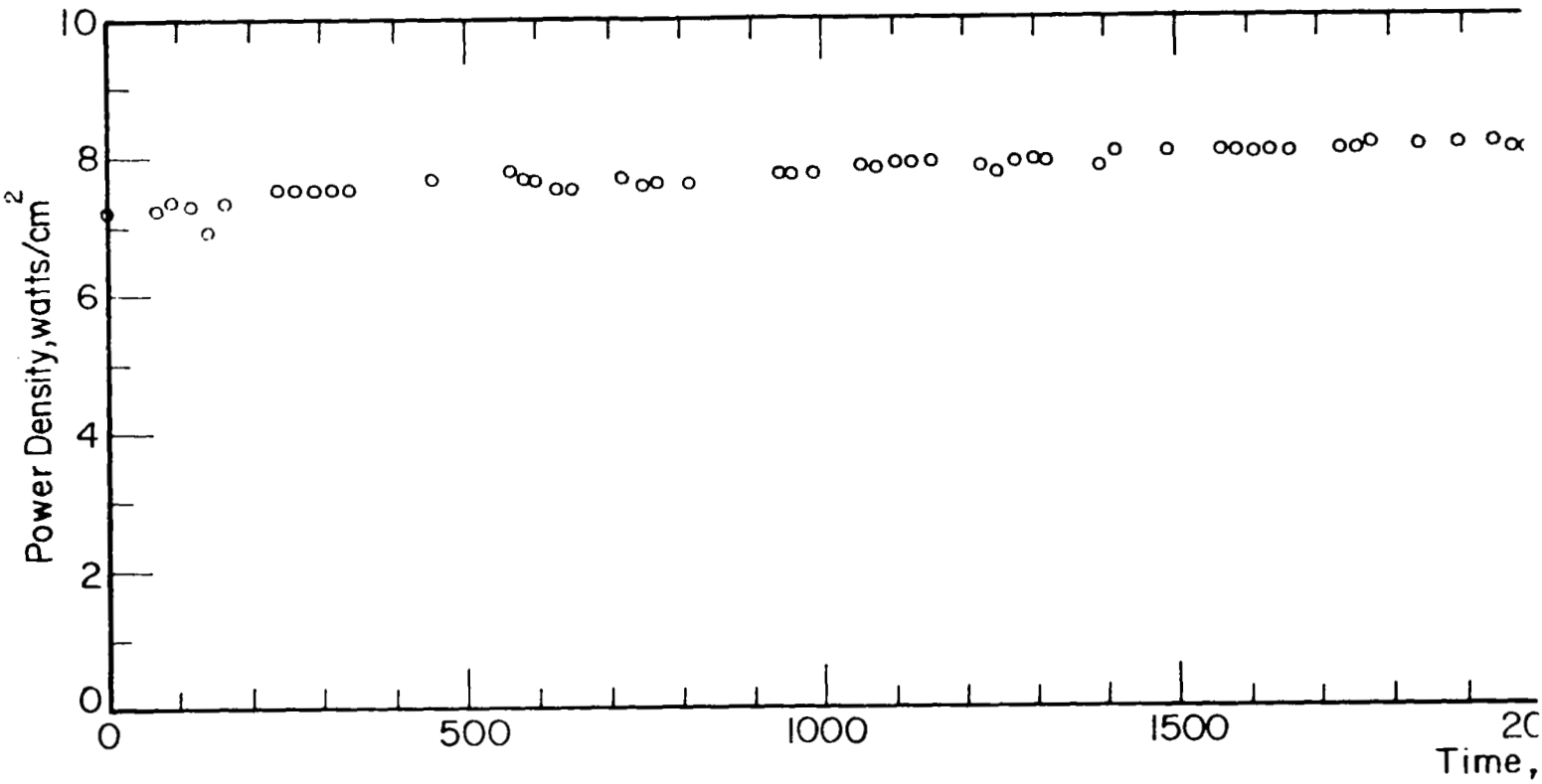

Figure VI-18, Life Test Data fo

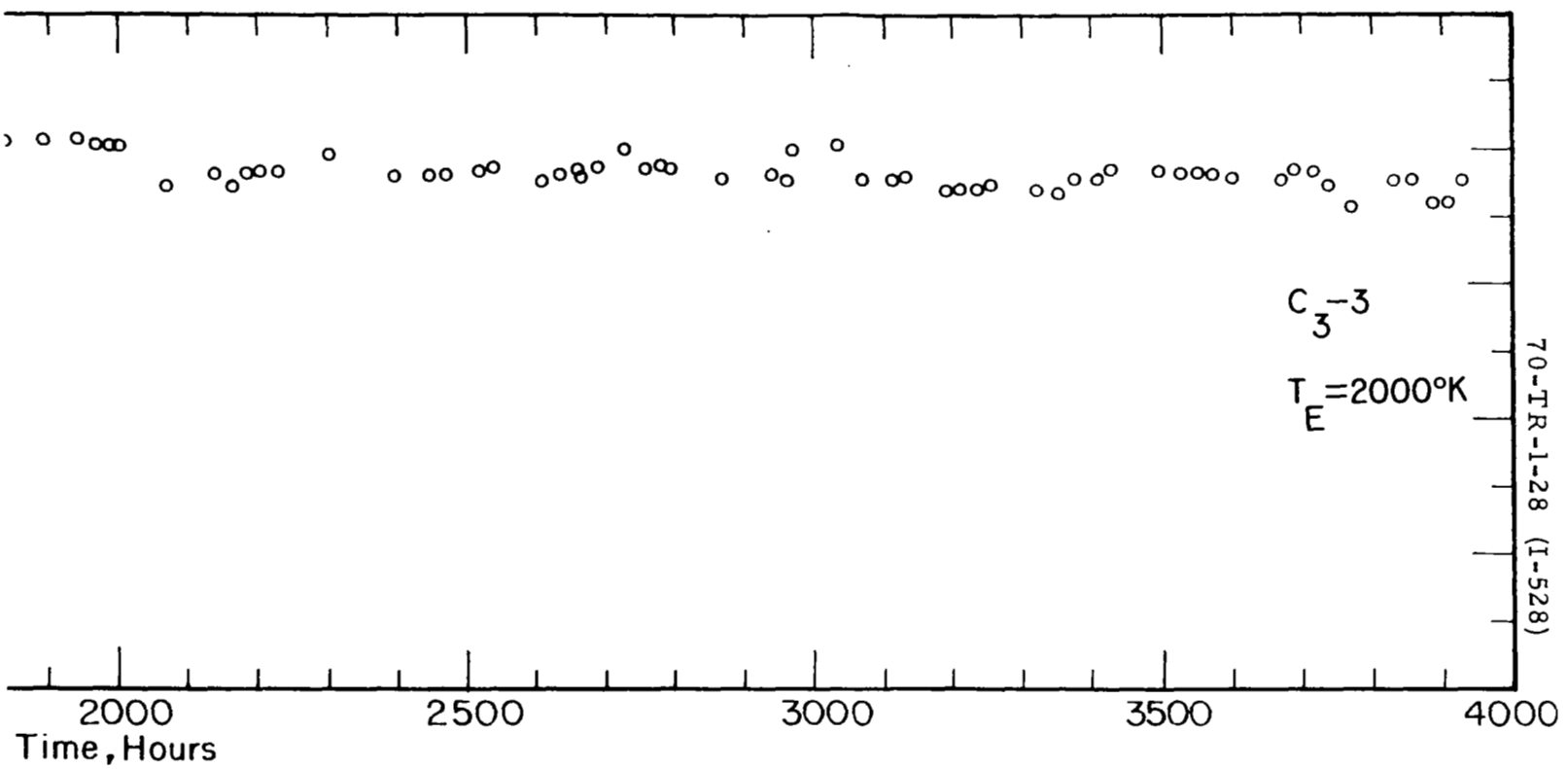

Data for Converter C_3-3 at T_E = 2000°K.

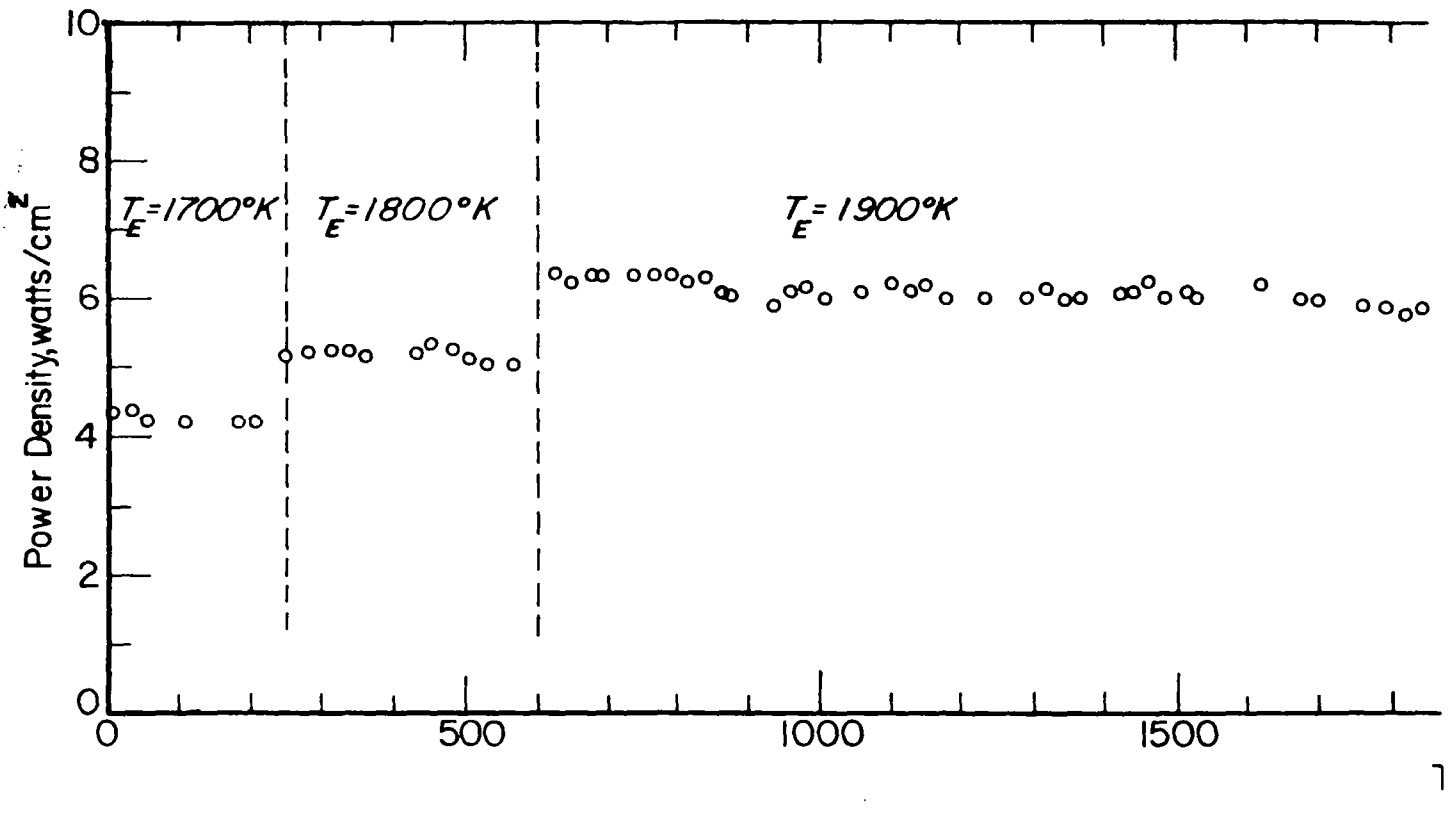

Figure VI-19. Life Test Da
and 1900°K.

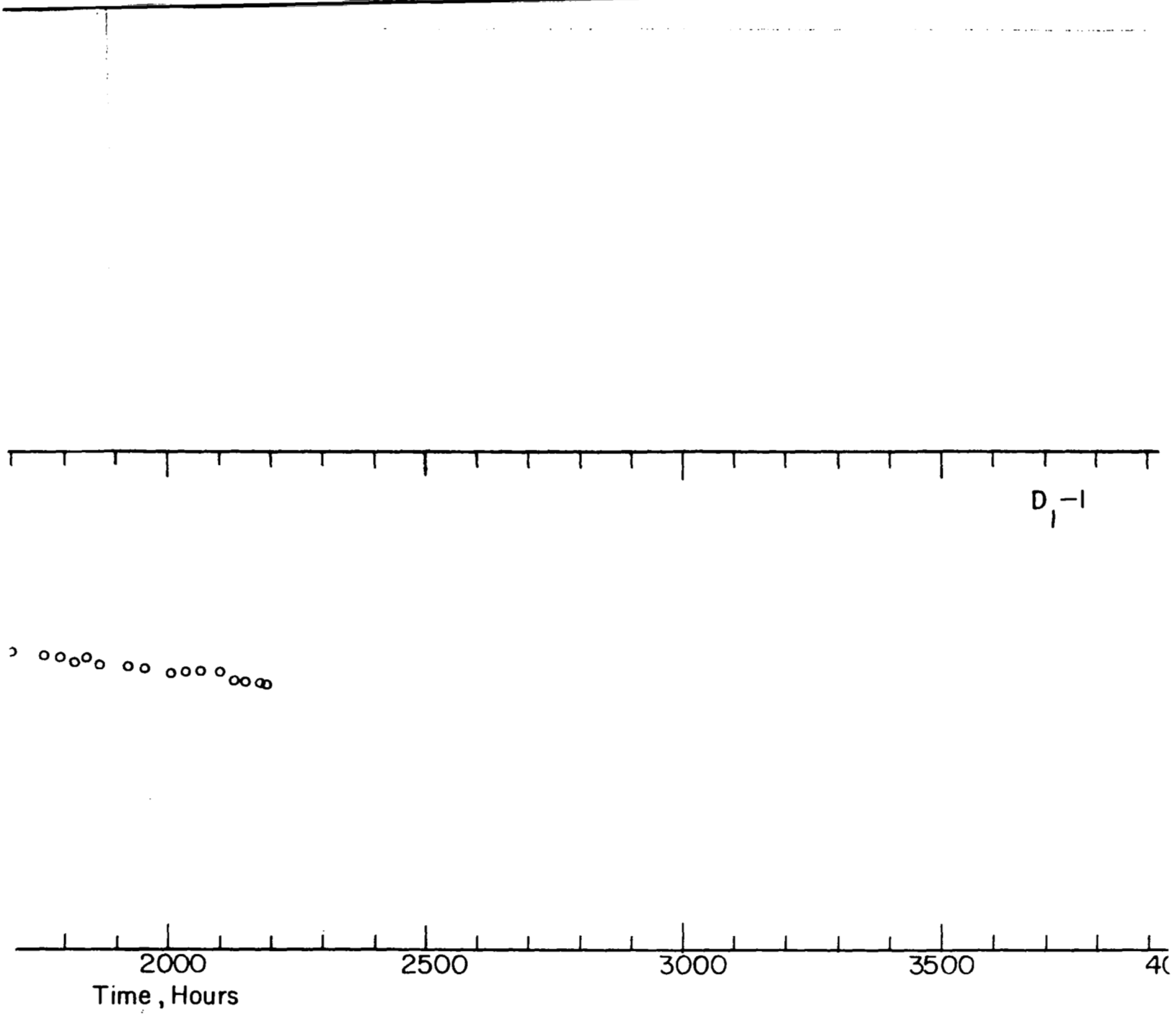

Test Data for Converter D_1-1 at T_E = 1700, 1800, 1900°K.

VII. CONCLUSIONS

Performance data from chemically vapor-deposited tungsten emitters in a series of planar converters with niobium collectors and interelectrode spacings of 8 ±0.5 mils show that the maximum power achieved at a given emitter temperature with chloride tungsten emitters is higher than that achieved with fluoride tungsten emitters. For example, at an emitter temperature of 2000 °K, the maximum power achieved with chloride tungsten is about twice that achieved with fluoride tungsten emitters. It was also found that chemical etching of fluoride tungsten makes a considerable improvement in its performance, whereas electropolishing reduces the performance of ground fluoride emitters. Additional deposition of a thin layer of chloride tungsten on the surface of fluoride tungsten improves its performance almost to the same level as etched fluoride tungsten, but not to the level of chloride tungsten. A qualitative correlation was observed among the degree of orientation, the cesiated work functions, and the performances of the emitters. Performance stability examined by life testing showed that performance is stable with respect to time for test periods up to 4000 hours at emitter temperatures up to 2030 °K.

VIII. REFERENCES

1. L. Yang and R. G. Hudson, Thermionic Conversion Specialist Conference, Houston, Texas, page 395 (1966).

2. J. W. Holland and J. Kay, Thermionic Conversion Specialist Conference, Palo Alto, California, page 10 (1967).

3a. G. Miskolczy, L. van Someren, S. S. Kitrilakis, D. Lieb, and J. H. Weinstein, "Final Report - Rhenium Thermionic Emitter Study," for Jet Propulsion Laboratory (Contract No. 950671), June 1965.

3b. L. van Someren, D. Lieb, G. Miskolczy, and S. S. Kitrilakis, "Evaluation of Thermionic Emitter Surfaces," Advanced Energy Conversion, Volume 7, pages 201-218 (1968).

4. V. C. Wilson and J. Lawrence, Thermionic Conversion Specialist Conference, Palo Alto, California, page 1 (1967).

5. "Studies of Thermionic Materials for Space Power Applications," Summary Report for the period 23 November 1965 through 31 January 1967, NASA Report No. CR-72315.

6. "Studies of Thermionic Materials for Space Power Applications," Semi-Annual Report for the period 1 February 1967 through 31 July 1967, NASA Report No. CR-72327.

7. Jun, C. K. and Hoch, M., "Thermal Conductivity of Tantalum, Tungsten, Rhenium, Ta-10W, T_{111}, T_{222}, W-25Re in the Temperature Range 1500 - 2800°K, Technical Report AFML-TR-66-367, November 1966.

8. "Applied Thermionic Research," First Quarterly Progress Report for the period 4 December 1967 through 4 March 1968, TECO Report No. 4092/3-123-68.

9. "Applied Thermionic Research," Second Quarterly Progress Report for the period 4 March 1968 through 4 June 1968, TECO Report No. 4092/3-183-68.

10. Gulf General Atomic Report No. GA8956, covering the period February 1, 1967 through July 31, 1969. Contract NAS3-8504.

APPENDIX A

MASS SPECTROMETRIC DATA OF CONVERTER D_1-1 DURING OUTGASSING

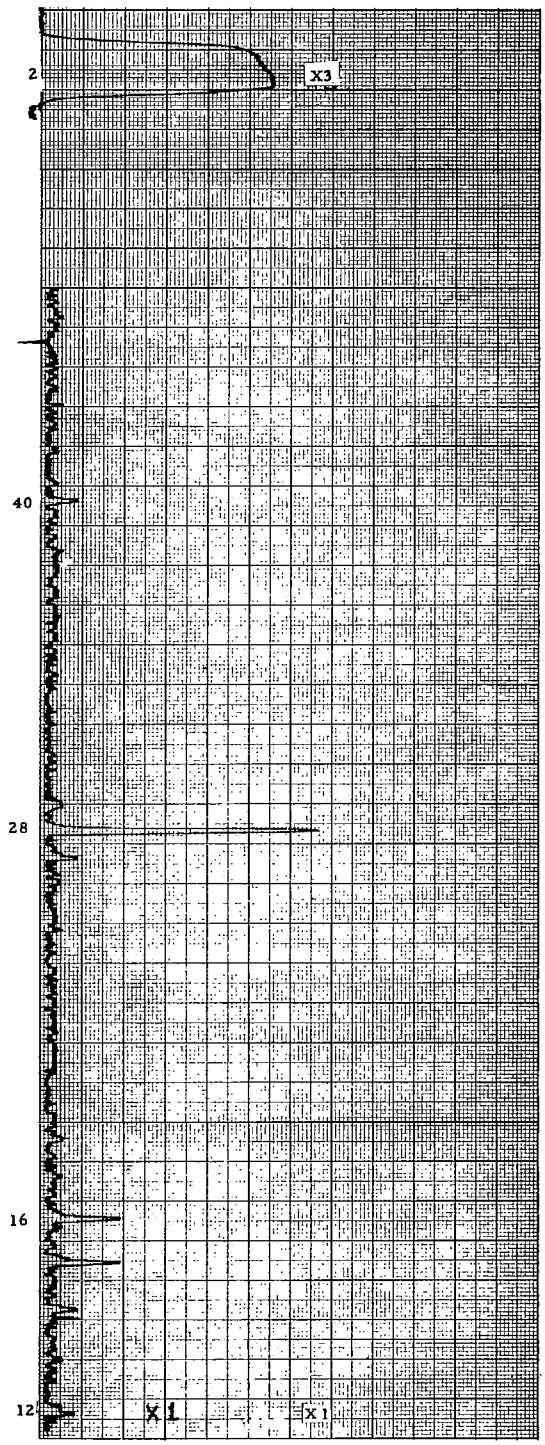

Figure A-1. Background.

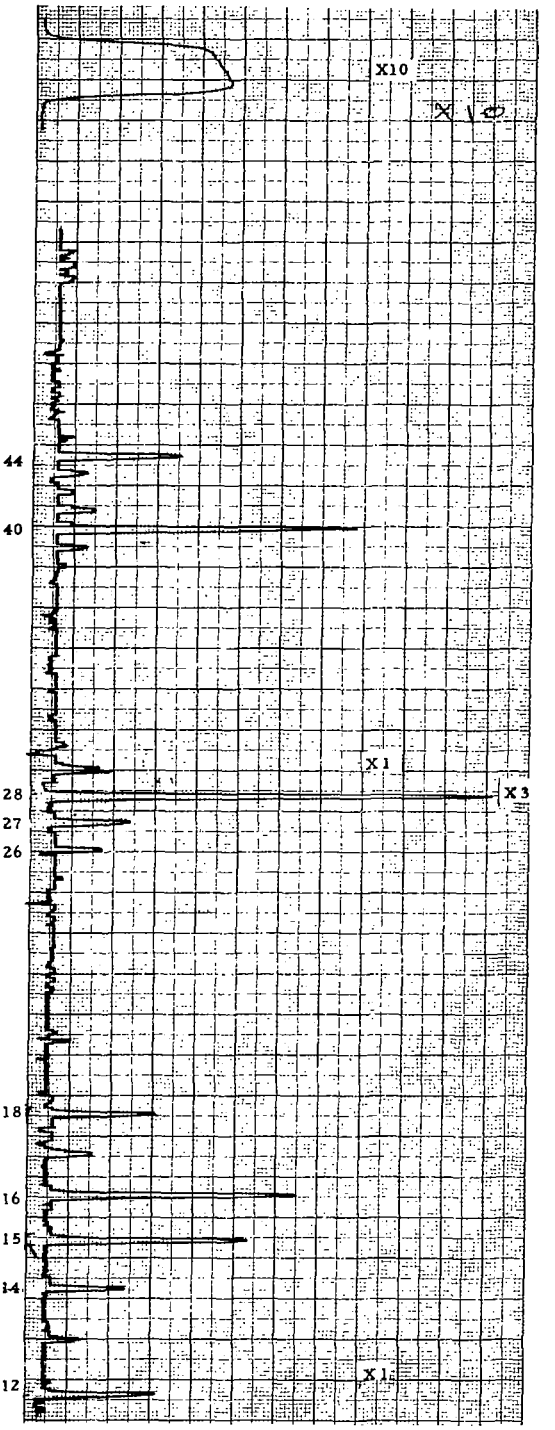

Figure A-2. Start of Heating Collector and Cesium Reservoir.

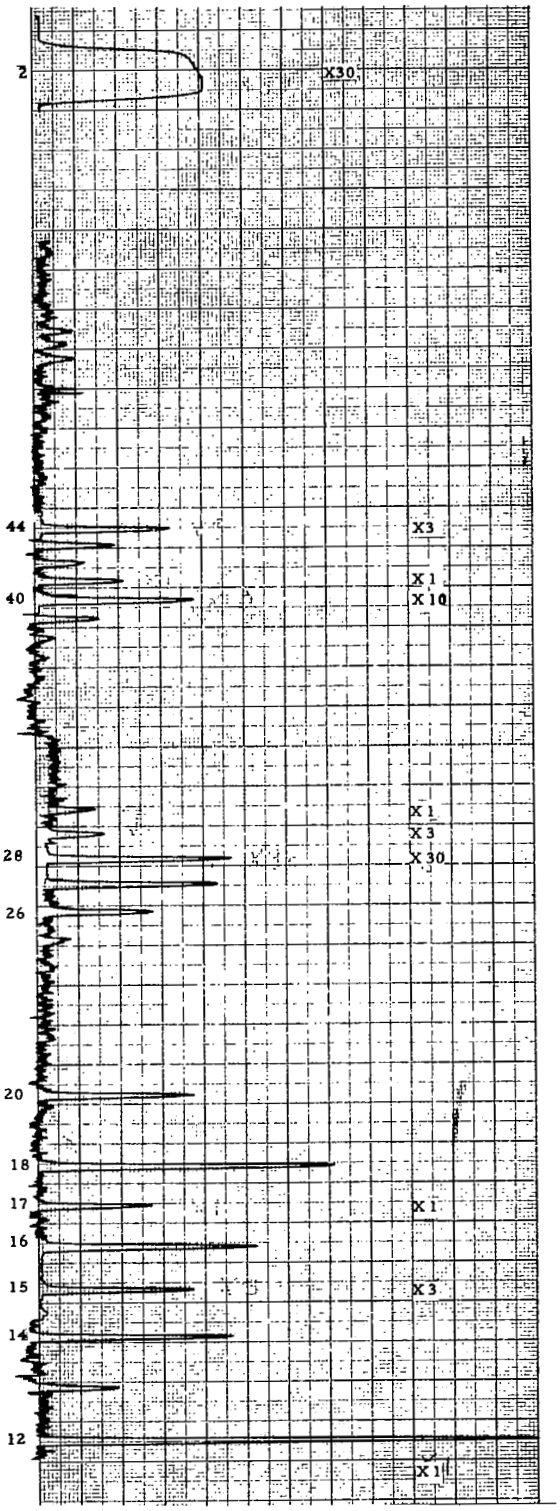

Figure A-3. Collector Temperature at 400°C and Cesium Reservoir Temperature at 275°C.

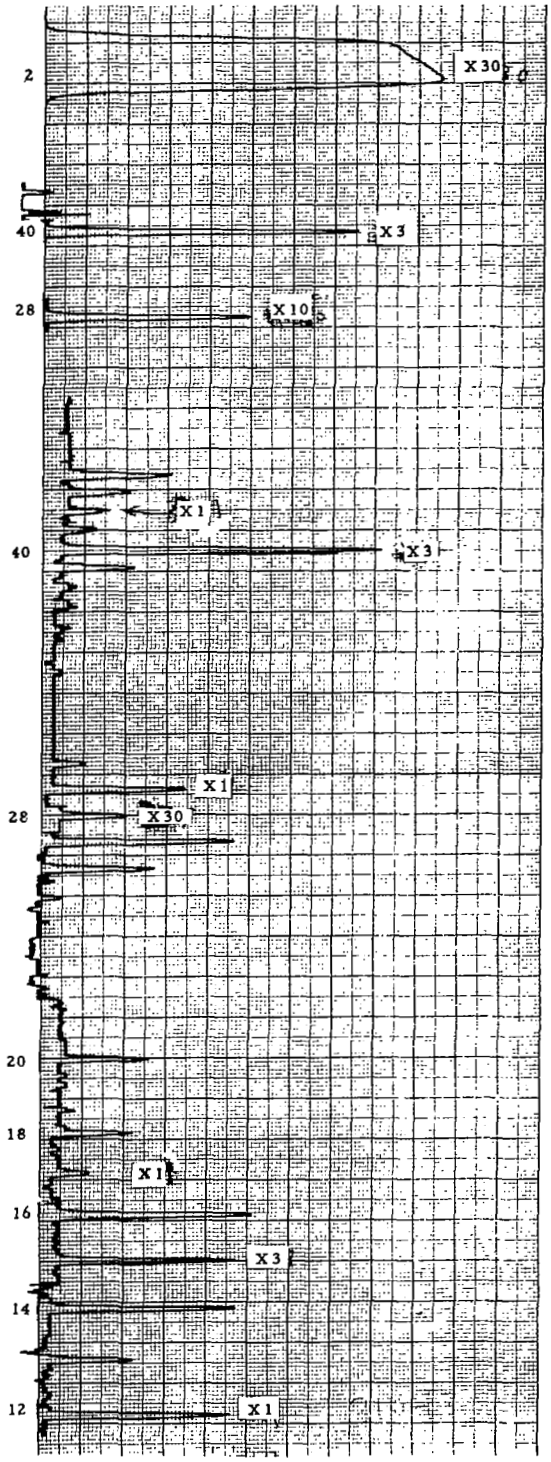

Figure A-4. Collector Temperature at 700°C and Cesium Reservoir Temperature at 400°C.

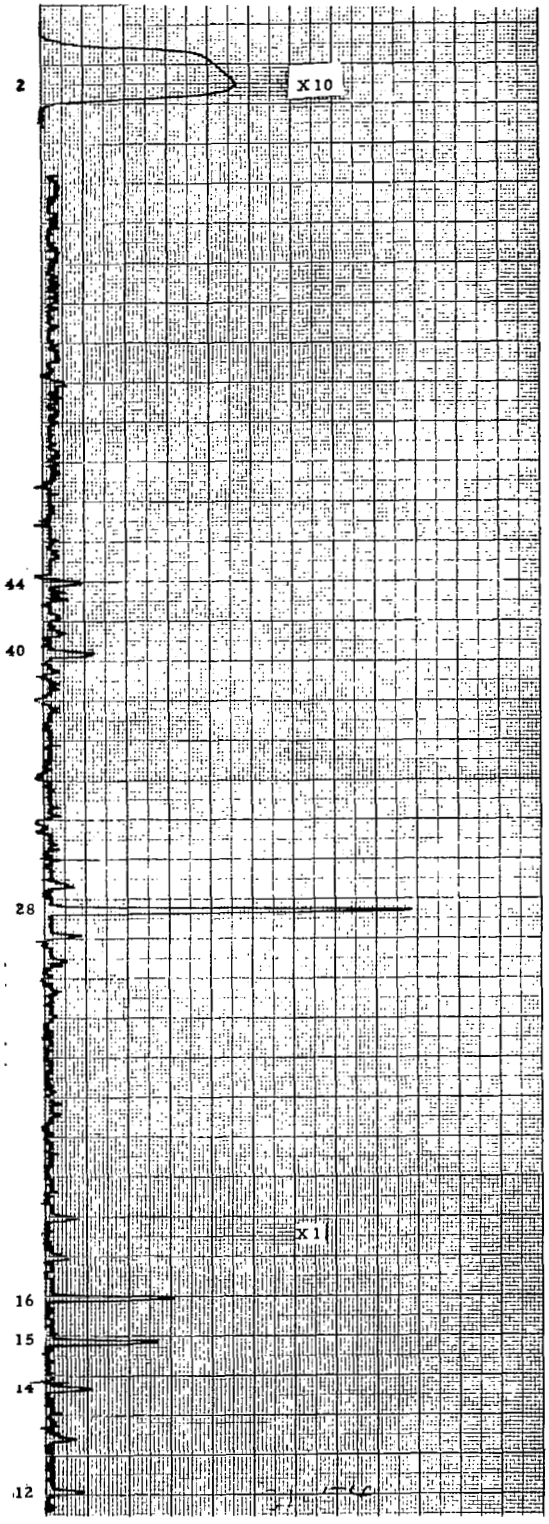

Figure A-5. Before Heating Up Emitter.

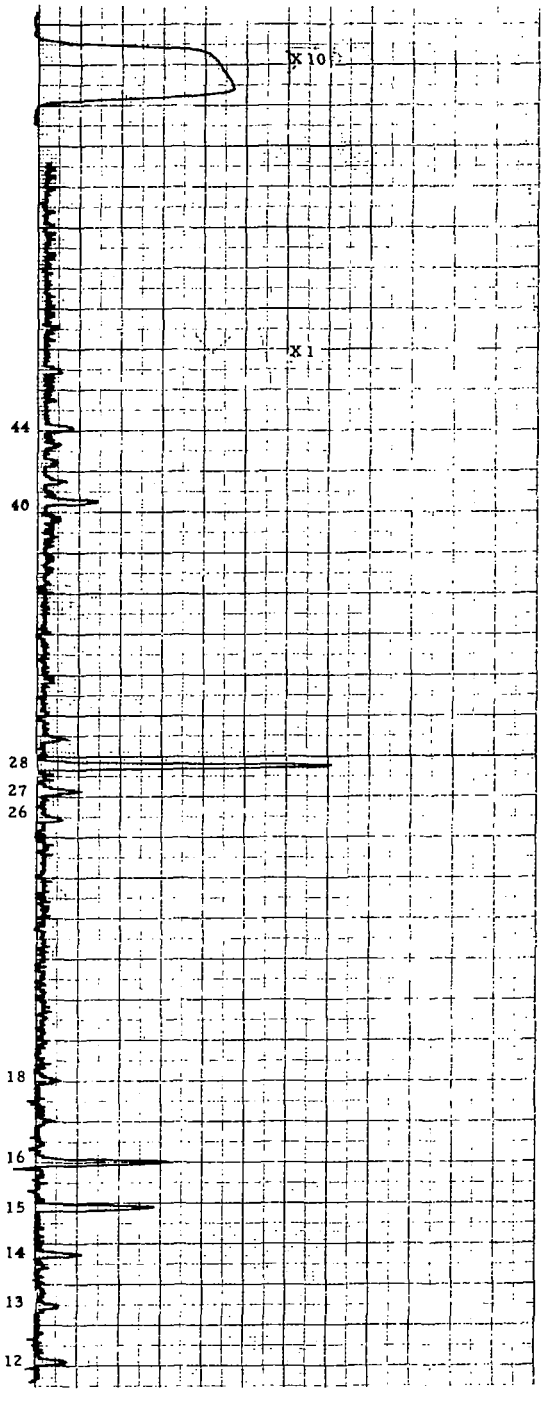

Figure A-6. Emitter Temperature up to 1700°C.

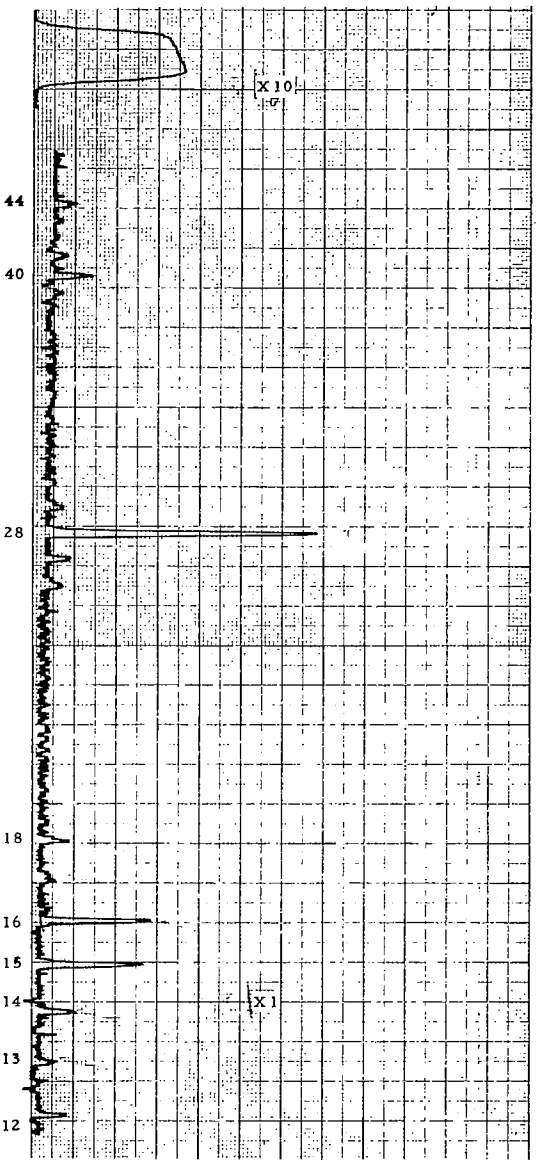

Figure A-7. End of Outgassing.

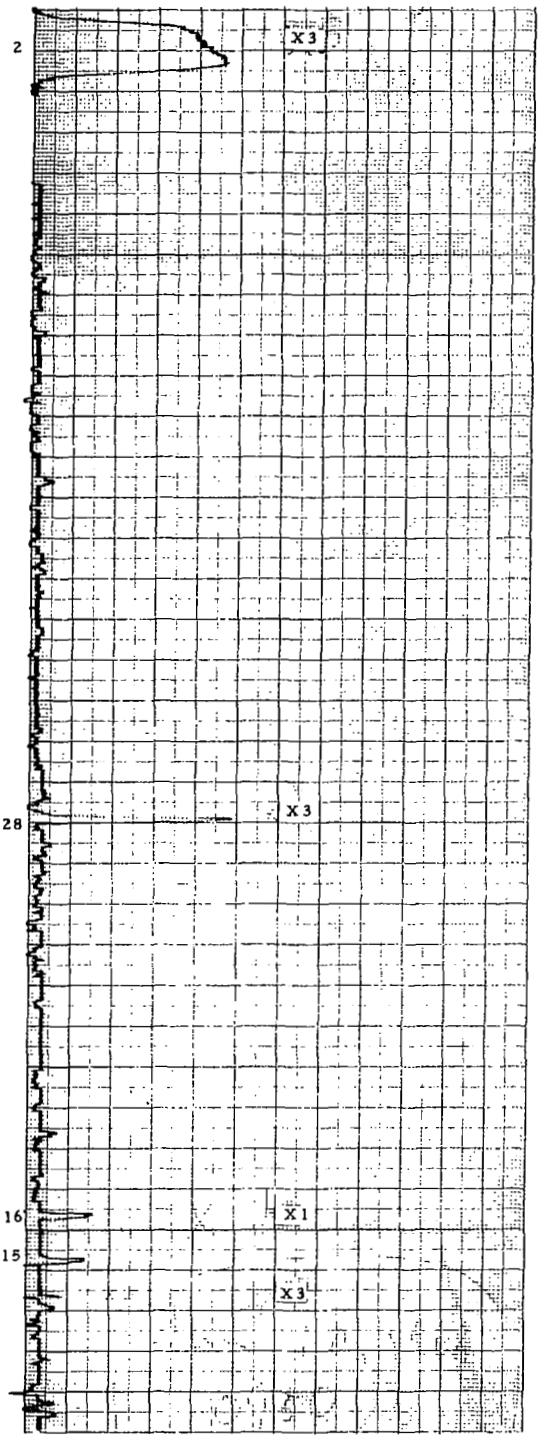

Figure A-8. Cool Converter After Outgassing.

APPENDIX B

CONVERTER CESIUM TEMPERATURE FAMILIES BEFORE LIFE TEST

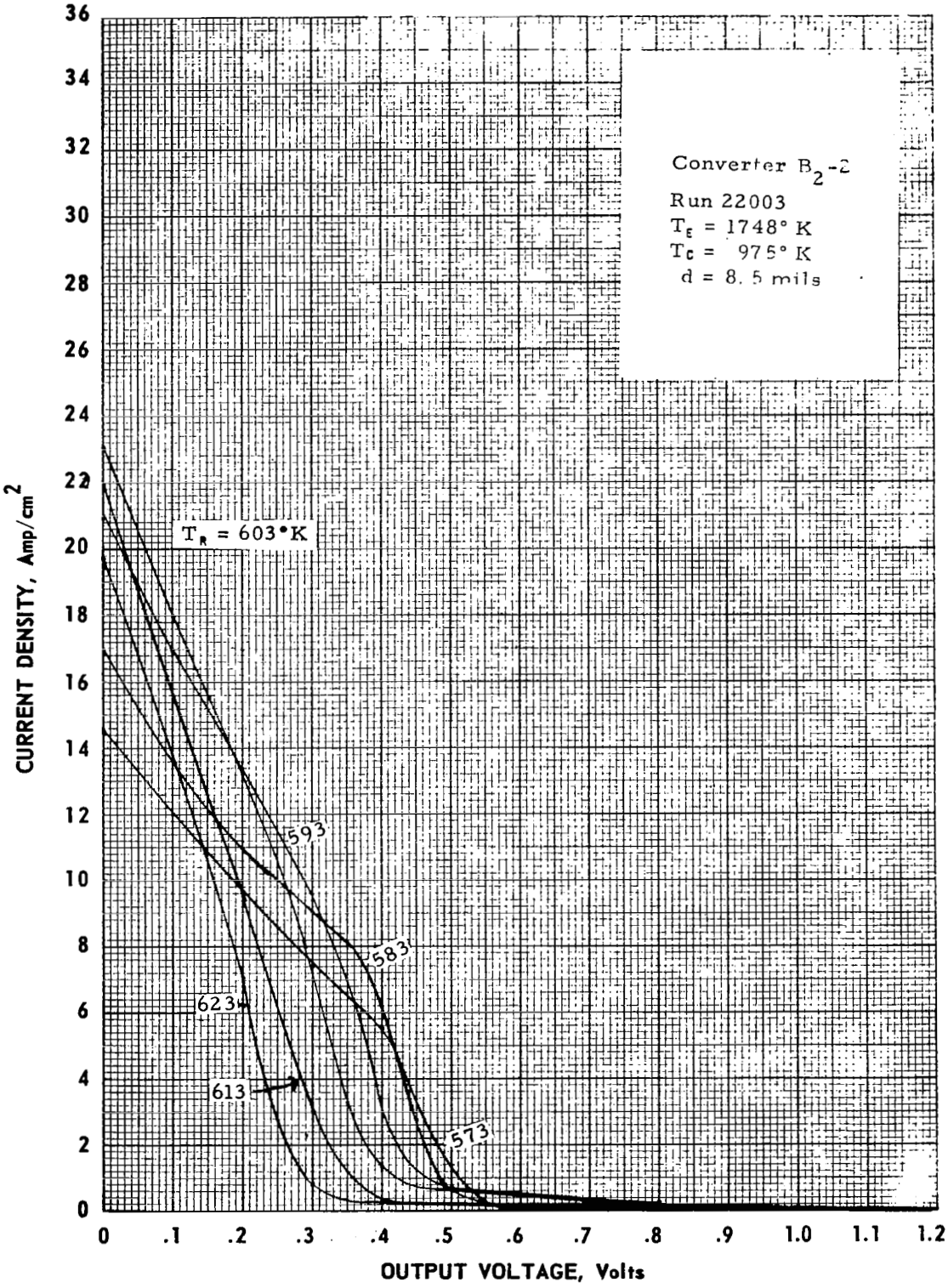

Figure B-1 Cesium-Temperature Family of Converter B_2-2 at T_E = 1748° K

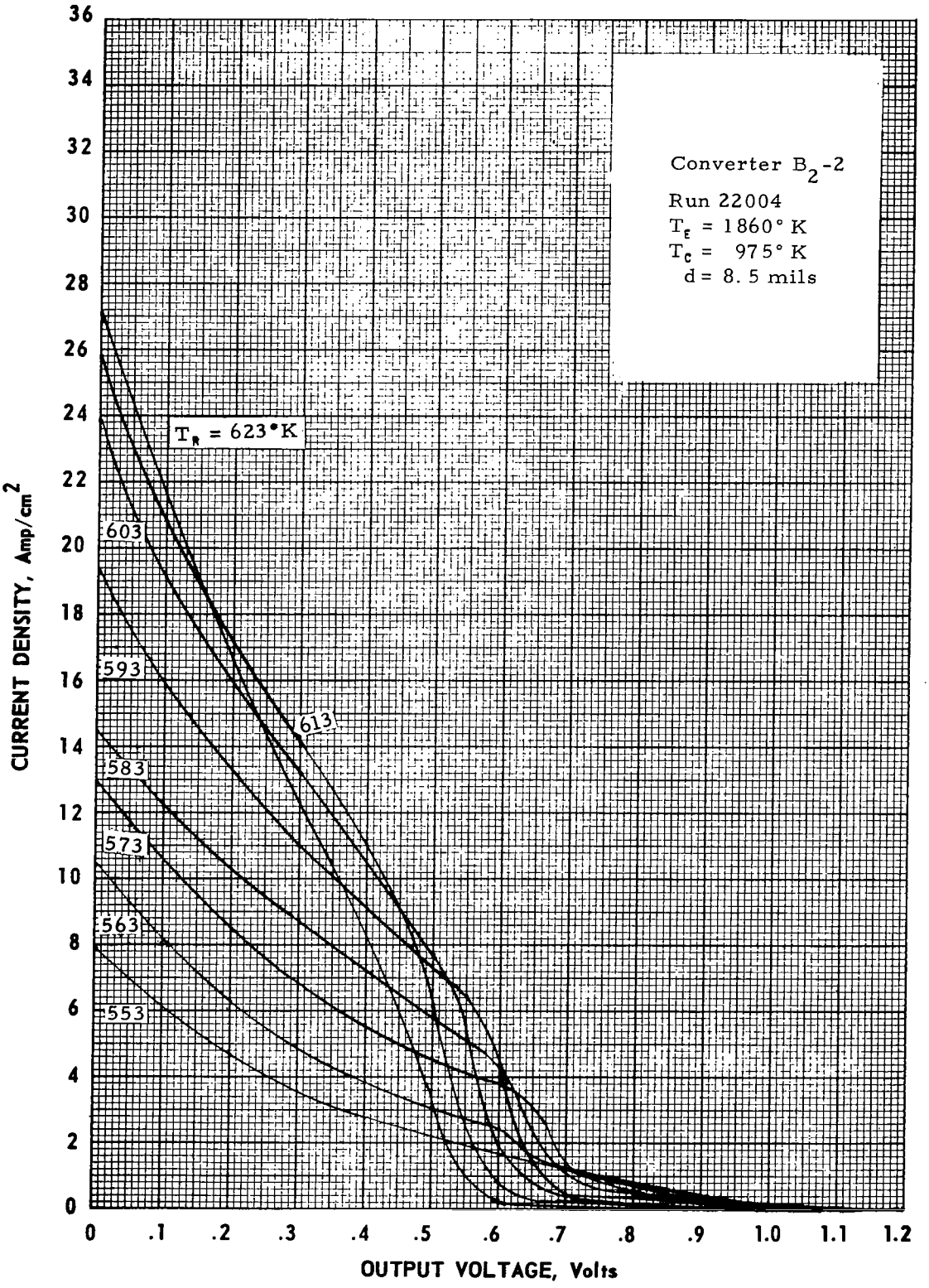

Figure B-2 Cesium-Temperature Family of Converter B_2-2 at T_E = 1860° K.

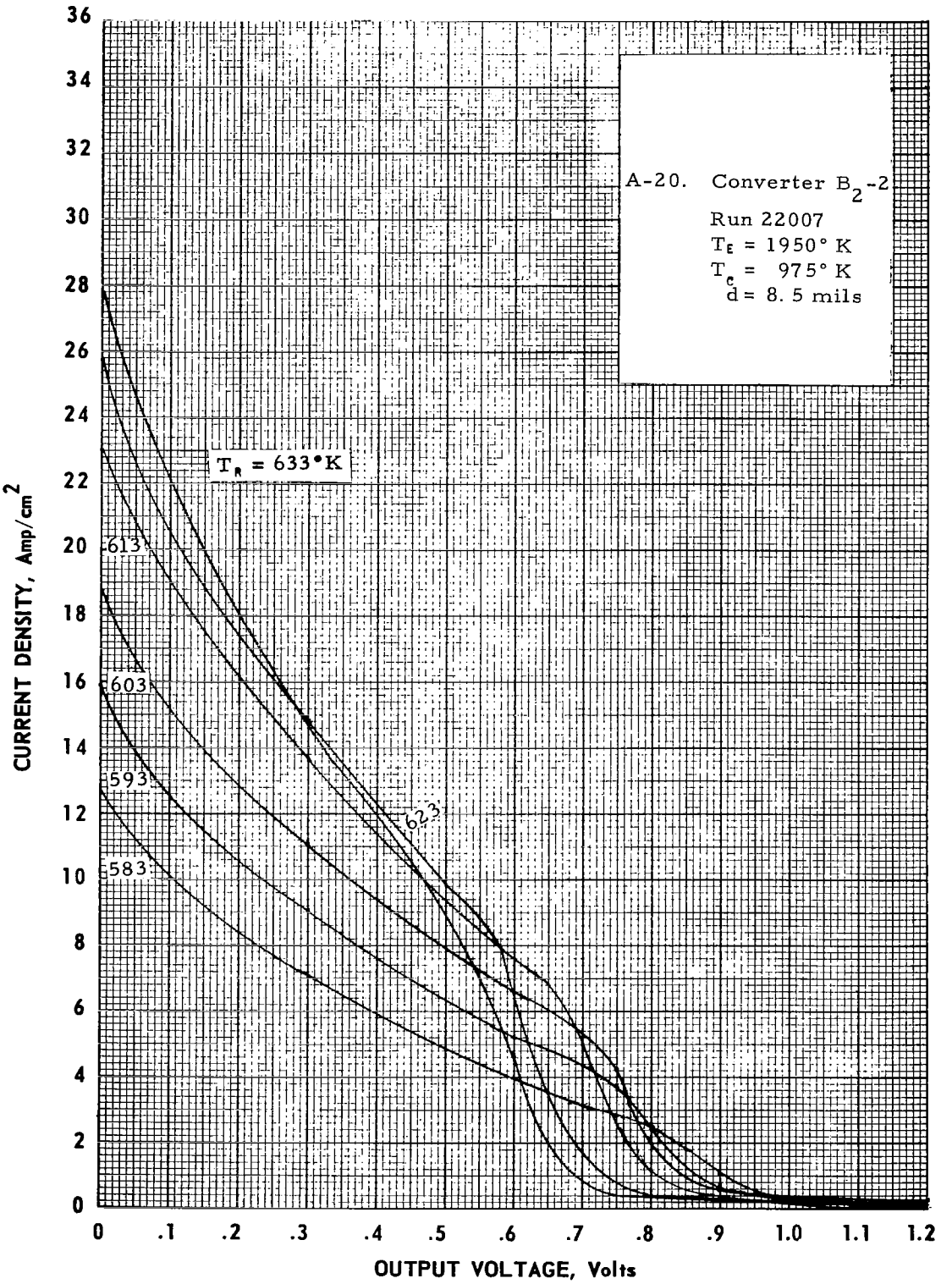

Figure B-3 Cesium-Temperature Family of Converter B_2-2 at T_E = 1950° K

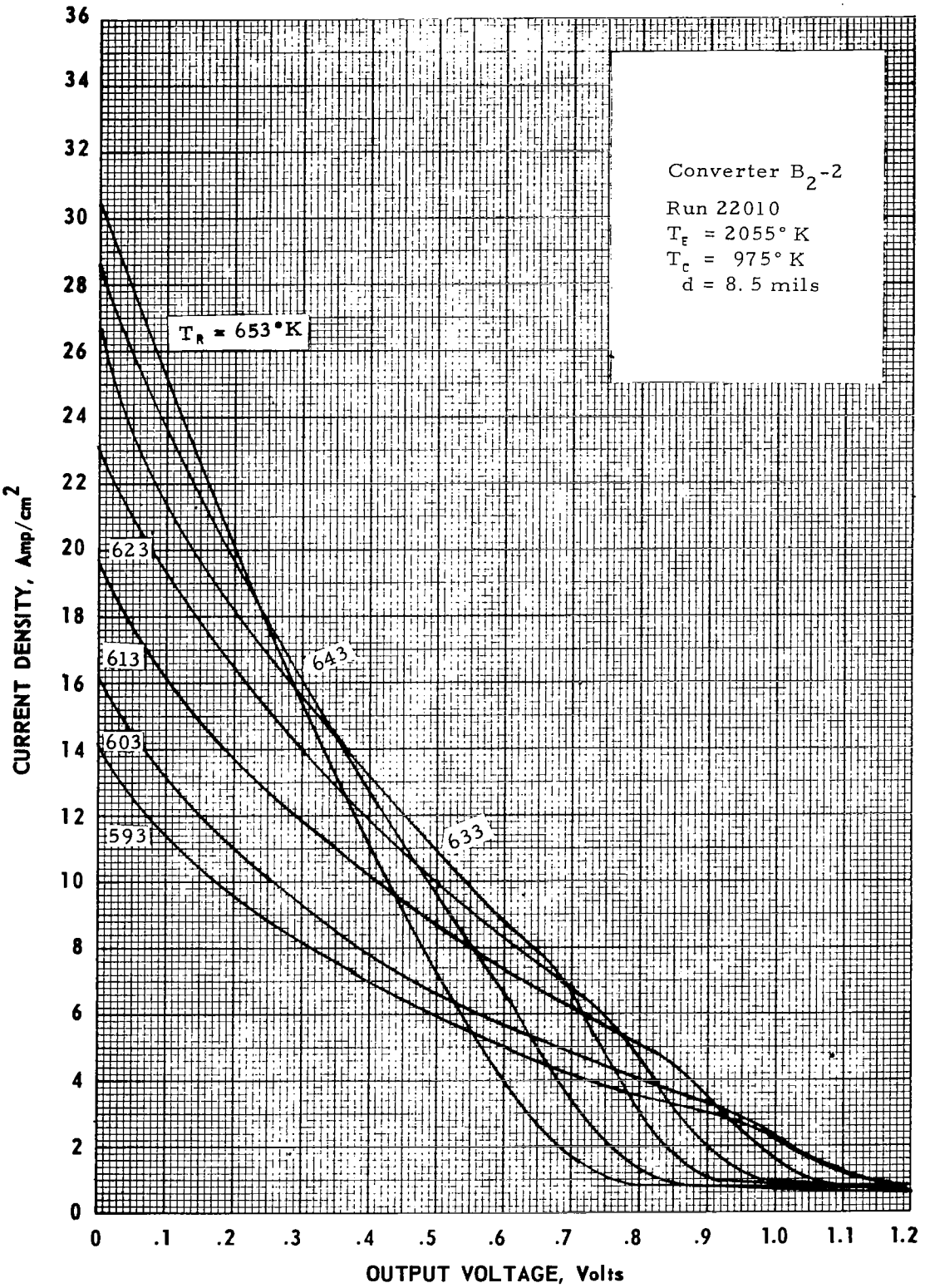

Figure B-4 Cesium-Temperature Family of Converter B_2-2 at T_E = 2055° K.

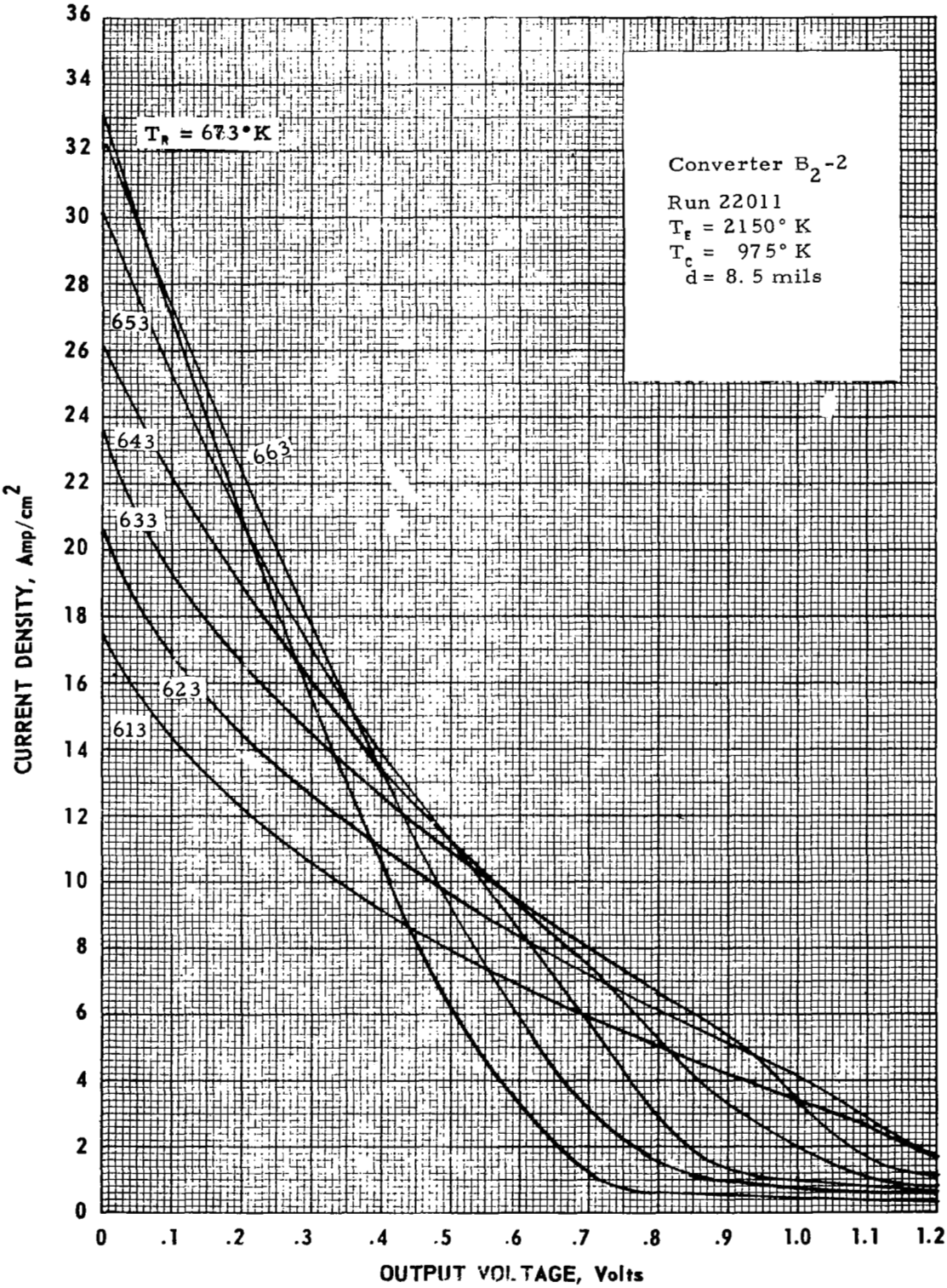

Figure B-5 Cesium-Temperature Family of Converter B_2-2 at T_E = 2150° K.

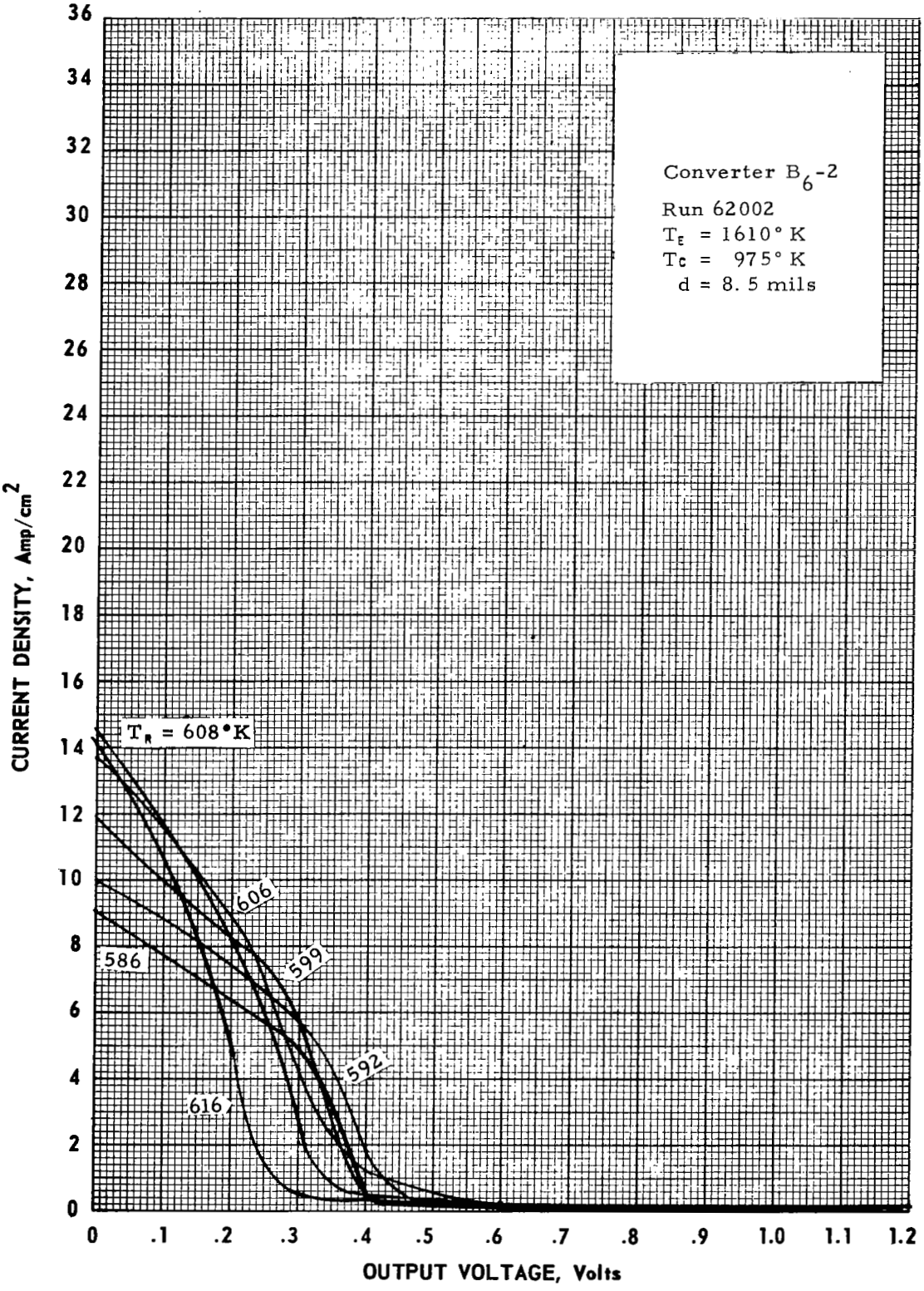

Figure B-6. Cesium-Temperature Family of Converter B_6-2 at T_E = 1610° K.

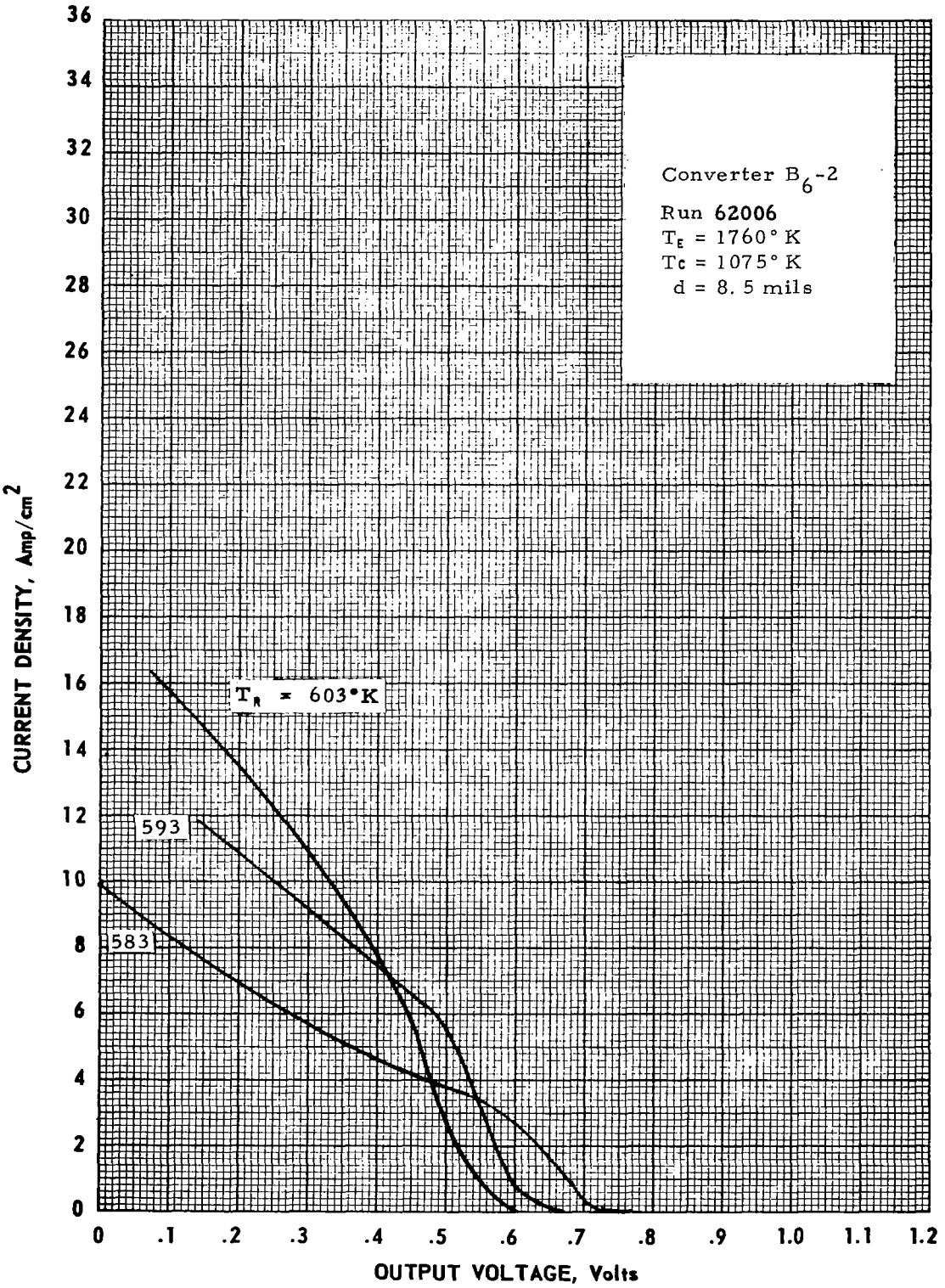

Figure B-7. Cesium-Temperature Family of Converter B_6-2 at T_E = 1760° K.

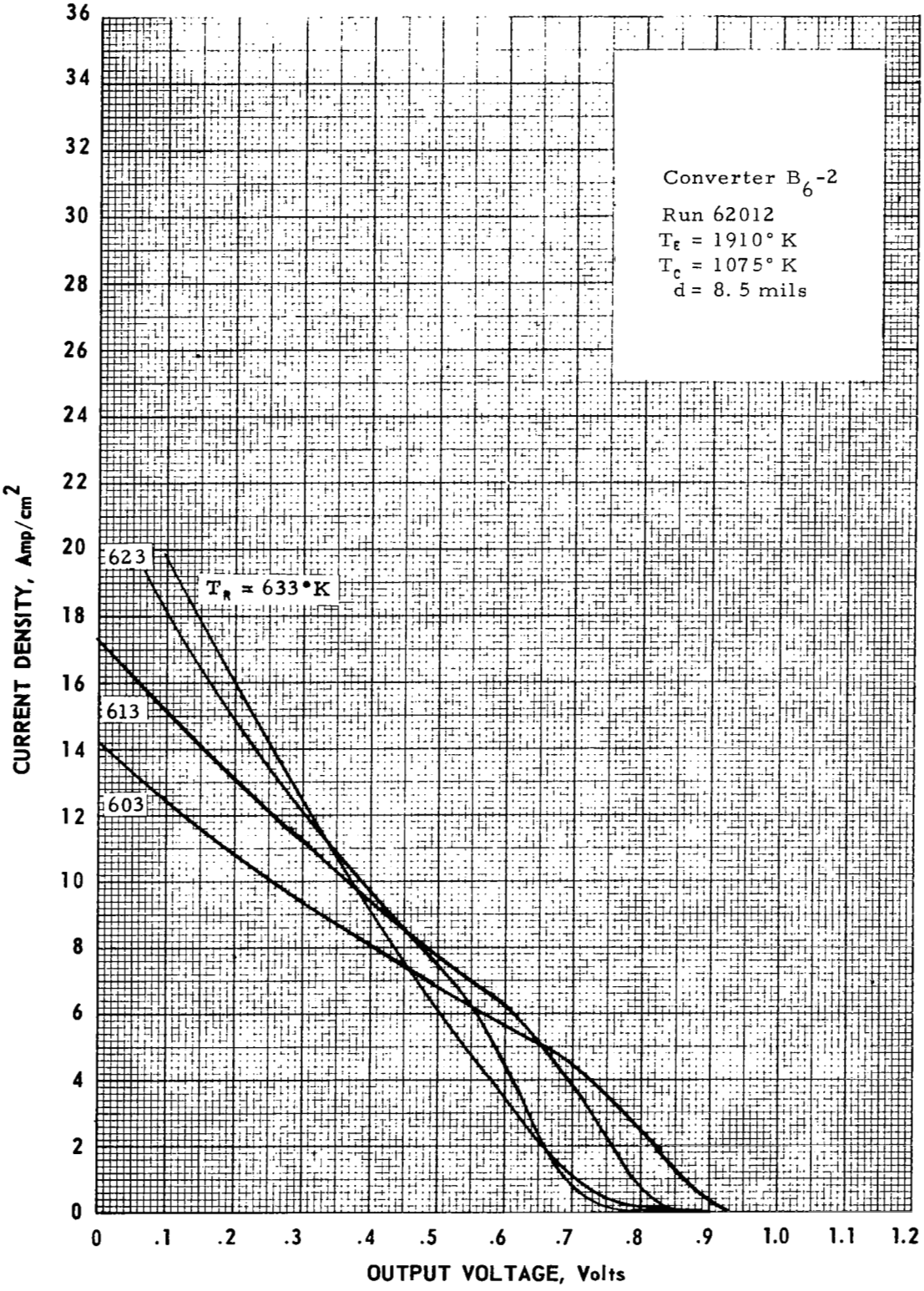

Figure B-8. Cesium-Temperature Family of Converter B_6-2 at T_E = 1910° K.

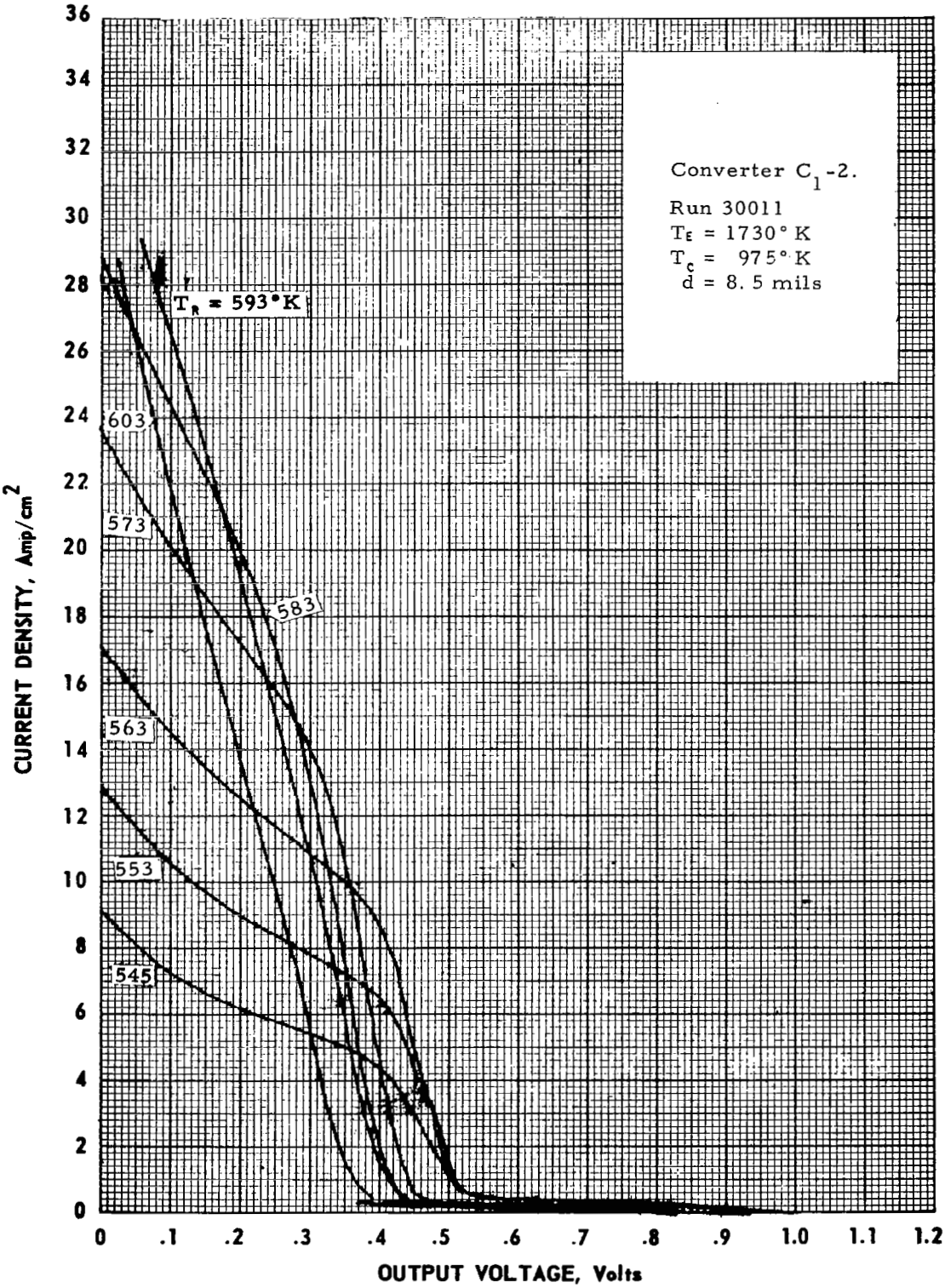

Figure B-9. Cesium-Temperature Family of Converter C_1-2 at T_E = 1730° K.

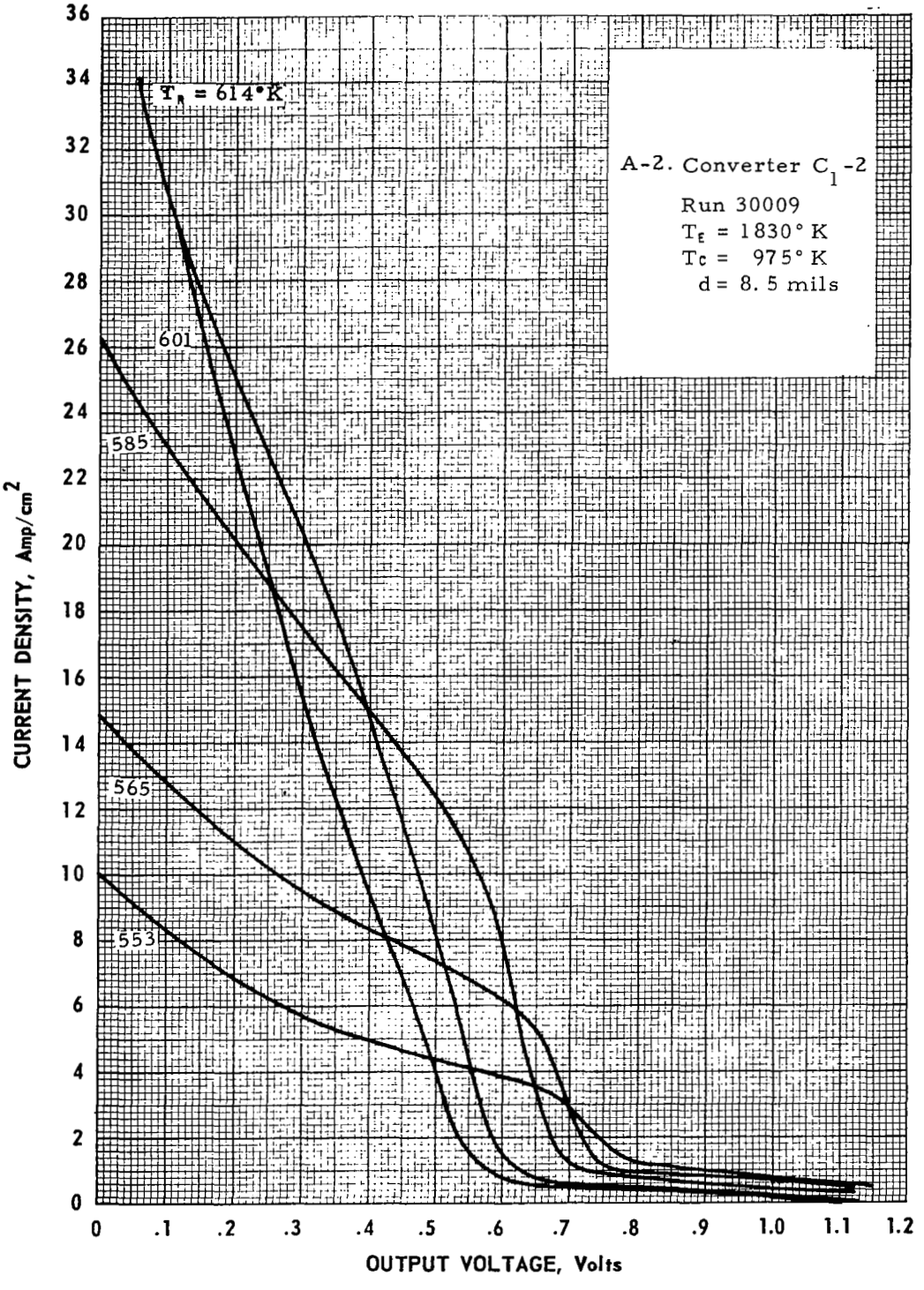

Figure B-10. Cesium-Temperature Family of Converter C_1-2 at T_E = 1830° K.

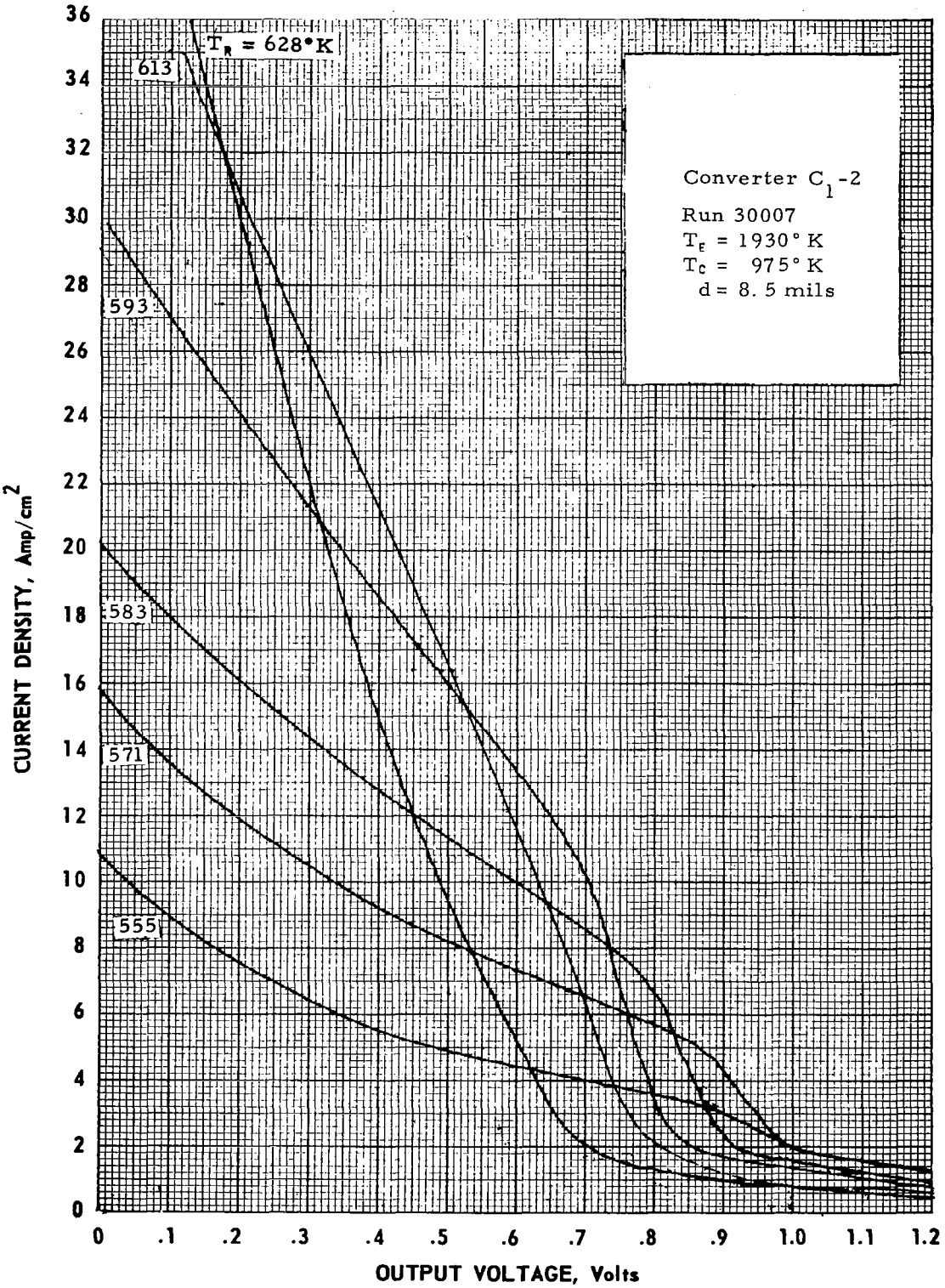

Figure B-11. Cesium-Temperature Family of Converter C_1-2 at T_E = 1930° K.

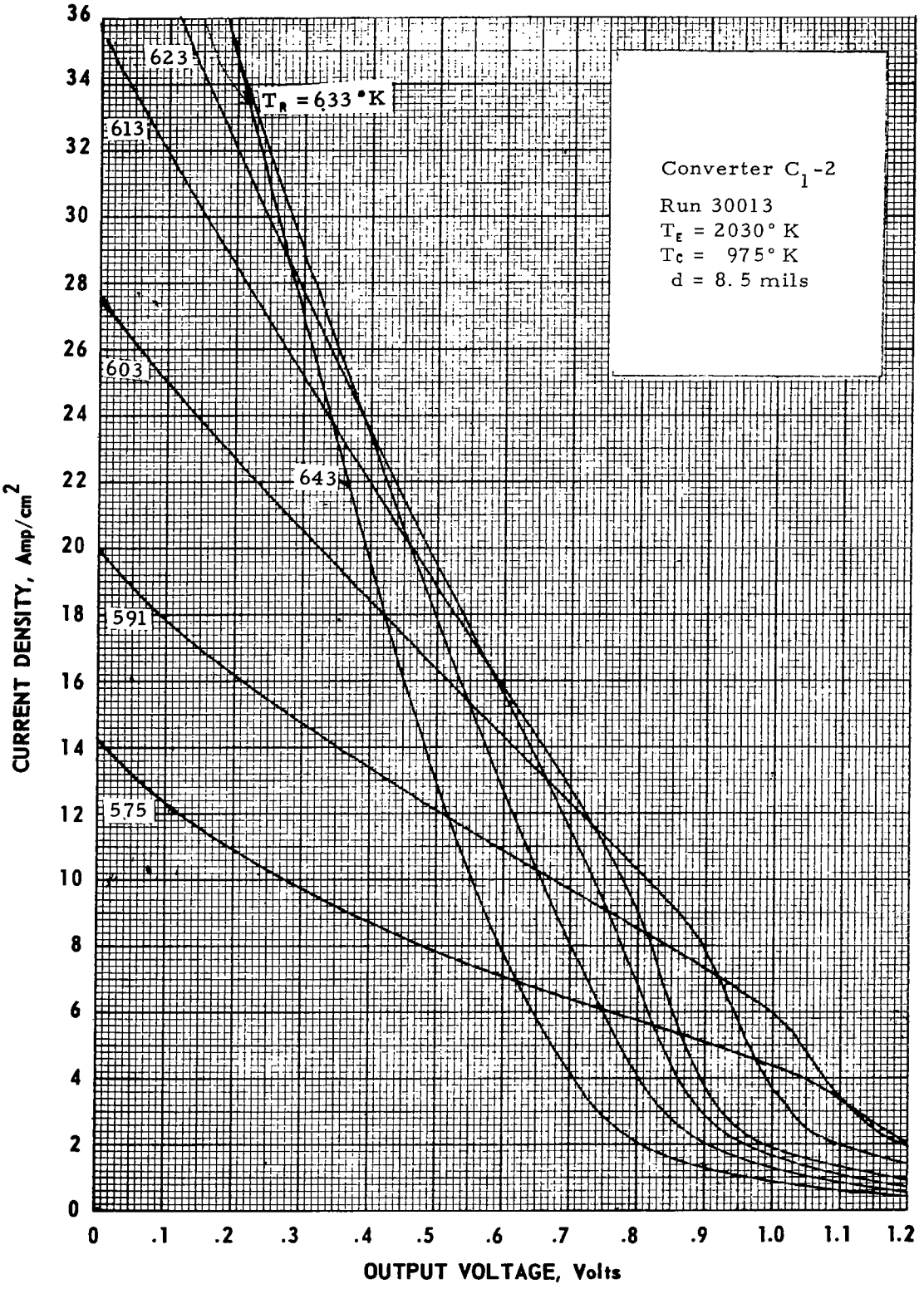

Figure B-12. Cesium-Temperature Family of Converter C_1-2 at T_E = 2030° K.

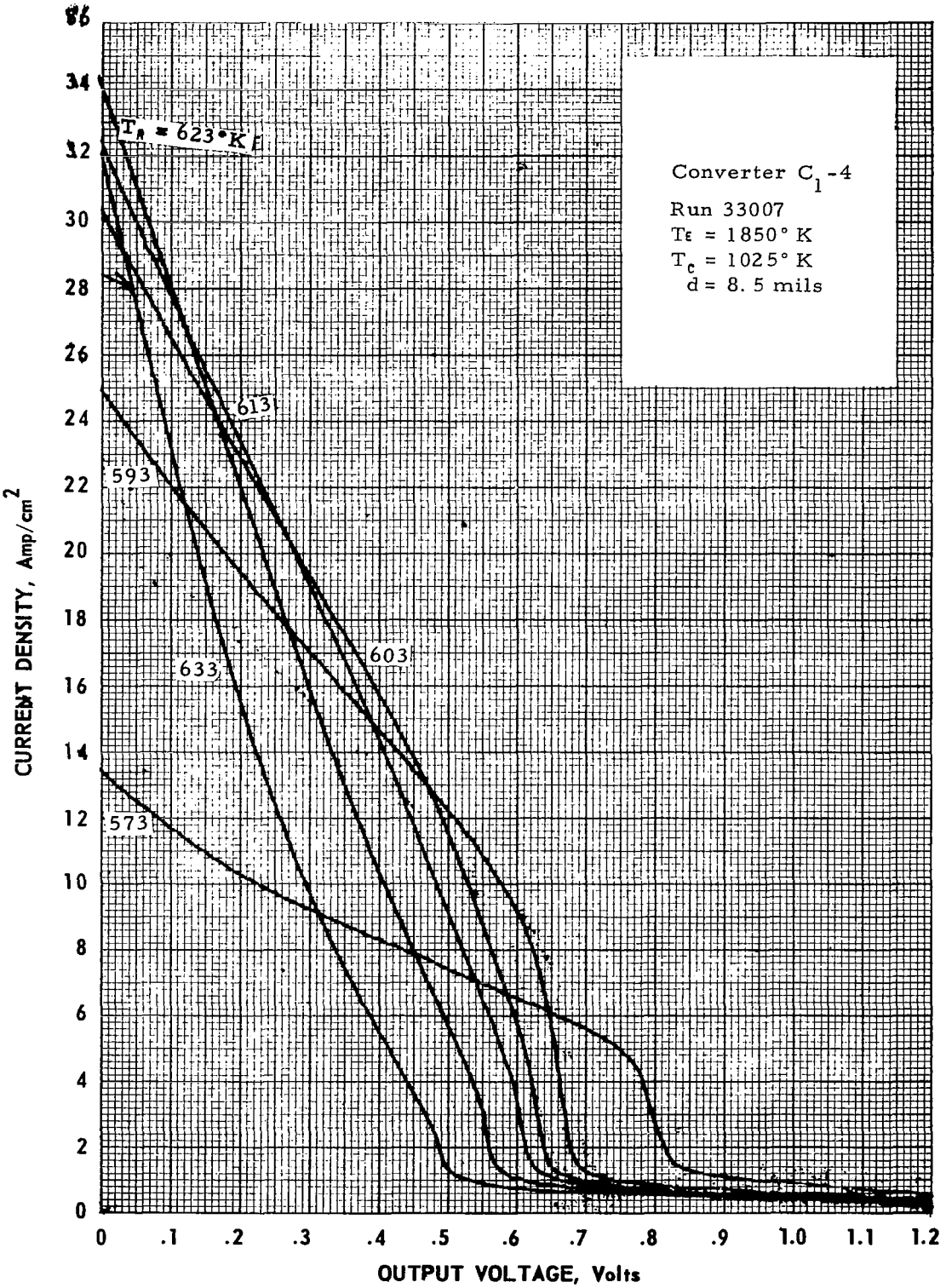

Figure B-15. Cesium-Temperature Family of Converter C_1-4 at T_E = 1850° K.

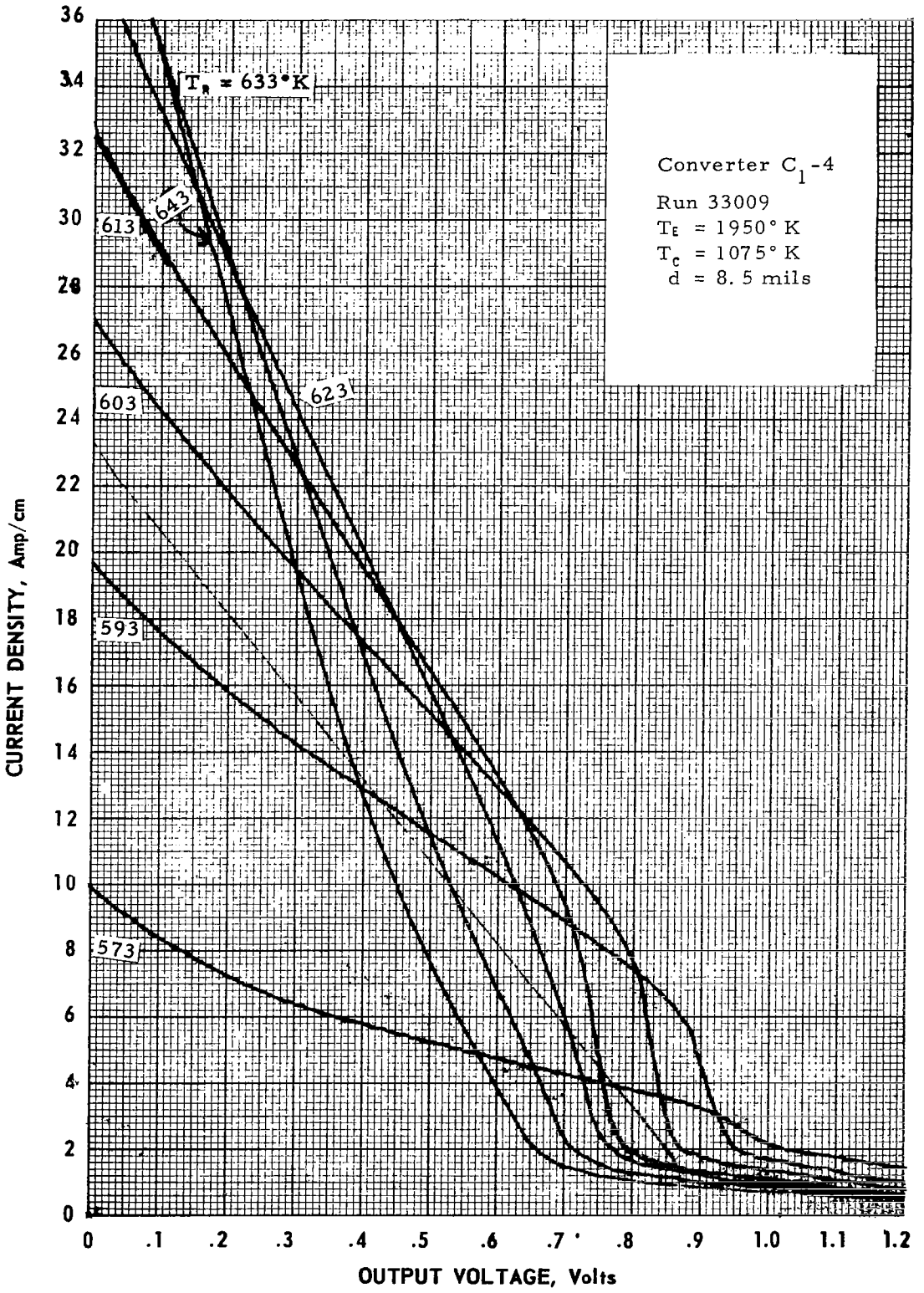

Figure B-16 Cesium-Temperature Family of Converter C_1-4 at T_E = 1950° K.

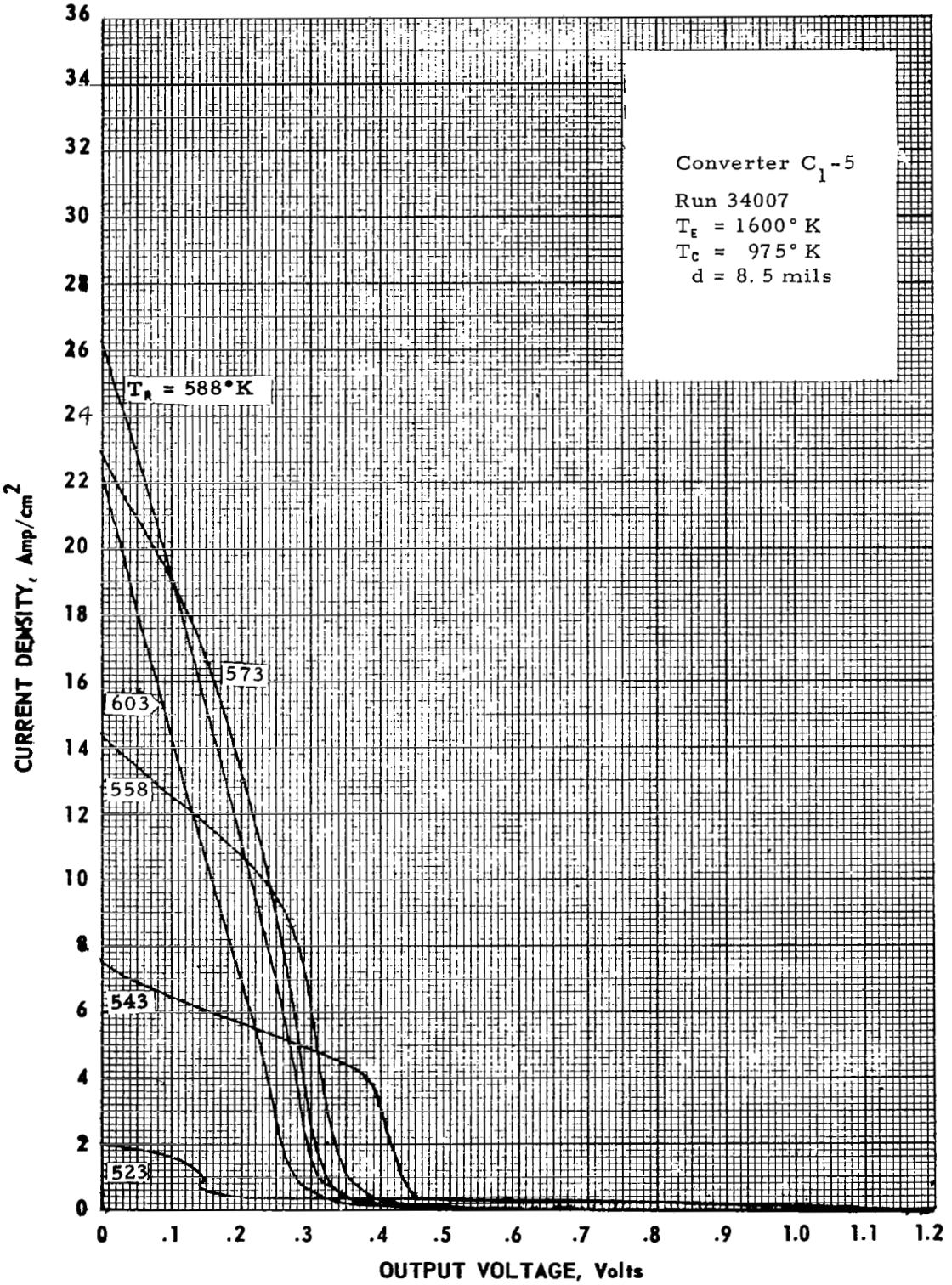

Figure B-17. Cesium-Temperature Family of Converter C_1-5 at T_E = 1600° K.

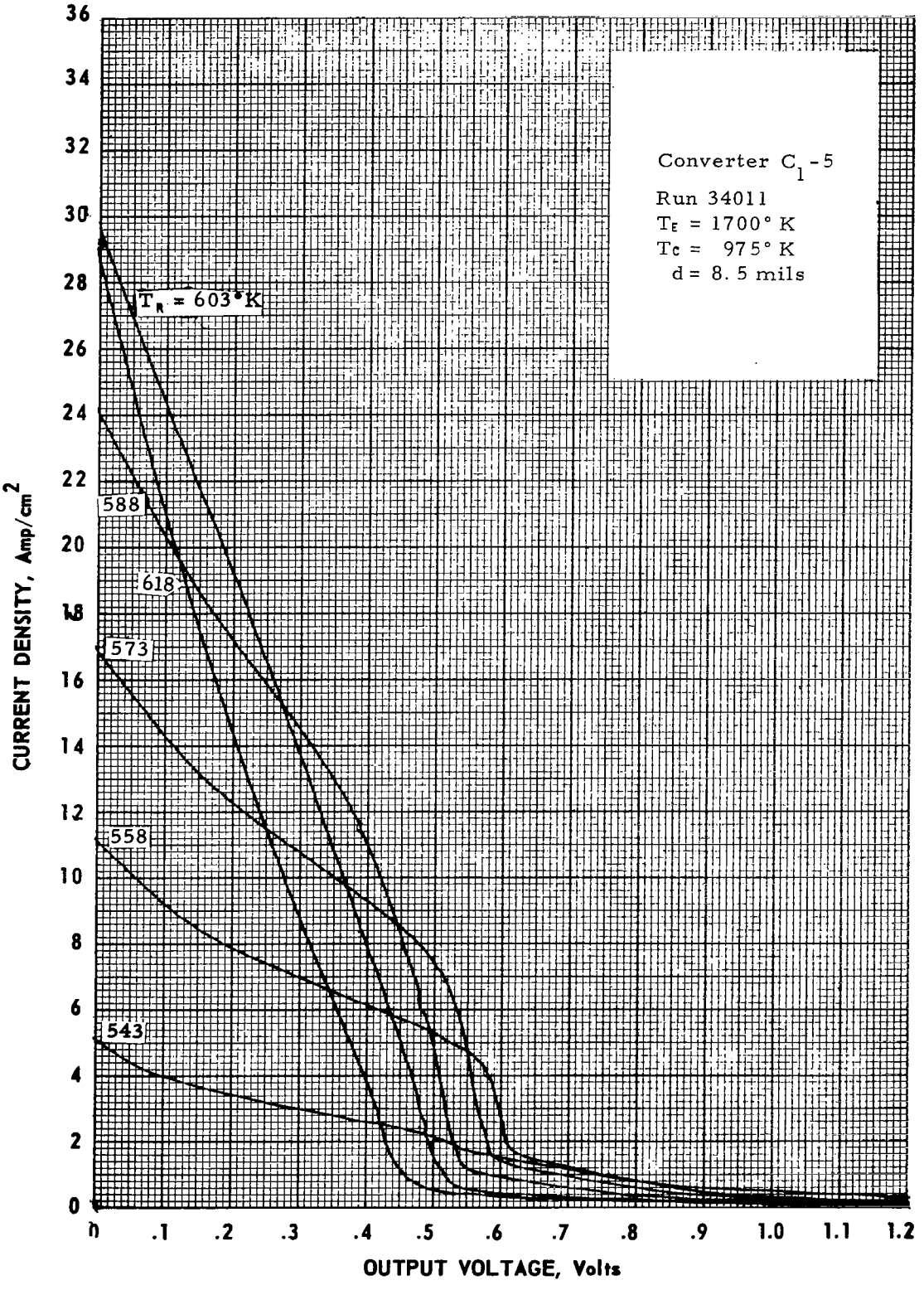

Figure B-18. Cesium-Temperature Family of Converter C_1-5 at T_E = 1700° K

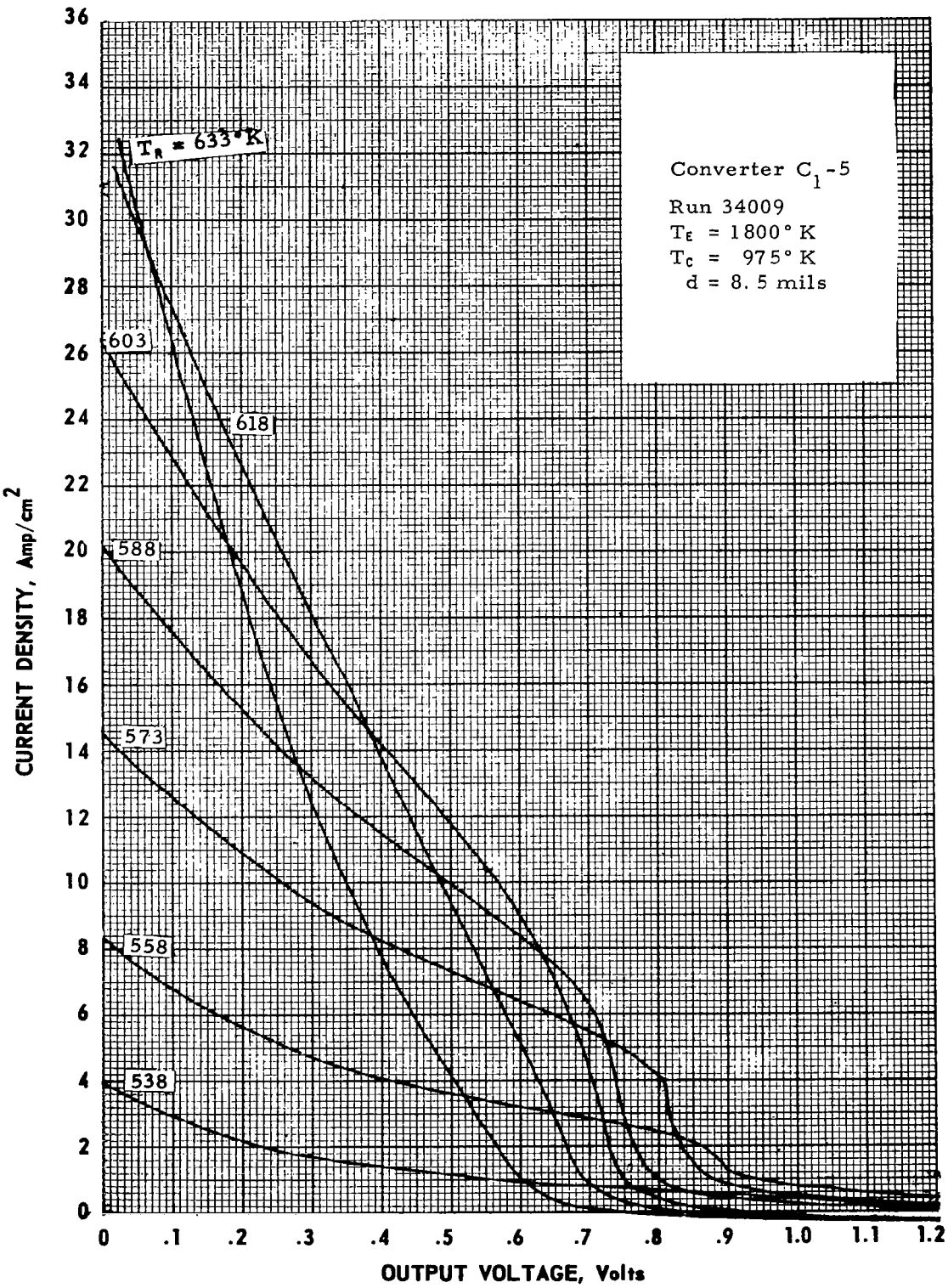

Figure B-19. Cesium-Temperature Family of Converter C_1-5 at T_E = 1800° K.

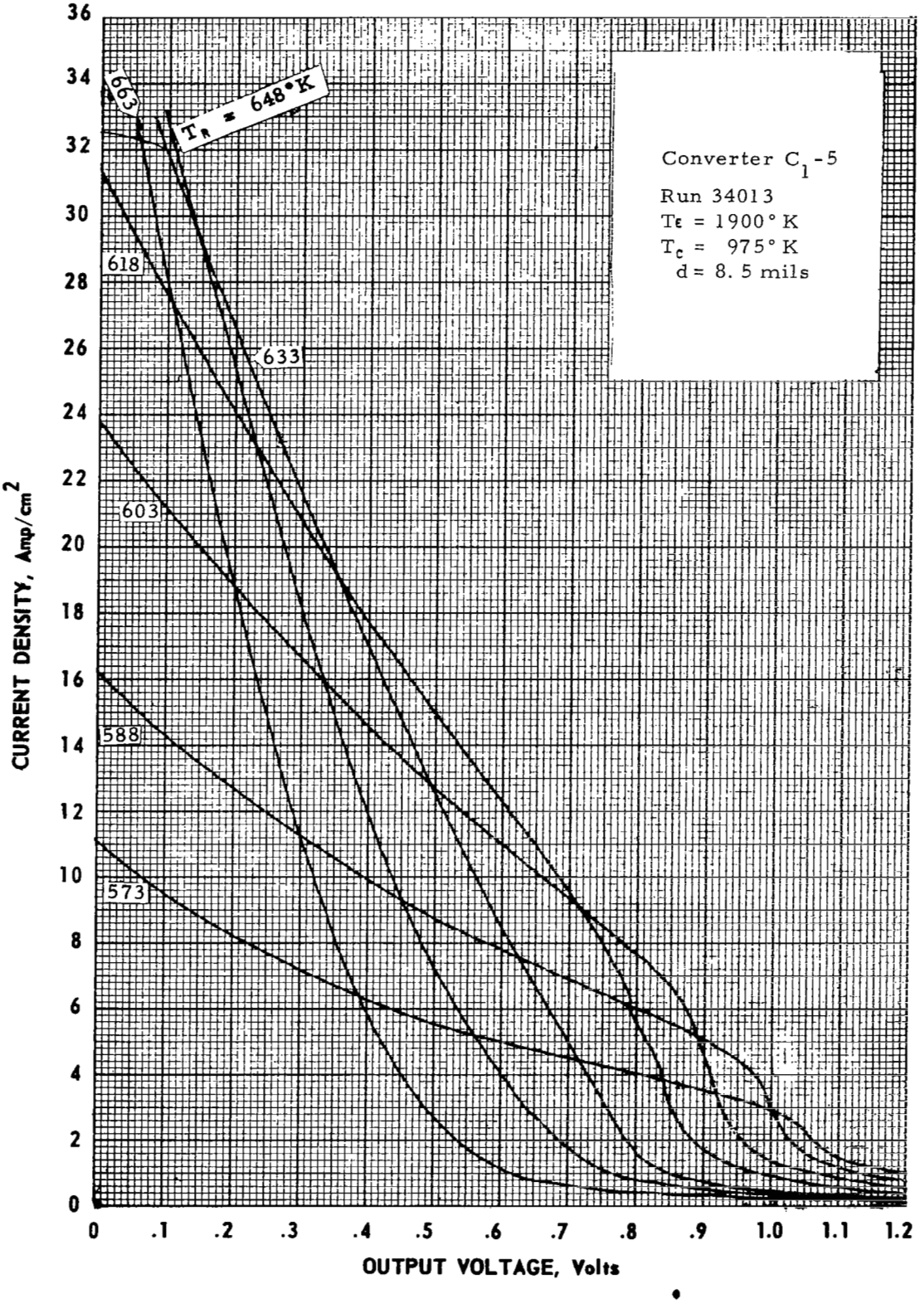

Figure B-20. Cesium-Temperature Family of Converter C_1-5 at T_ε = 1900° K.

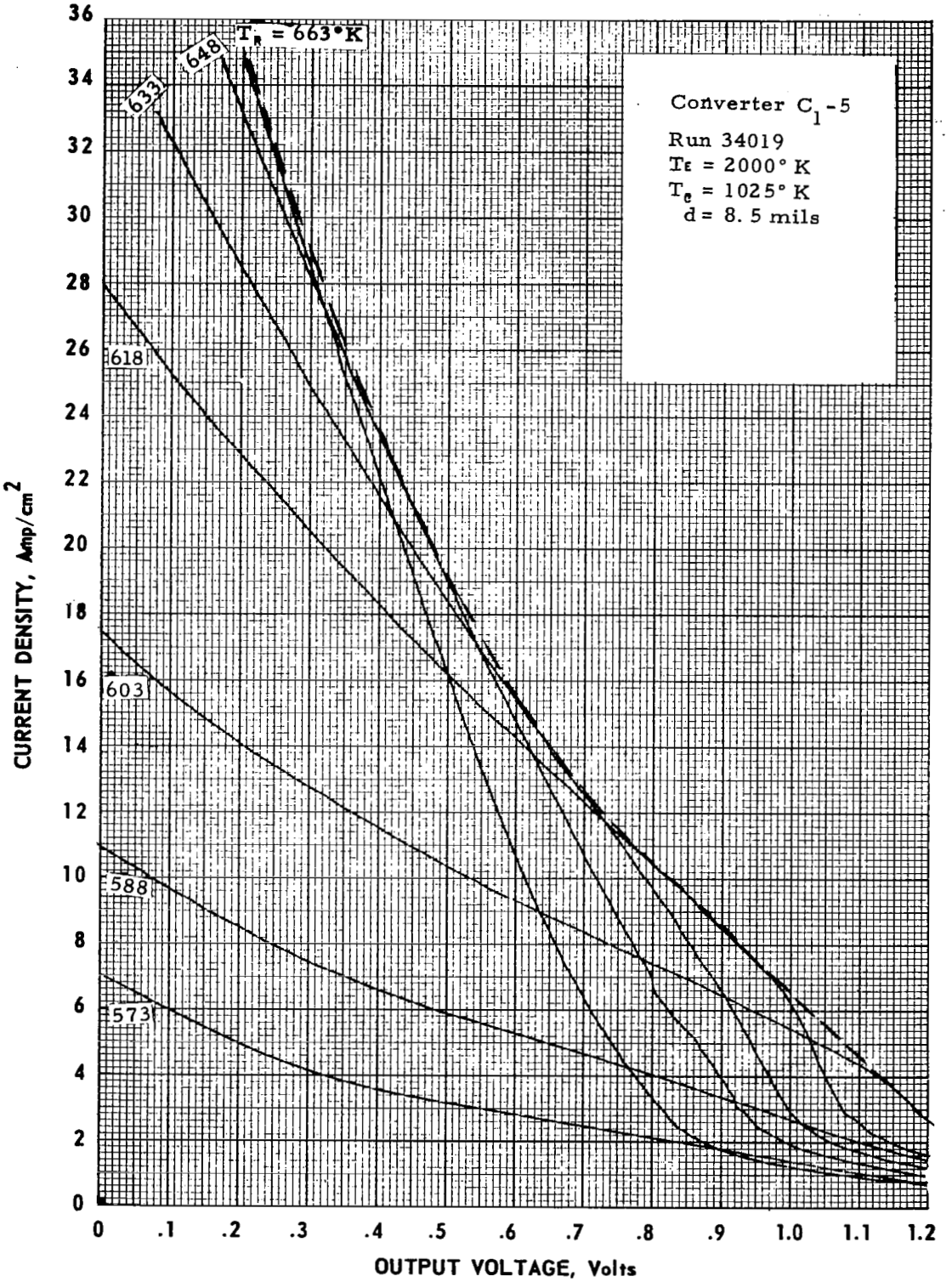

Figure B-21. Cesium-Temperature Family of Converter C_1-5 at T_E = 2000° K.

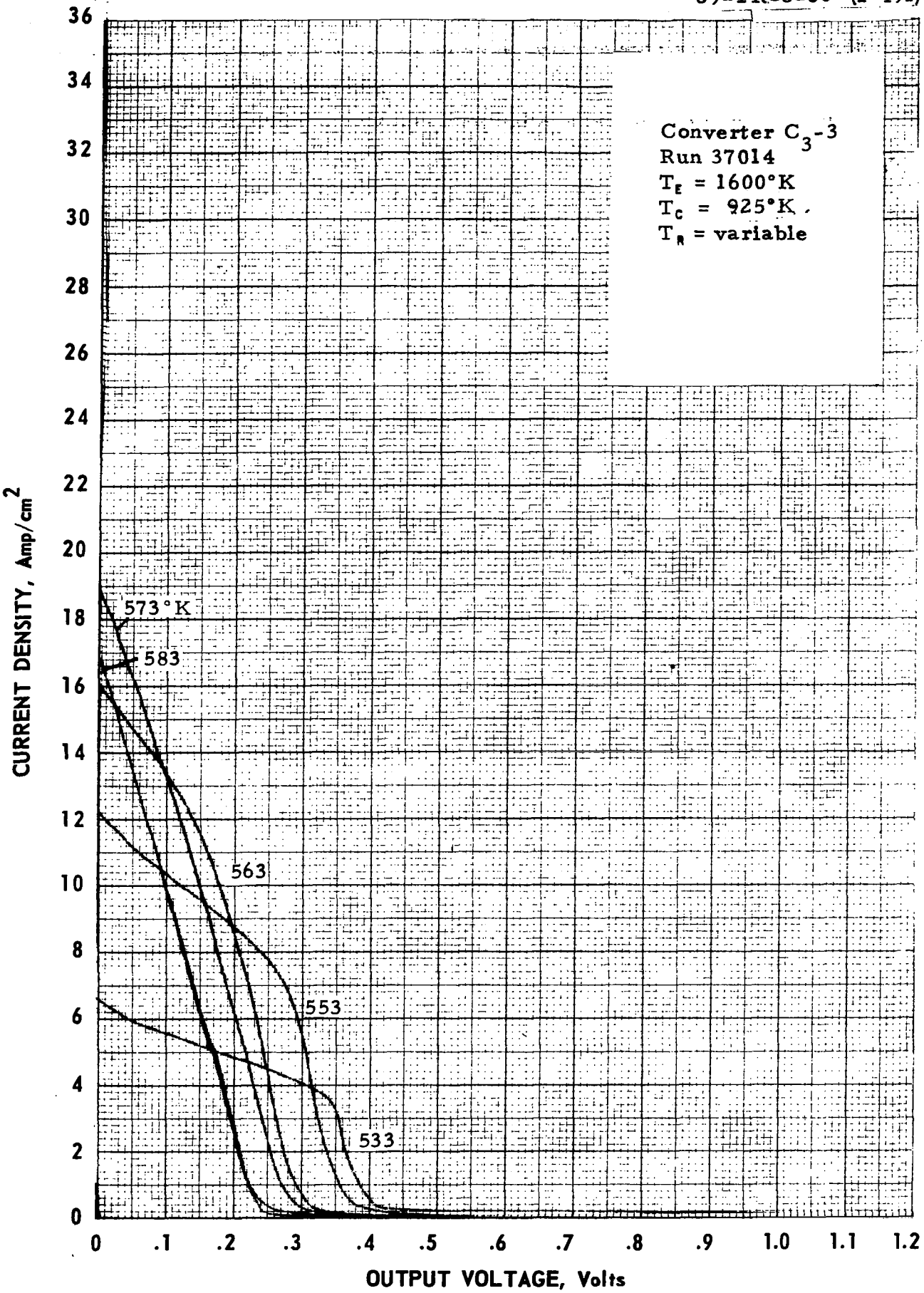

Figure B-22. Cesium Temperature Family of Converter C_3-3 at T_E = 1600°K.

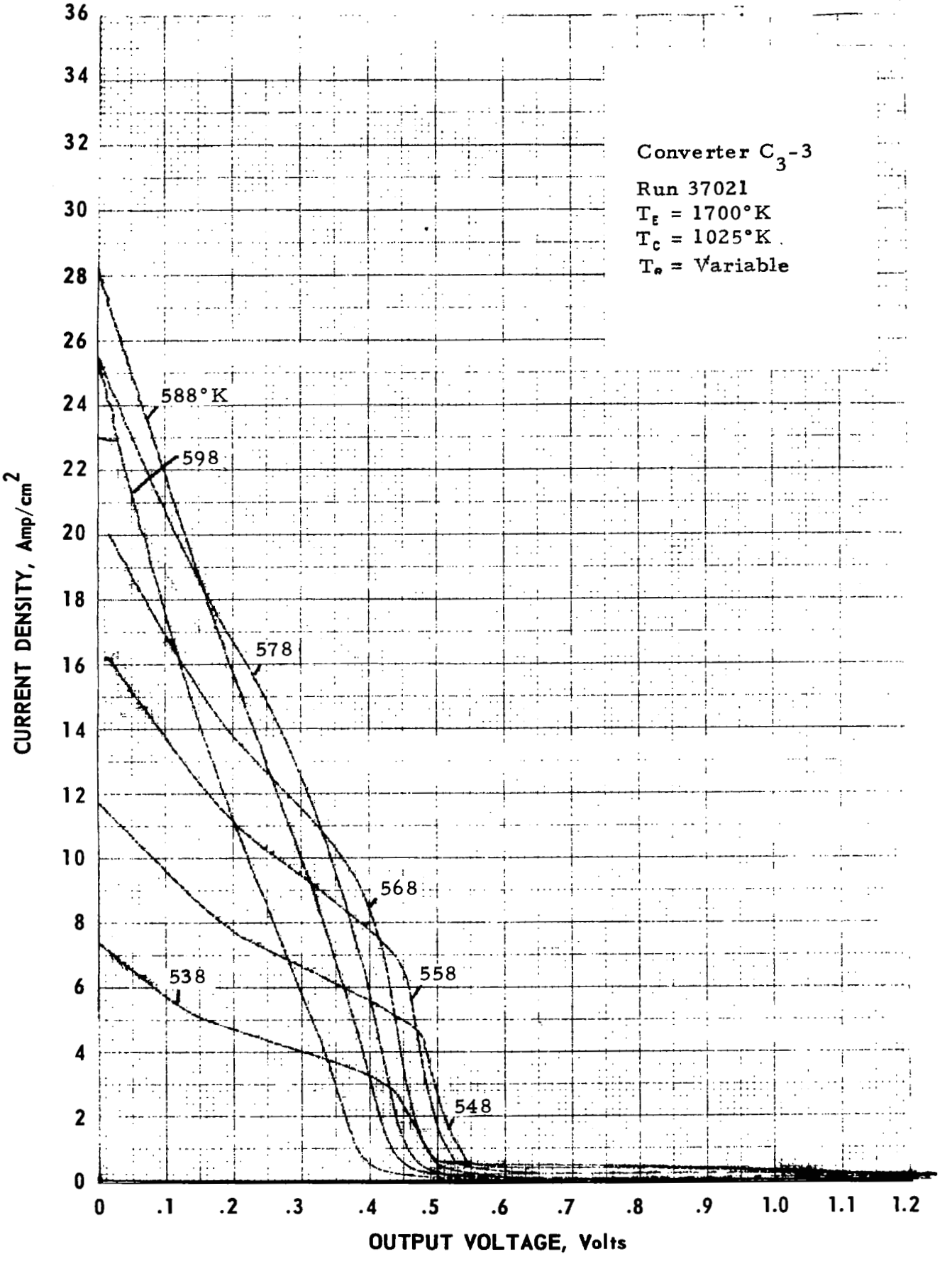

Figure B-23. Cesium Temperature Family of Converter C_3-3 at T_E = 1700°K.

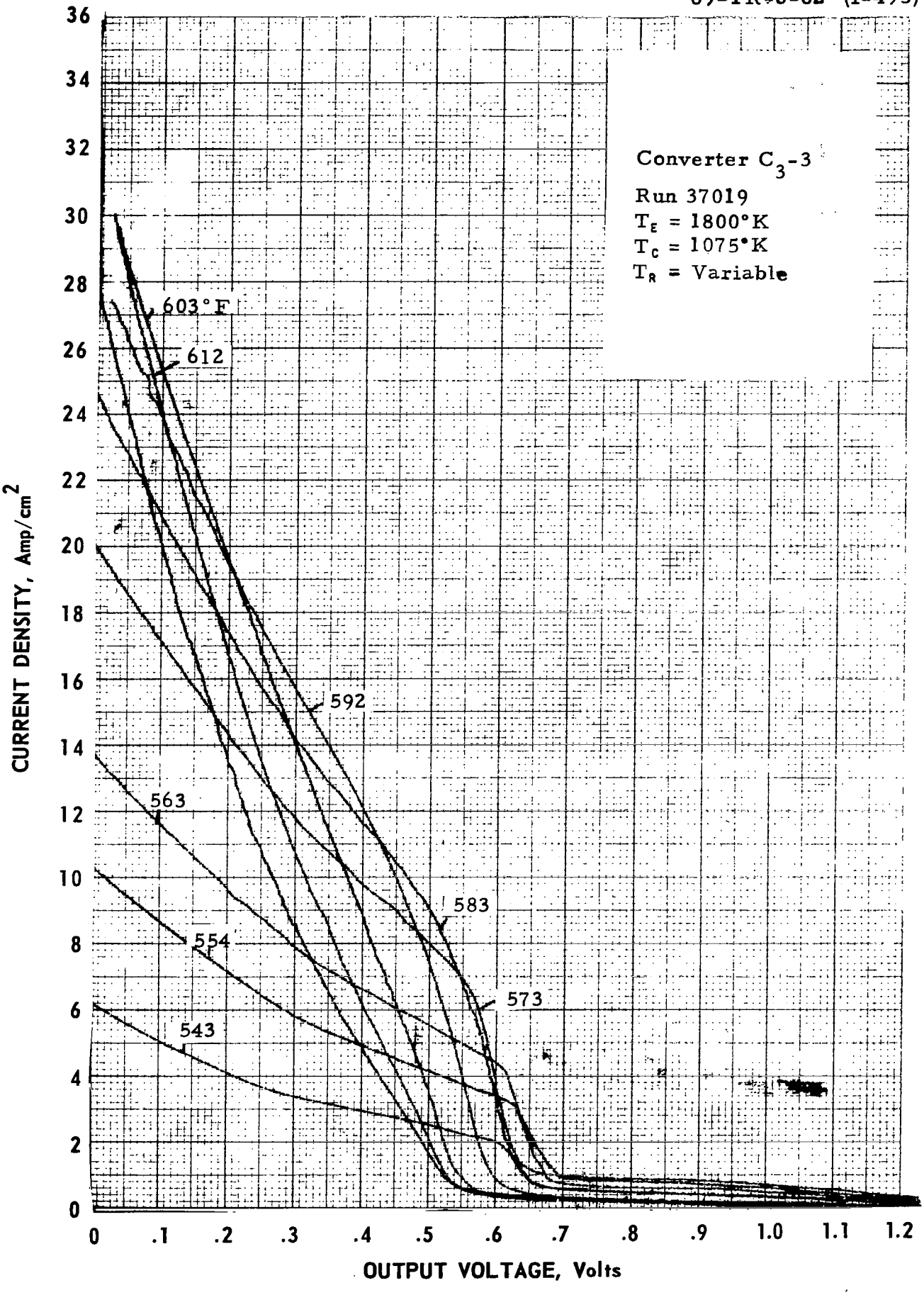

Figure B-24. Cesium Temperature Family of Converter C_3-3 at T_E = 1800°K.

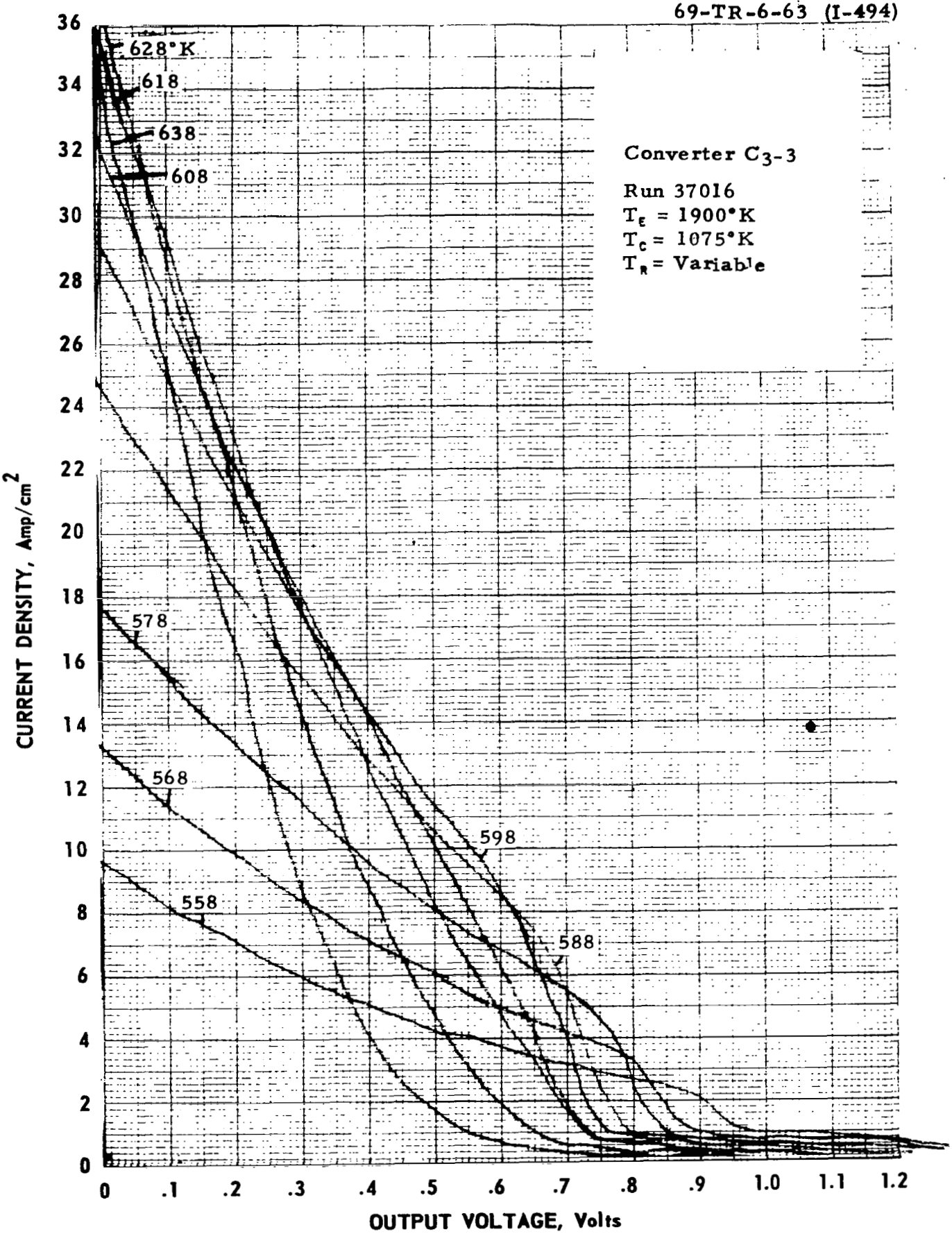

Figure B-25. Cesium Temperature Family of Converter C_3-3 at T_ε = 1900°K.

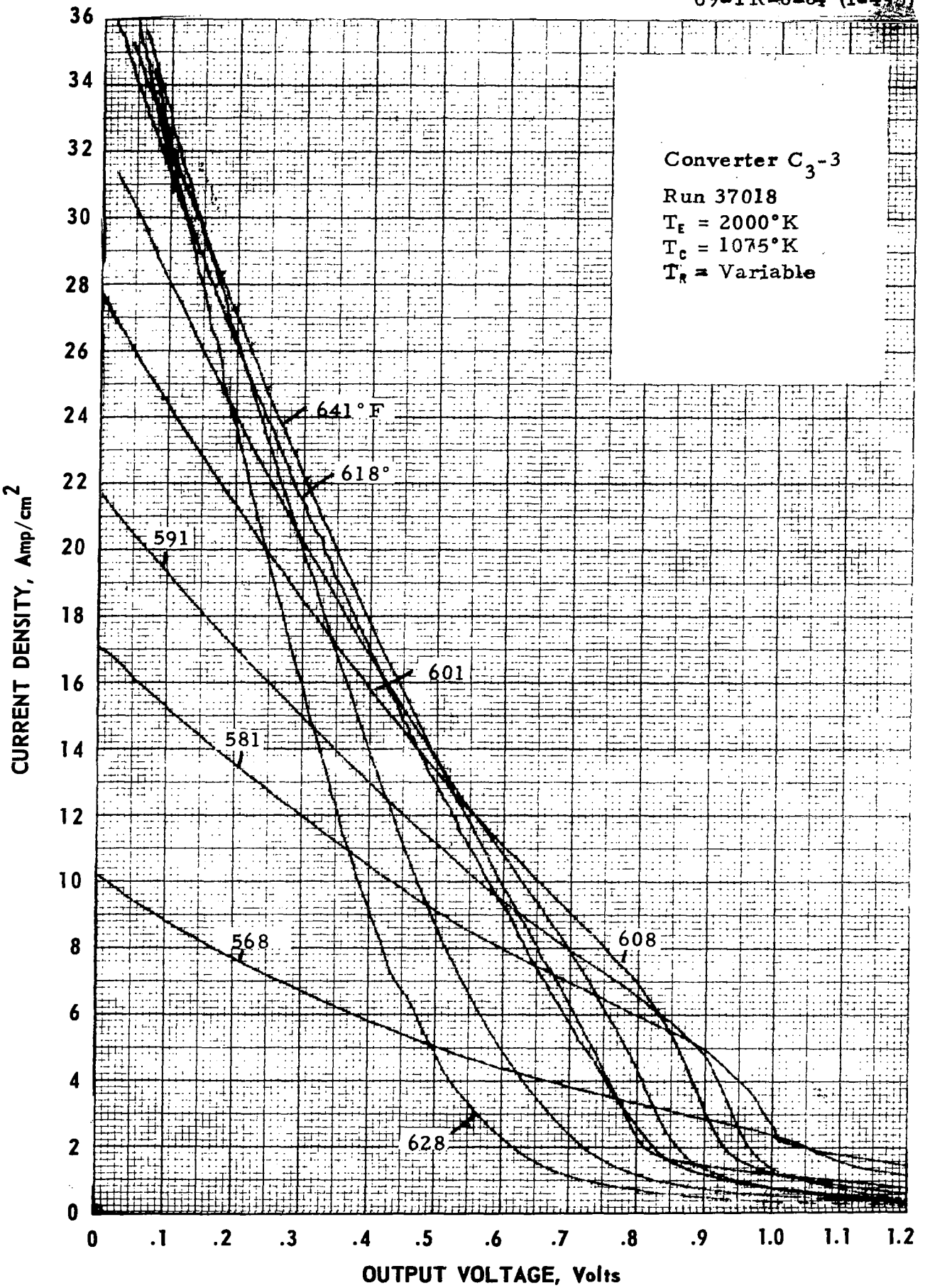

Figure B-26. Cesium Temperature Family of Converter C_3-3 at T_E = 2000°K.

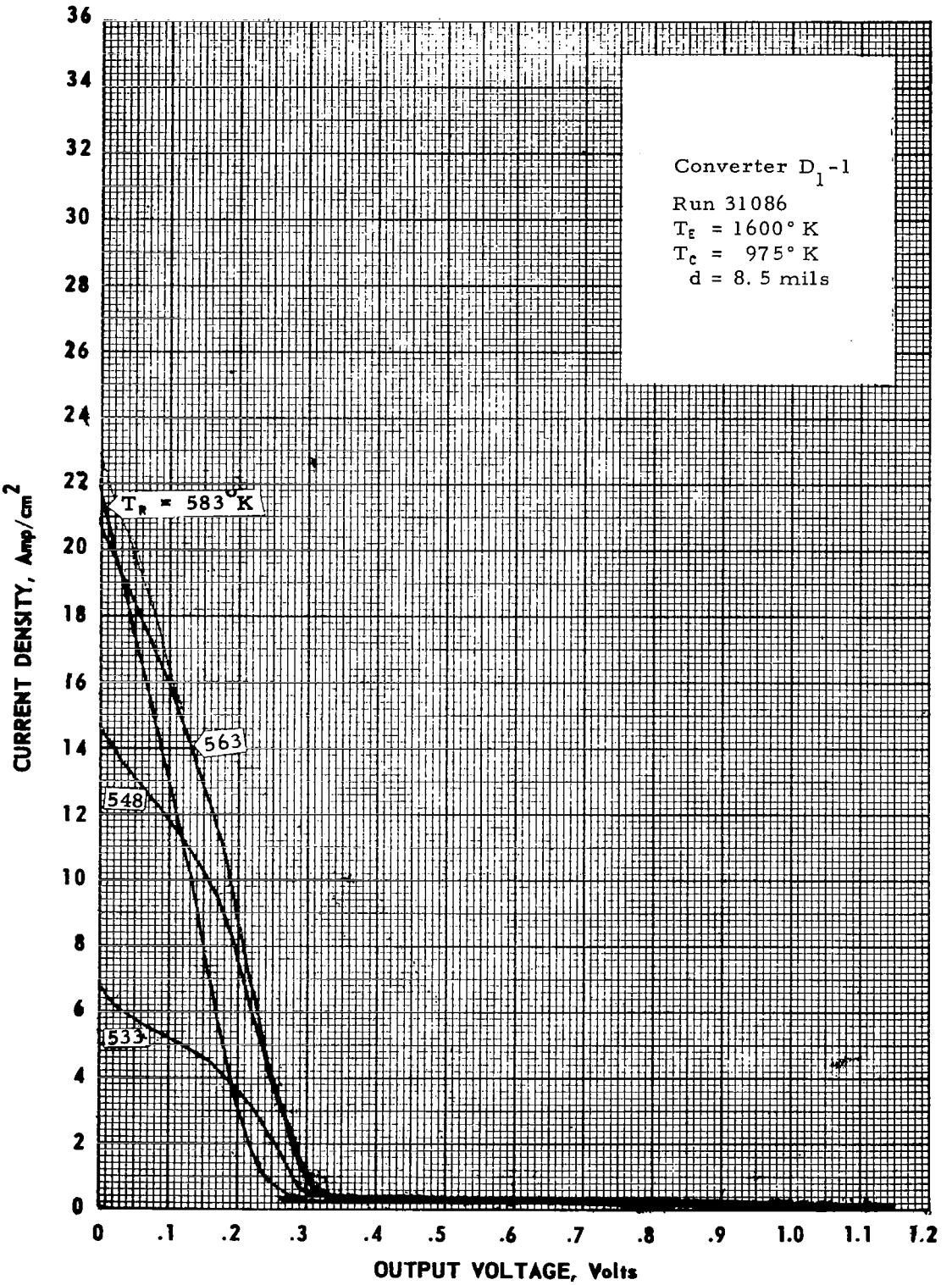

Figure B-27. Cesium-Temperature Family of Converter D_1-1 at T_E = 1600° K.

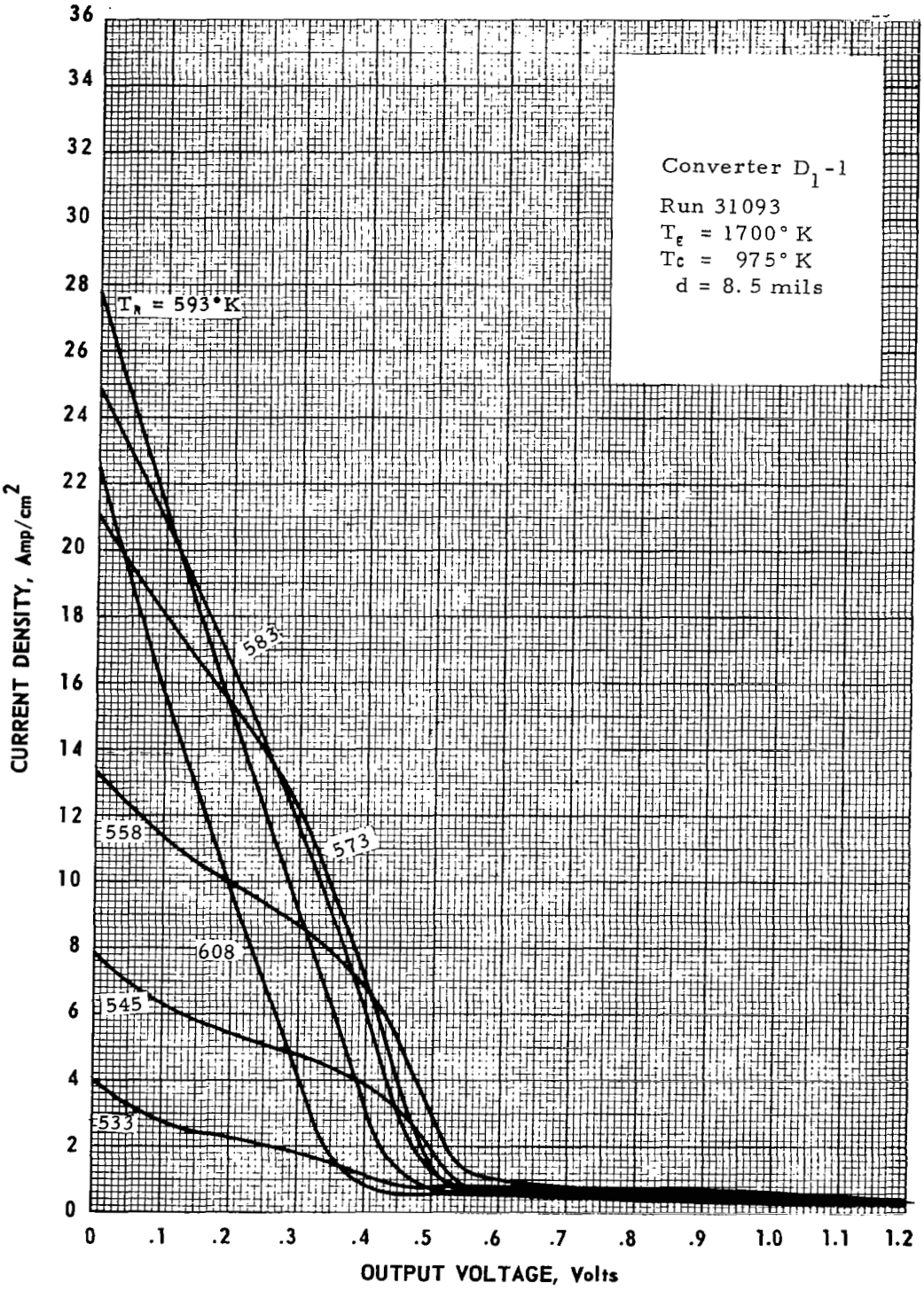

Figure B-28. Cesium-Temperature Family of Converter D_1-1 at T_e = 1700° K.

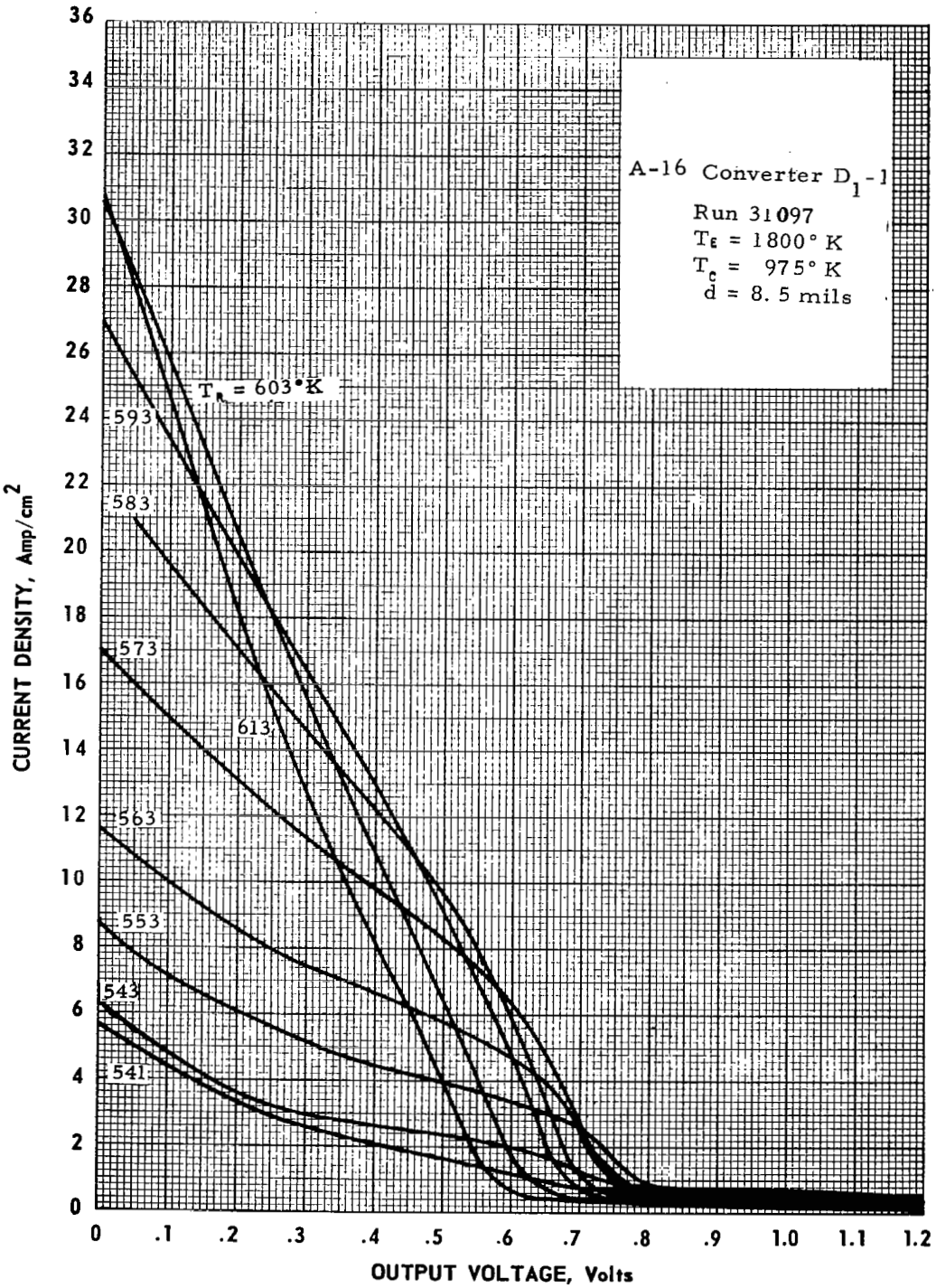

Figure B-29. Cesium-Temperature Family of Converter D_1-1 at T_e = 1800° K.

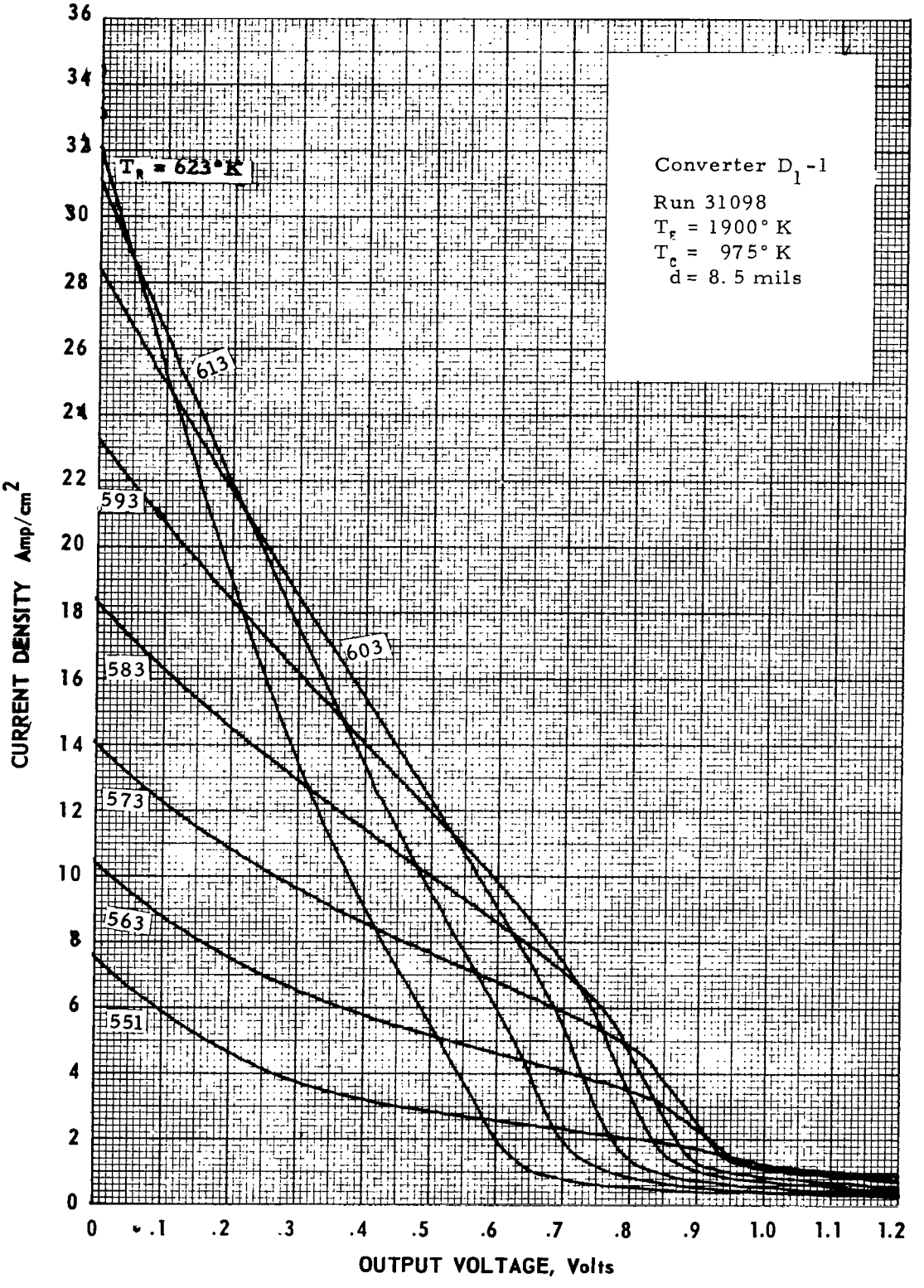

Figure B-30. Cesium-Temperature Family of Converter D_1-1 at T_e = 1900° K.

APPENDIX C

CESIUM TEMPERATURE FAMILIES AFTER 3000-HOUR LIFE TEST

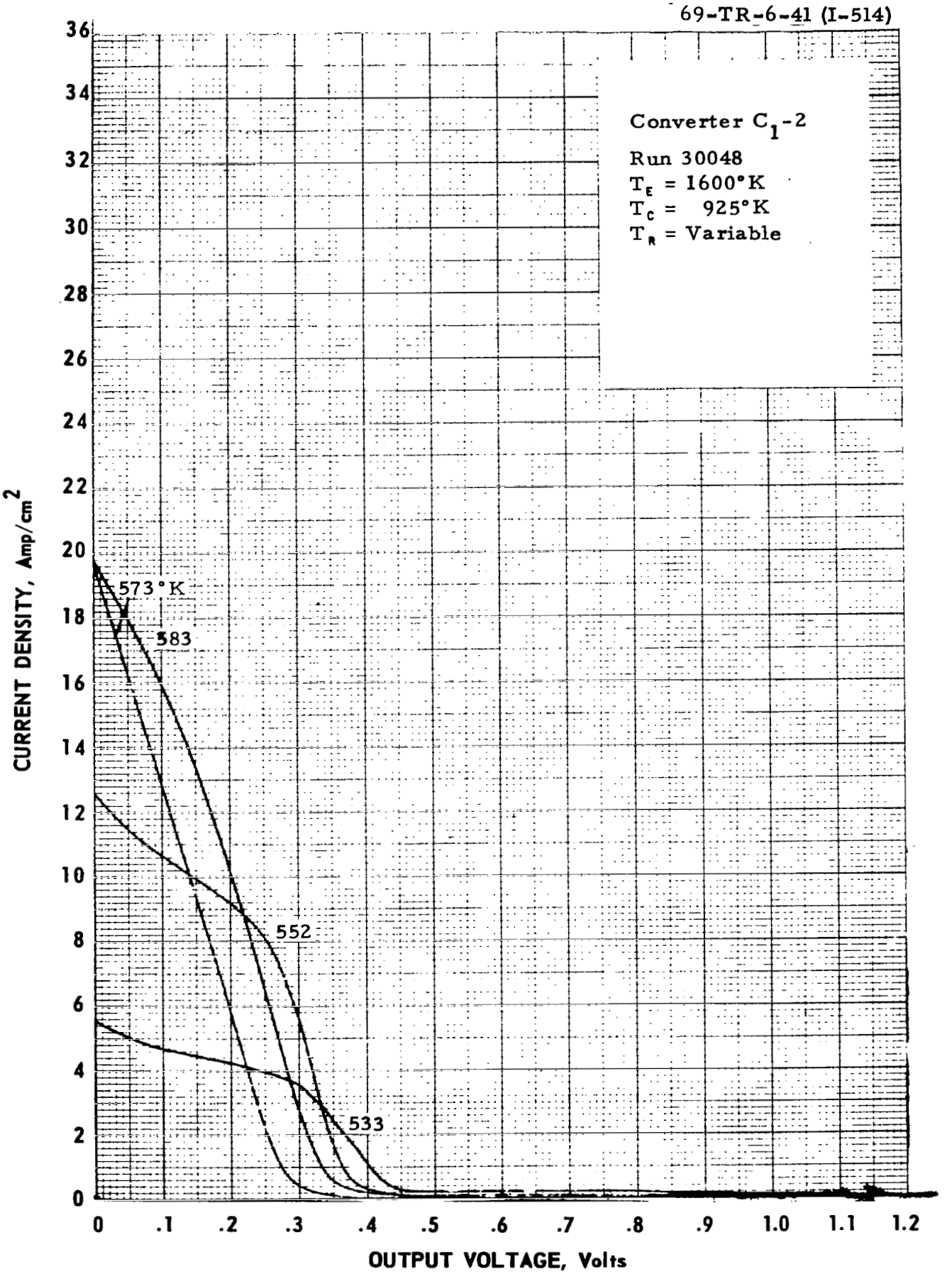

Figure C-1. Cesium Temperature Family of Converter C_1-2 at T_E = 1600°K.

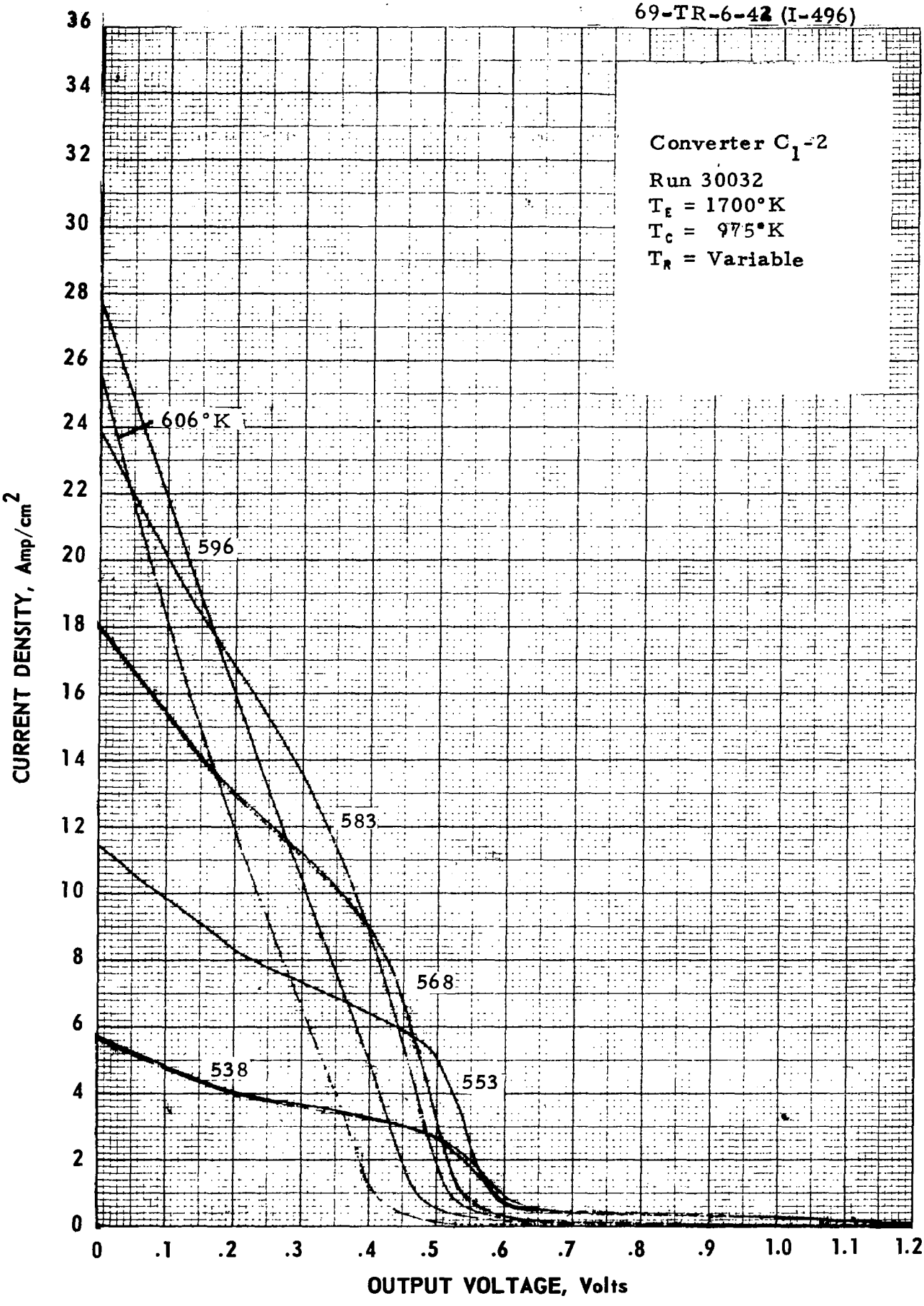

Figure C-2. Cesium Temperature Family of Converter C_1-2 at T_E = 1700°K.

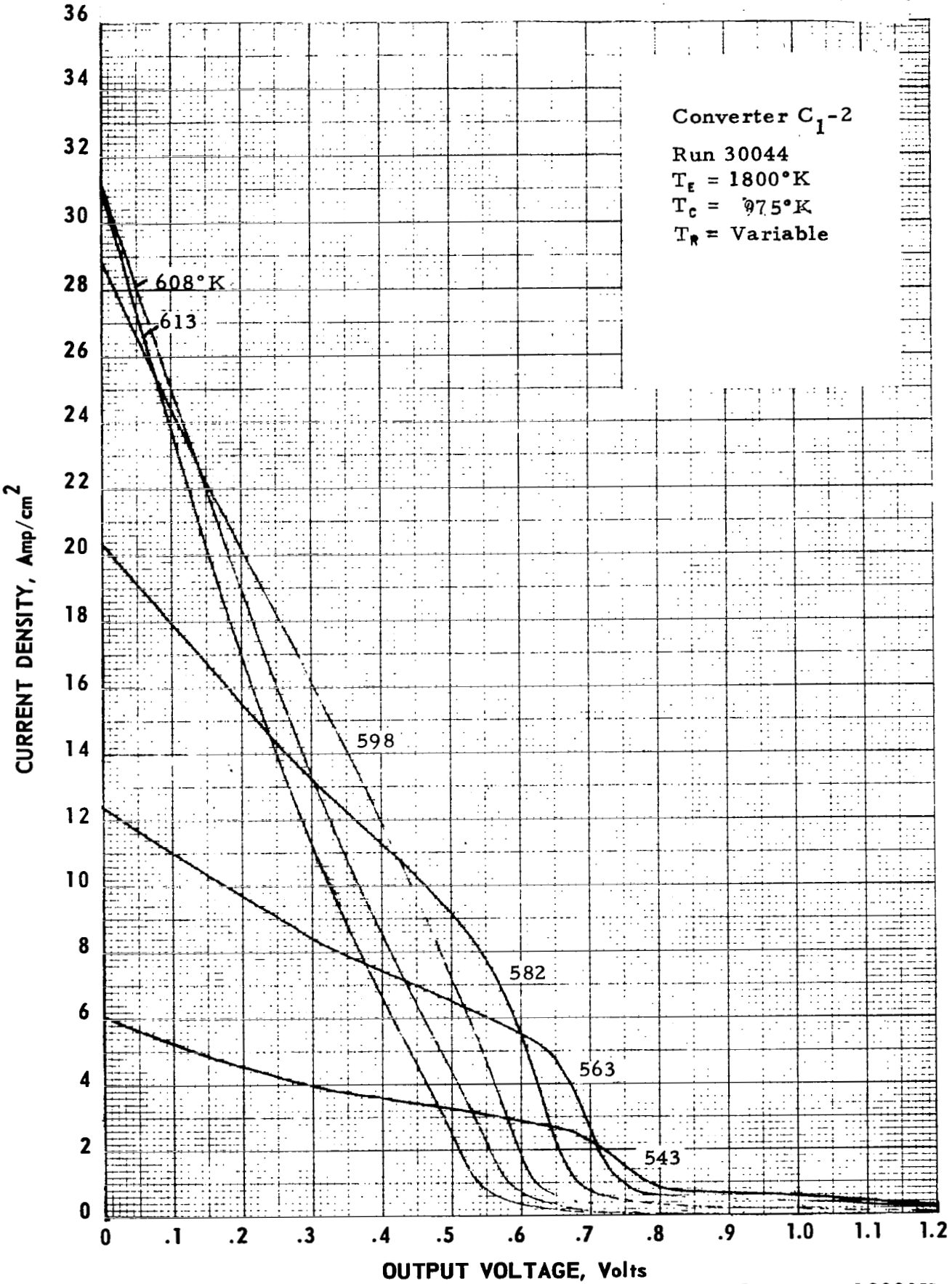

Figure C-3. Cesium Temperature Family of Converter C_1-2 at T_E = 1800°K.

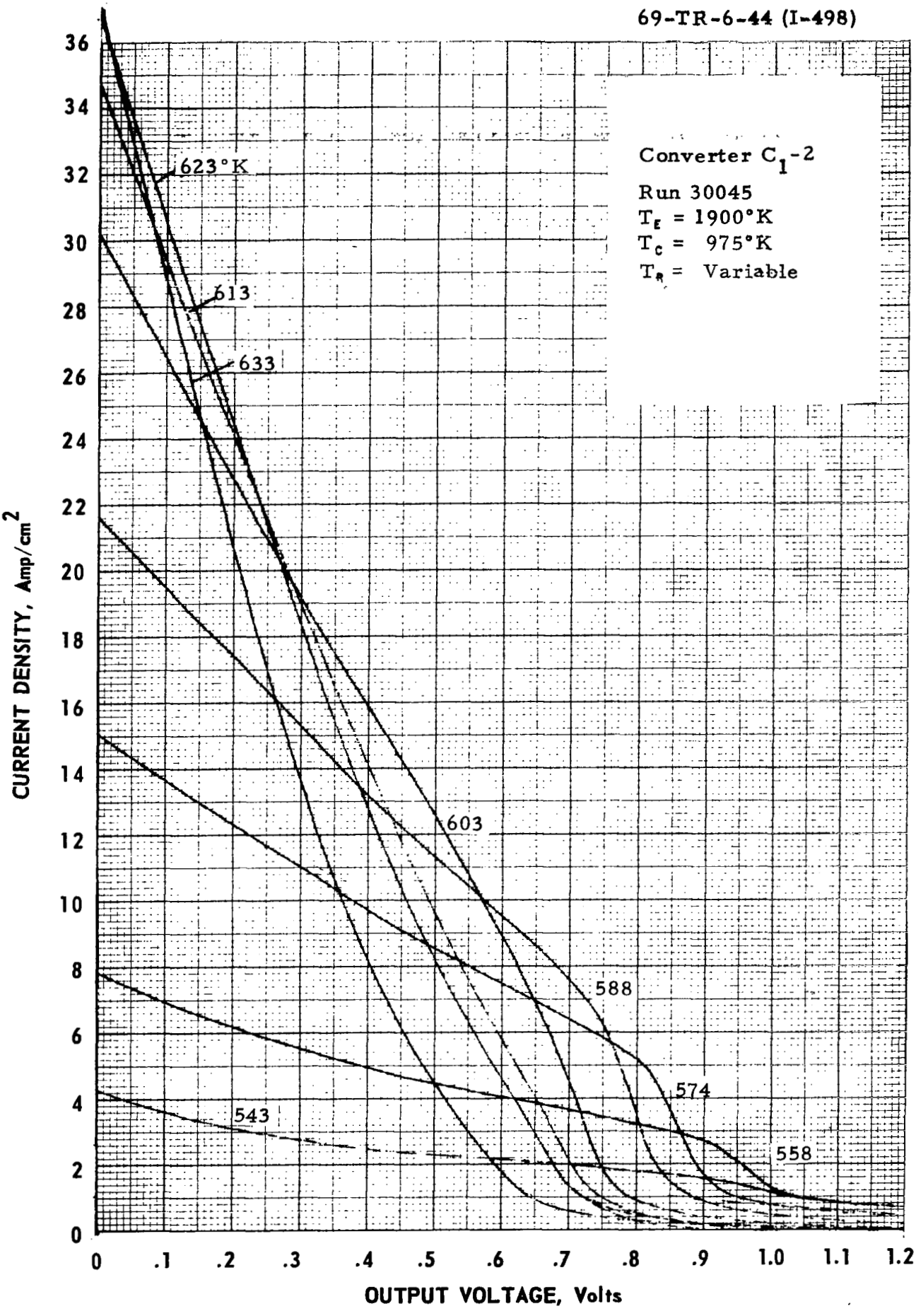

Figure C-4. Cesium Temperature Family of Converter C_1-2 at T_E = 1900°K.

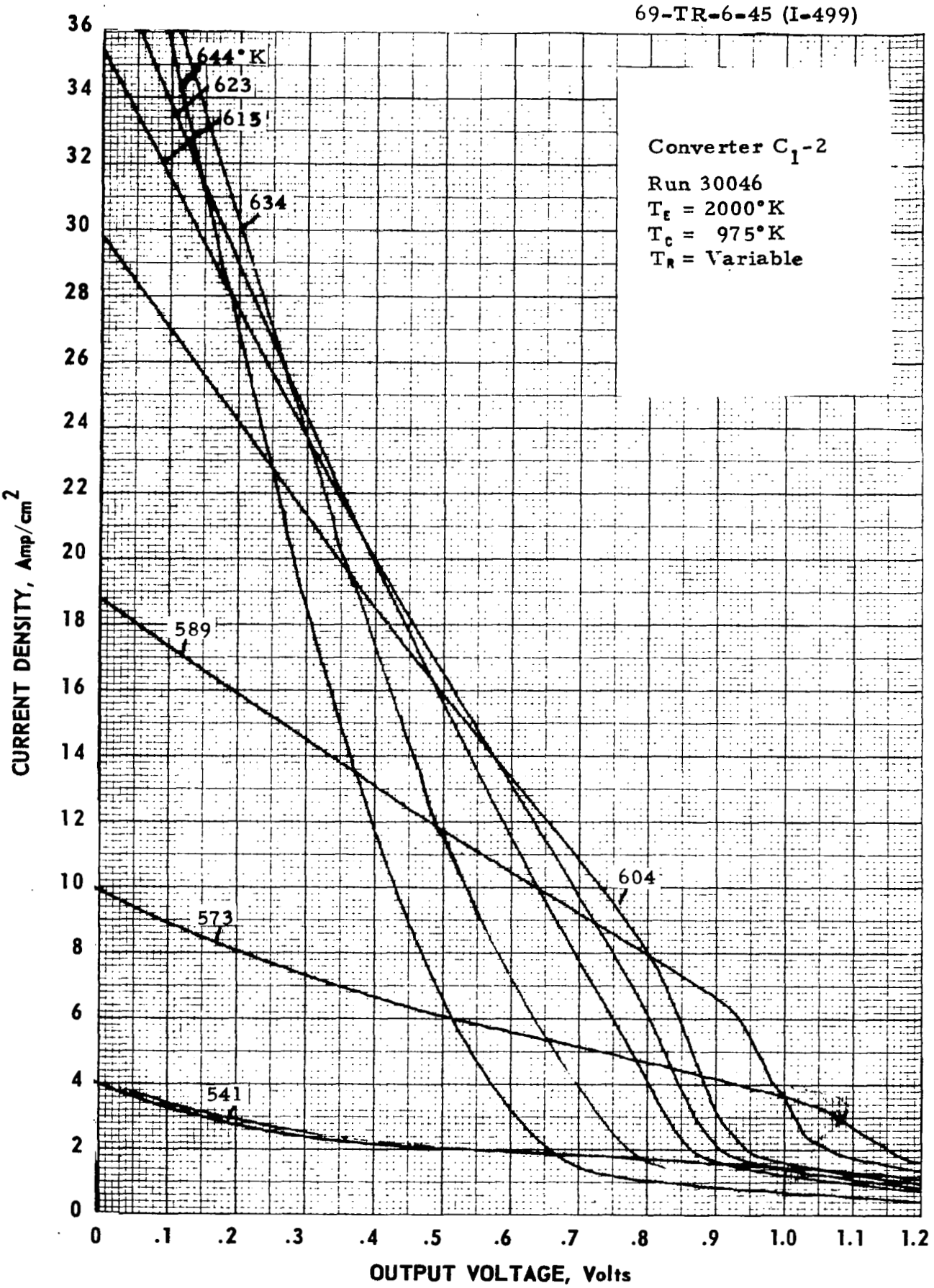

Figure C-5. Cesium Temperature Family of Converter C_1-2 at T_E = 2000°K.

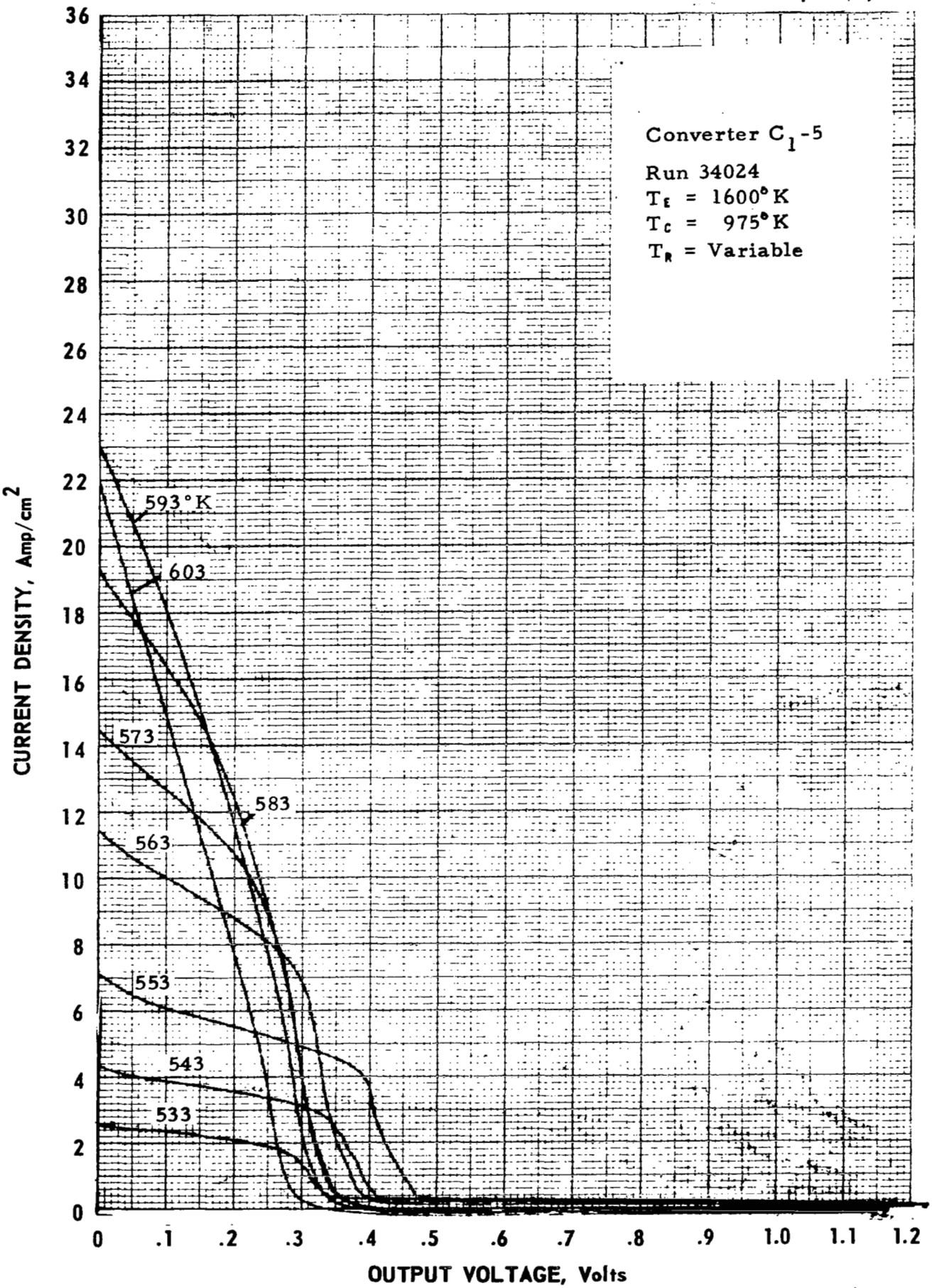

Figure C-6. Cesium Temperature Family of Converter C_1-5 at T_E = 1600°K.

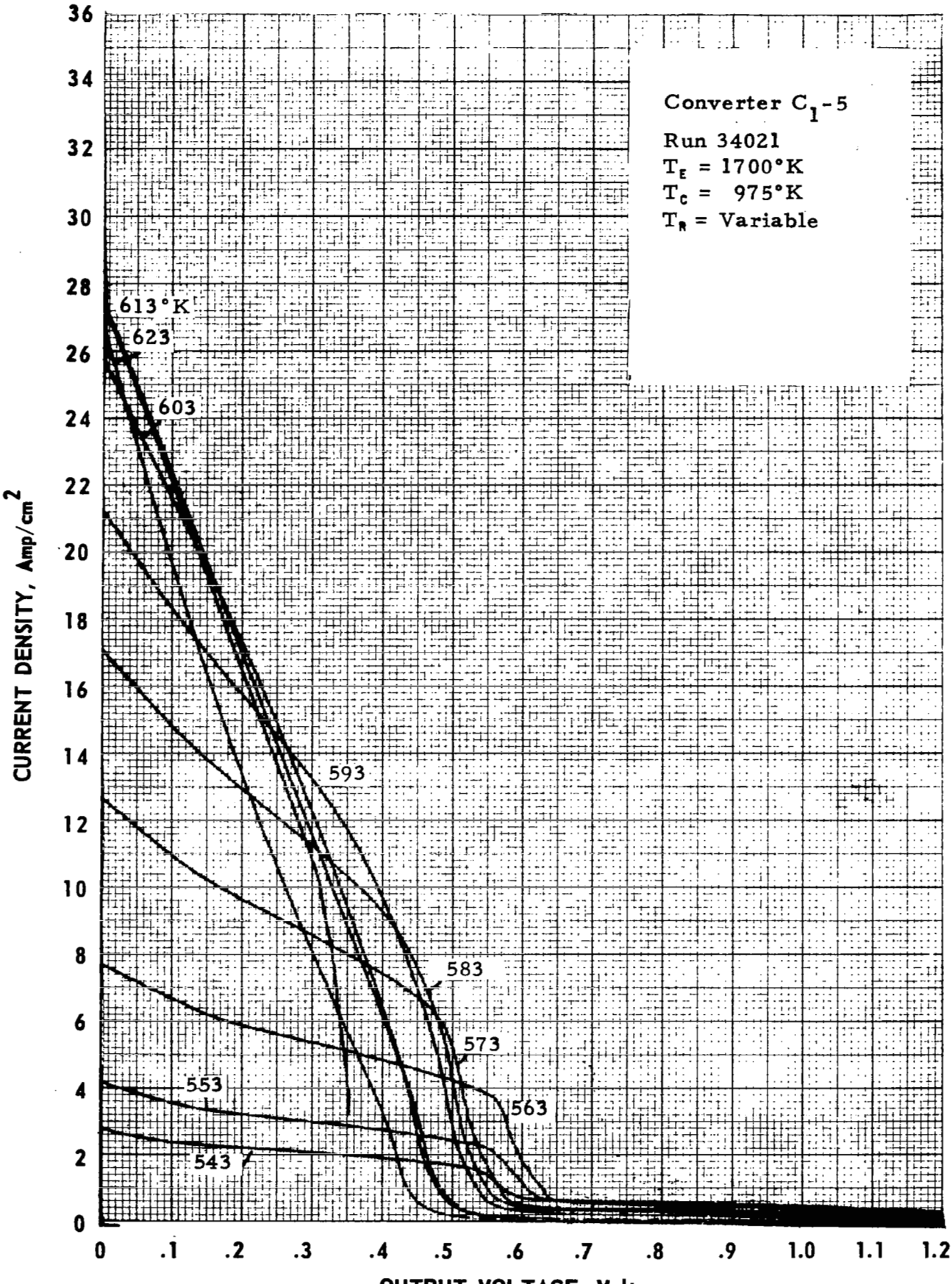

Figure C-7. Cesium Temperature Family of Converter C_1-5 at T_E = 1700°K.

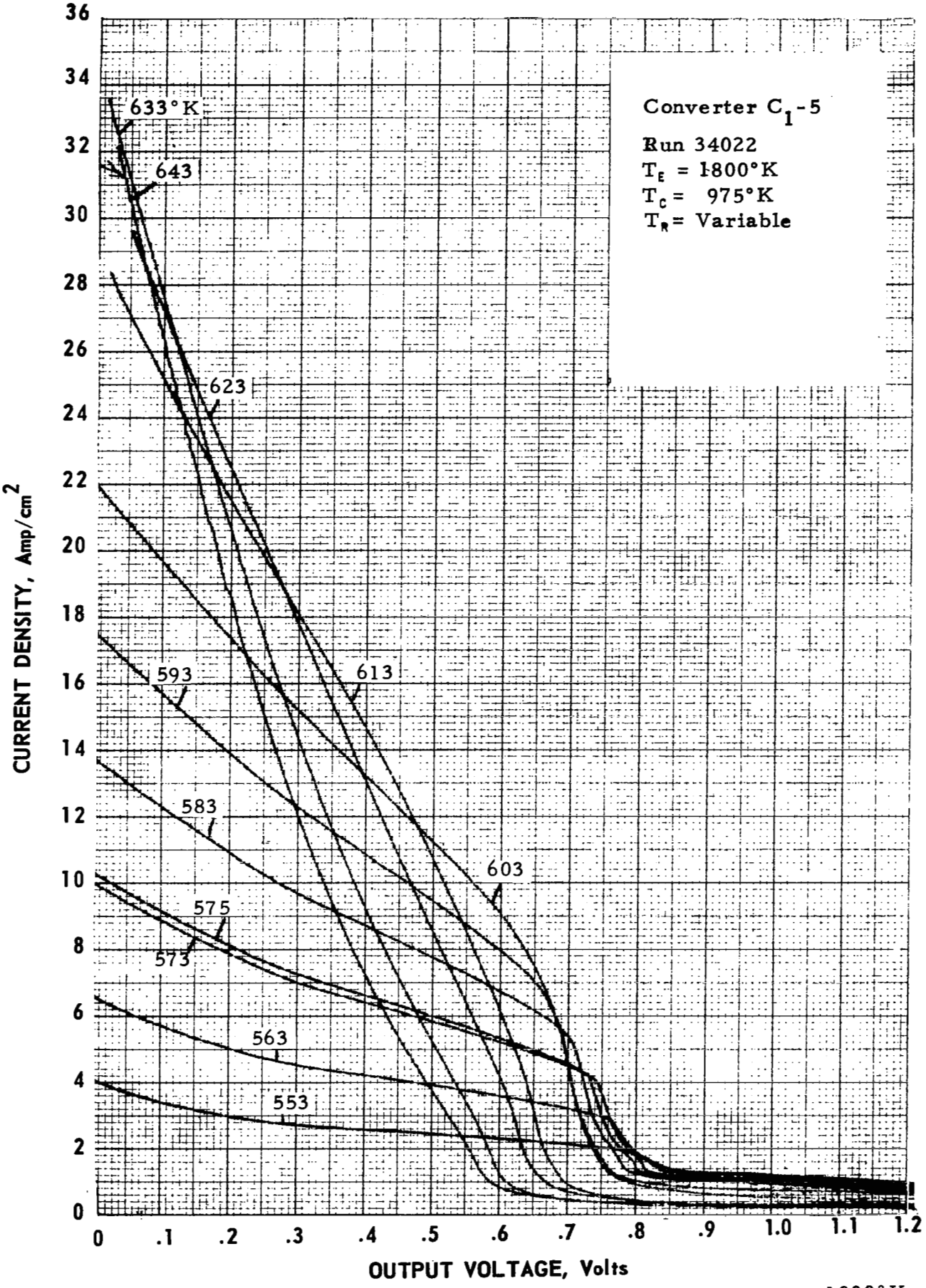

Figure C-8. Cesium Temperature Family of Converter C_1-5 at T_E = 1800°K.

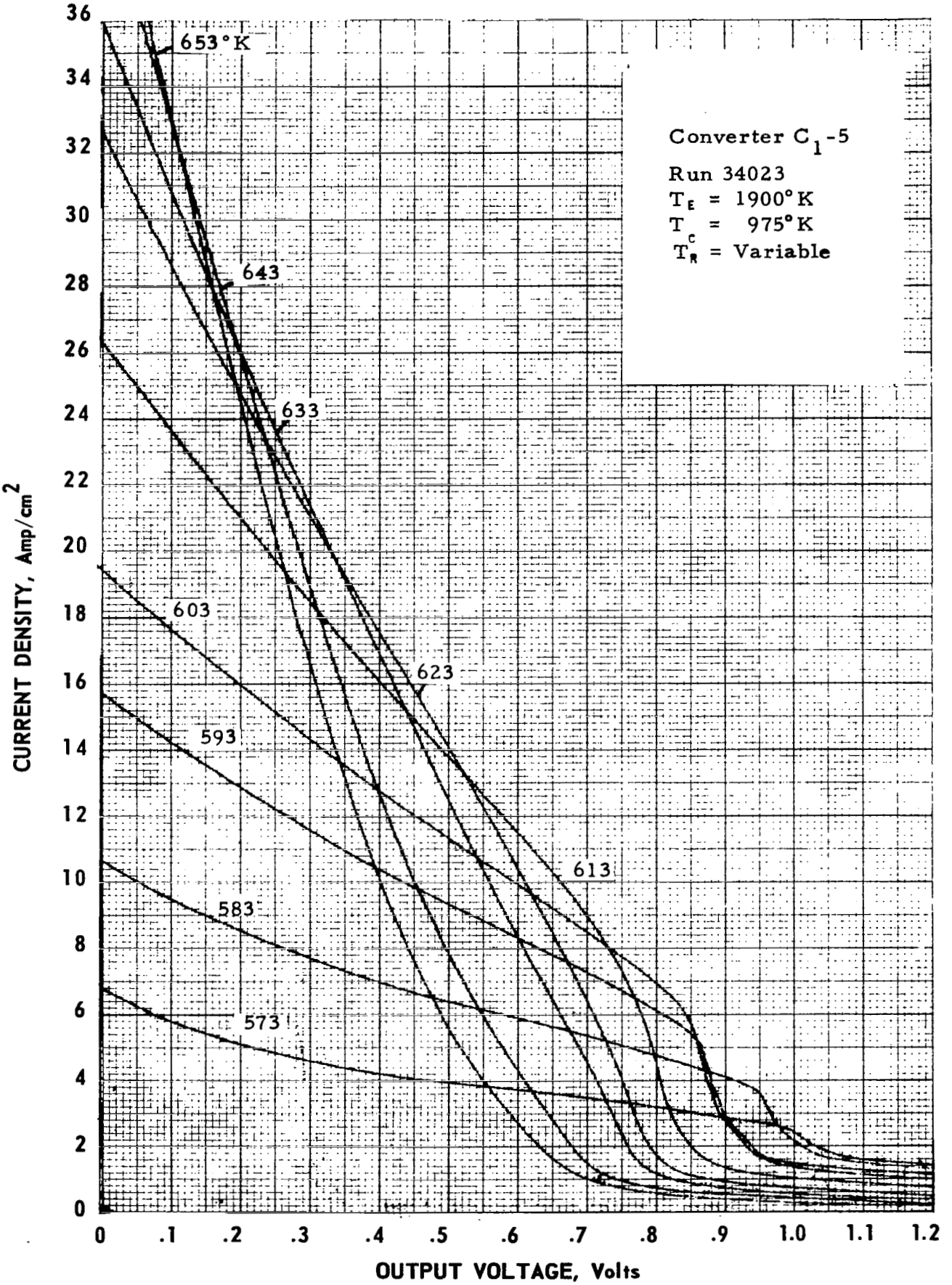

Figure C-9. Cesium Temperature Family of Converter C_1-5 at T_E = 1900°K.

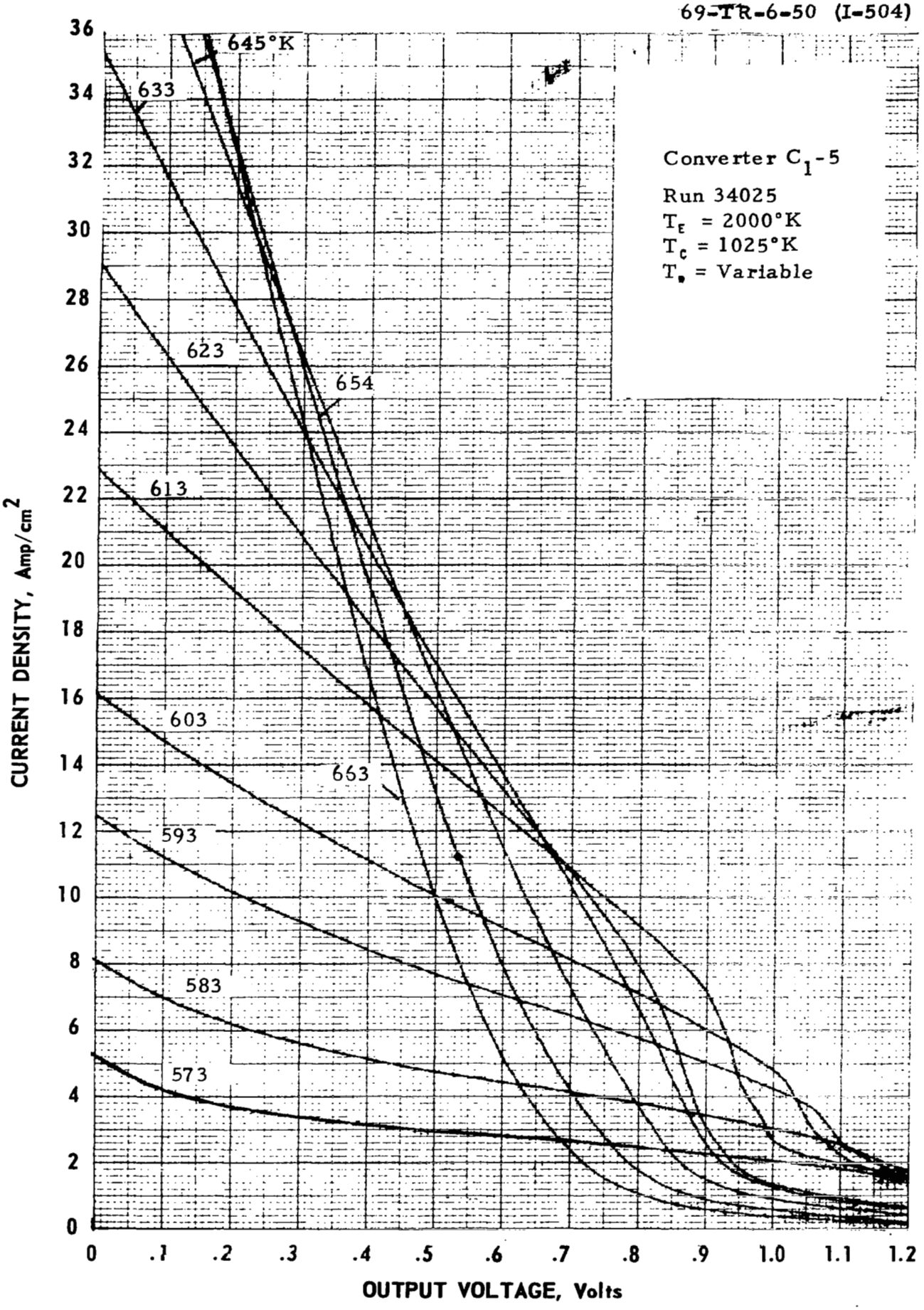

Figure C-10. Cesium Temperature Family of Converter C_1-5 at T_E = 2000°K.

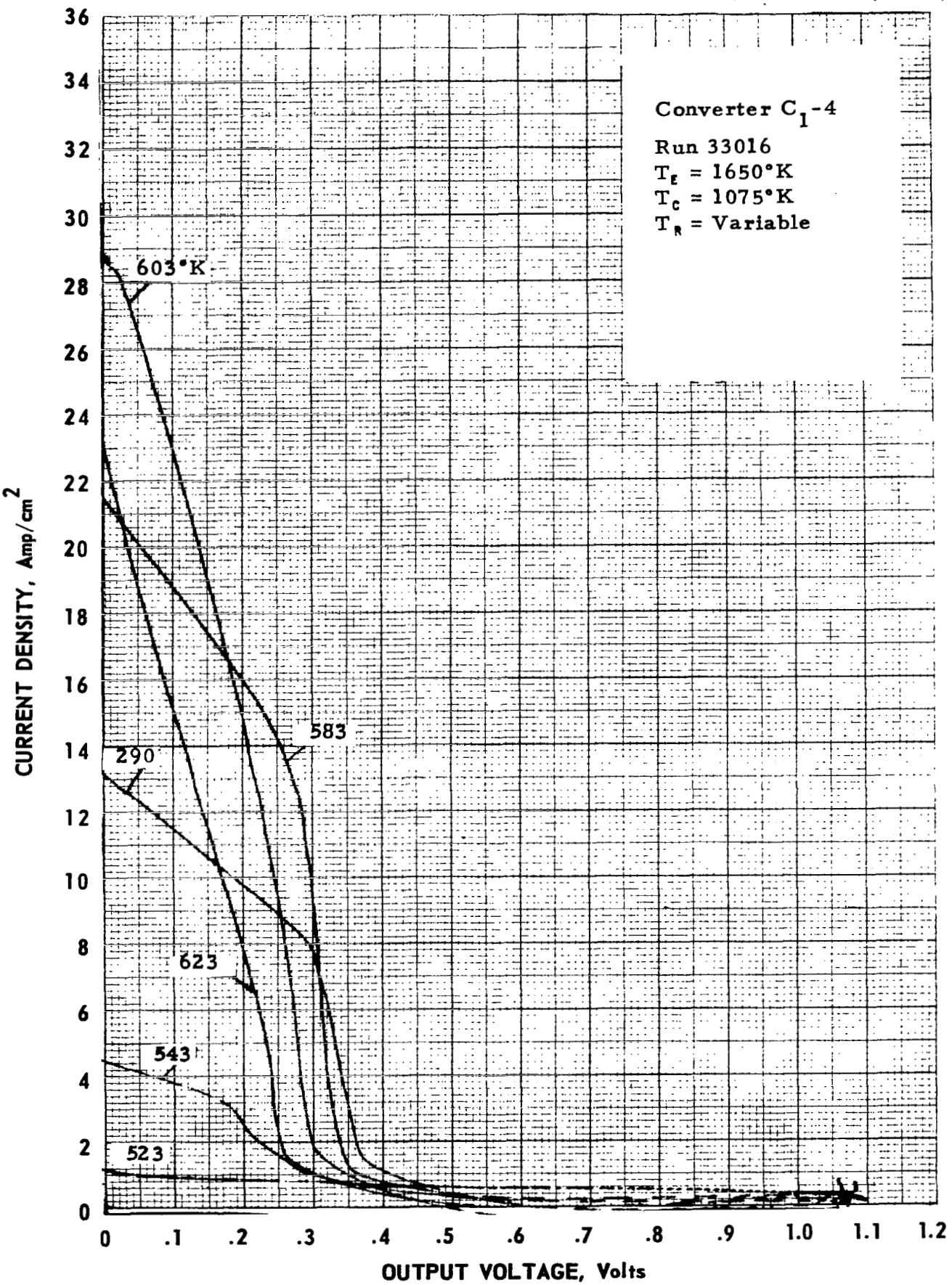

Figure C-11. Cesium Temperature Family of Converter C_1-4 at T_E = 1650°K.

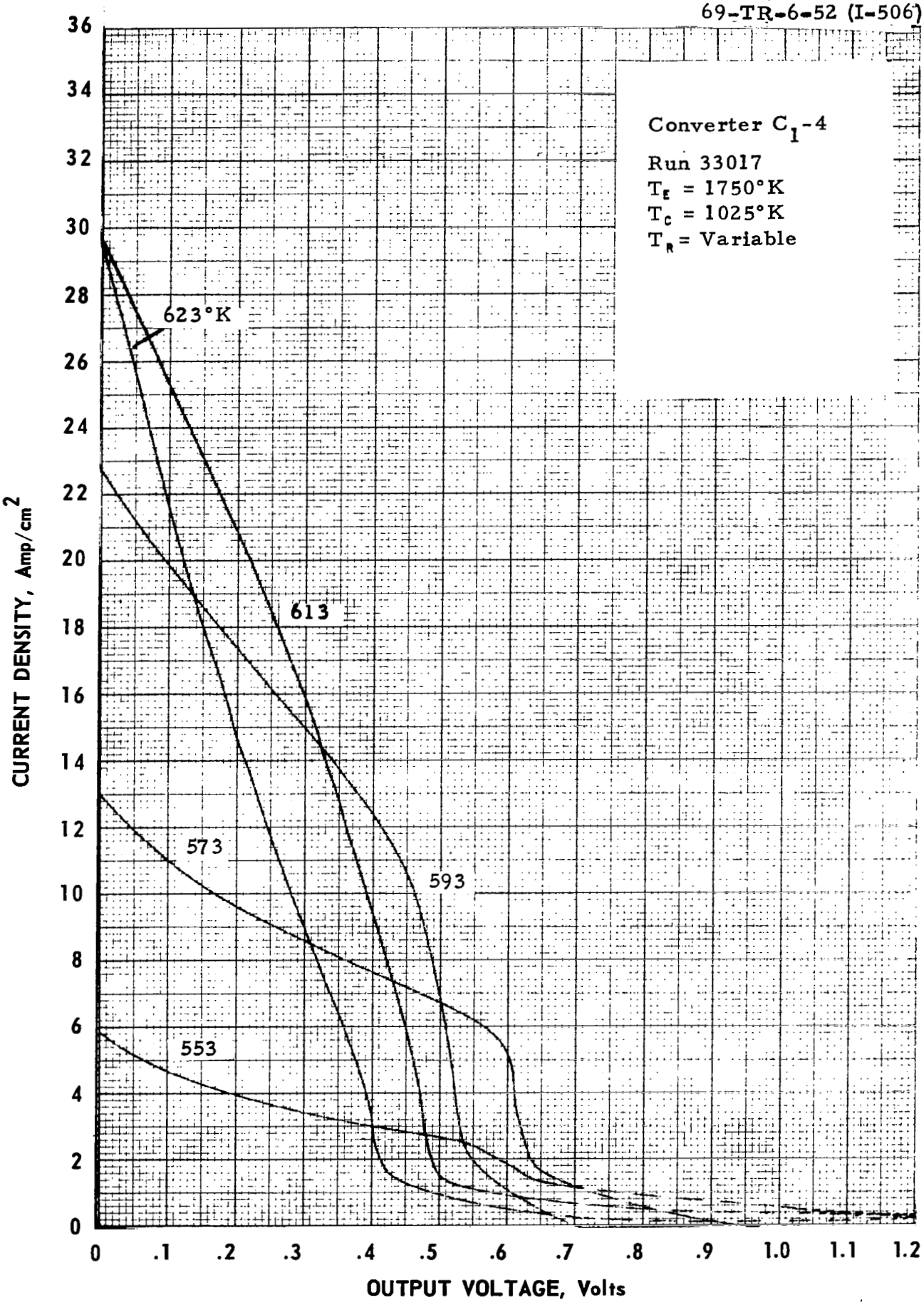

Figure C-12. Cesium Temperature Family of Converter C_1-4 at T_E = 1750°K.

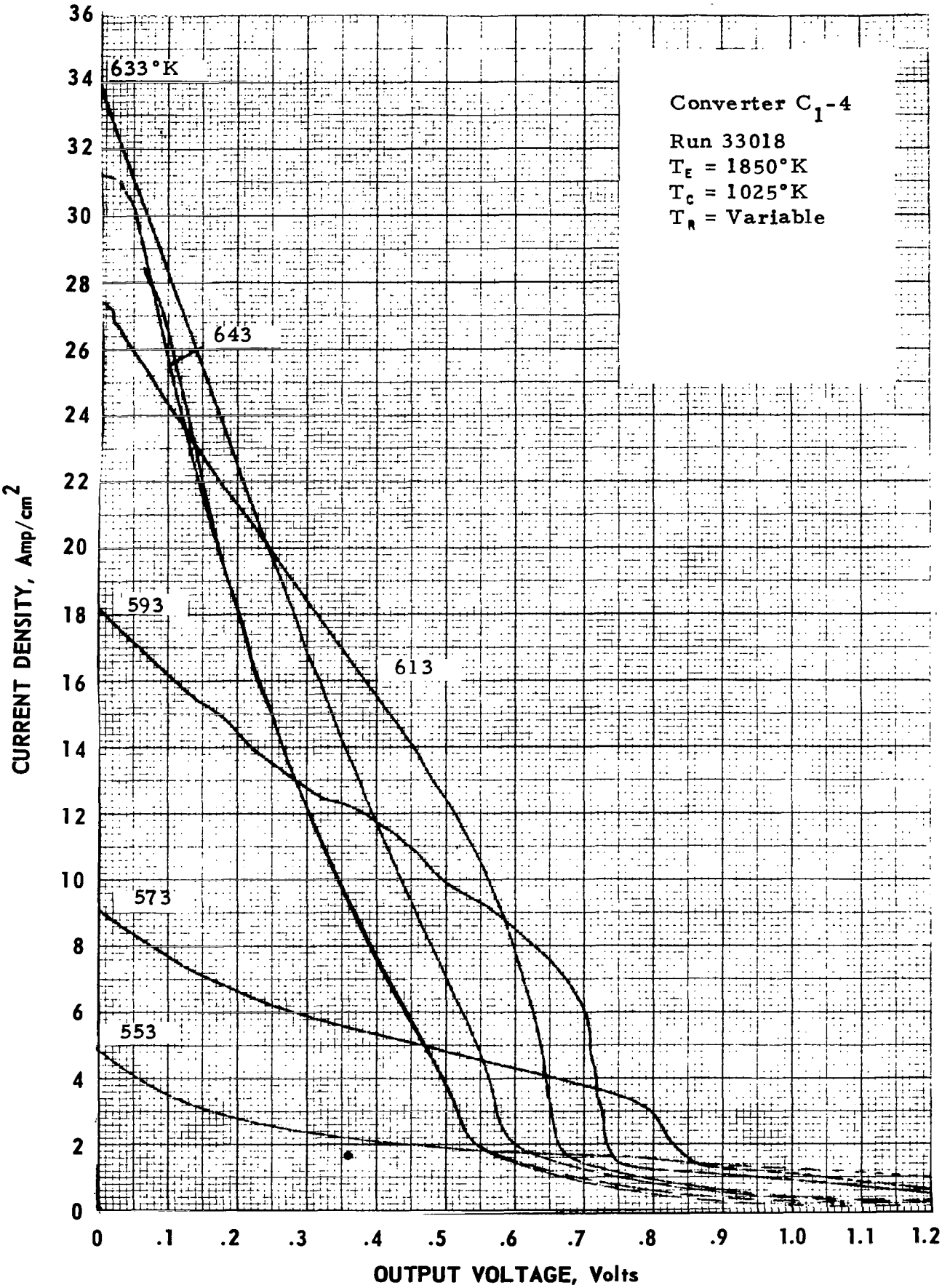

Figure C-13. Cesium Temperature Family of Converter C_1-4 at T_E = 1850°K.

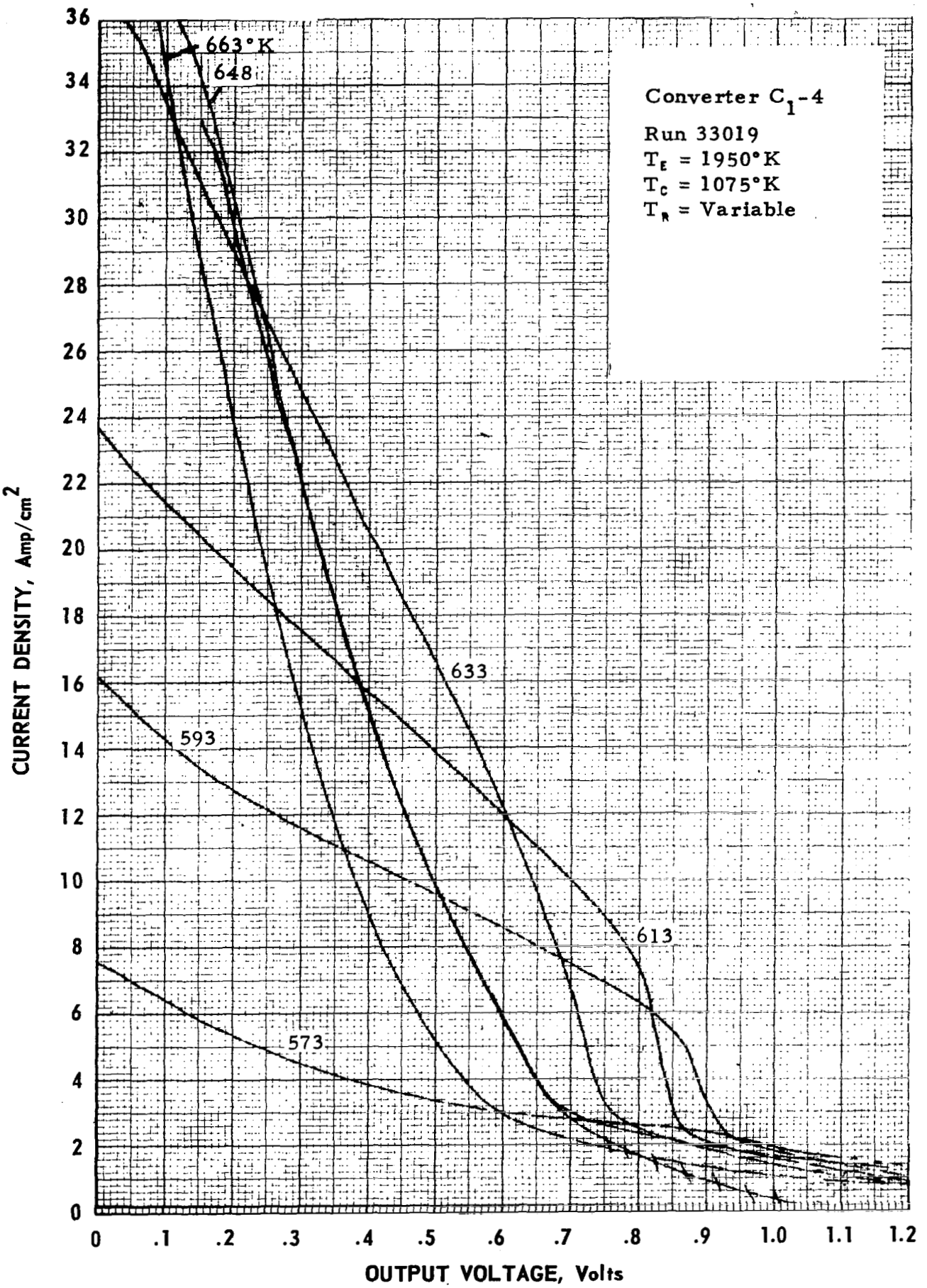

Figure C-14. Cesium Temperature Family of Converter C_1-4 at T_E = 1950°K.

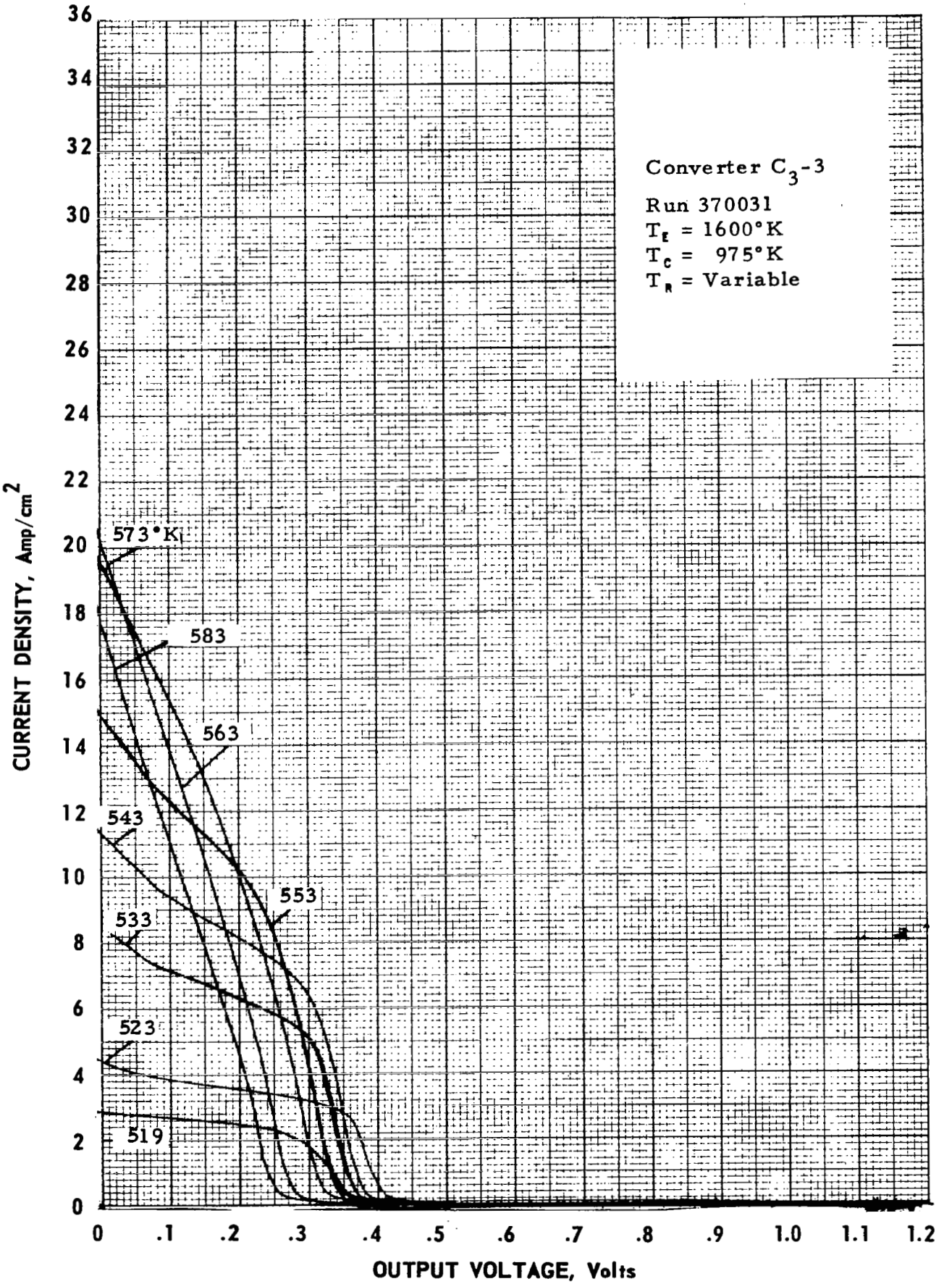

Figure C-15. Cesium Temperature Family of Converter C_3-3 at T_E = 1600°K.

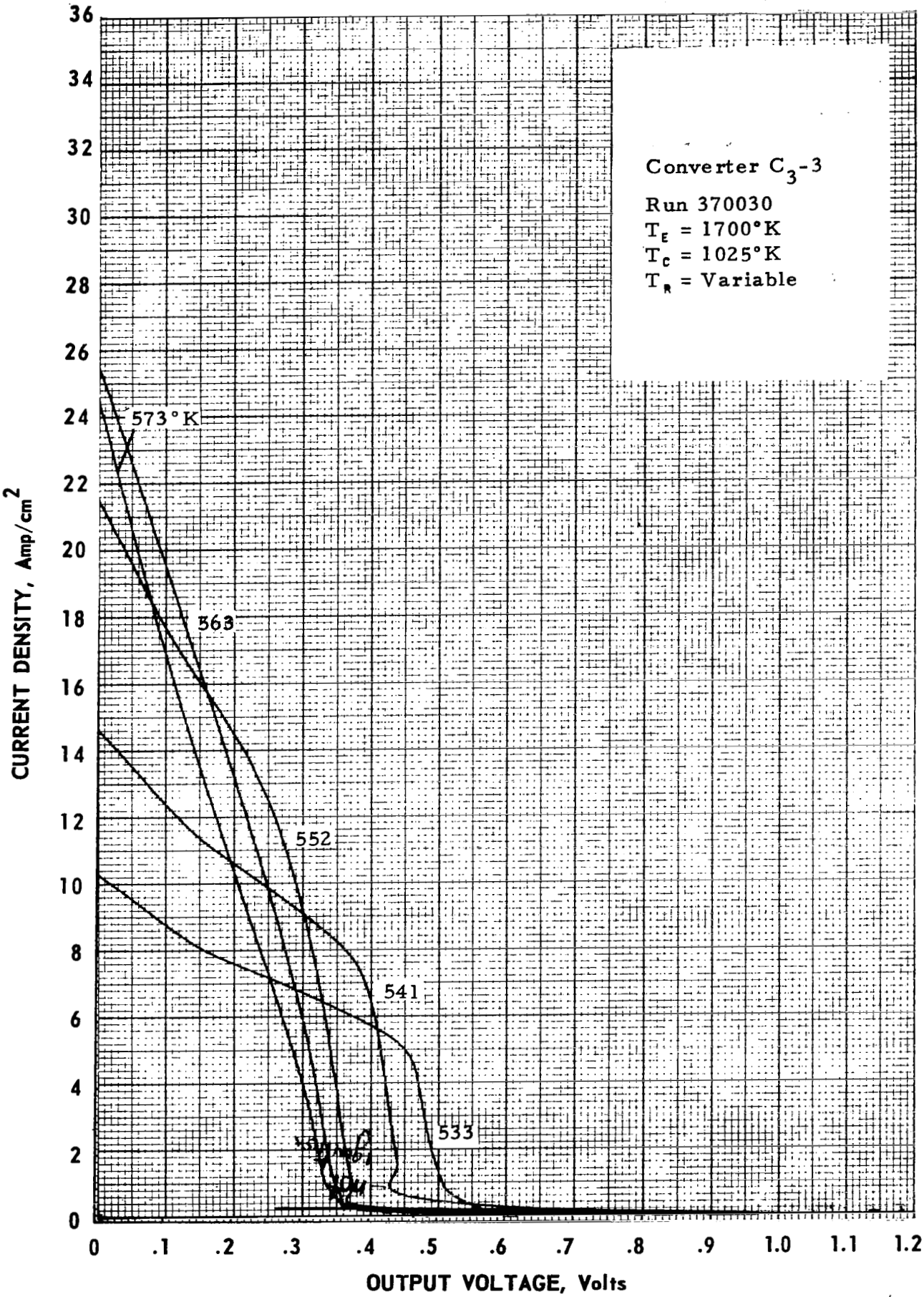

Figure C-16. Cesium Temperature Family of Converter C_3-3 at T_E = 1700°K.

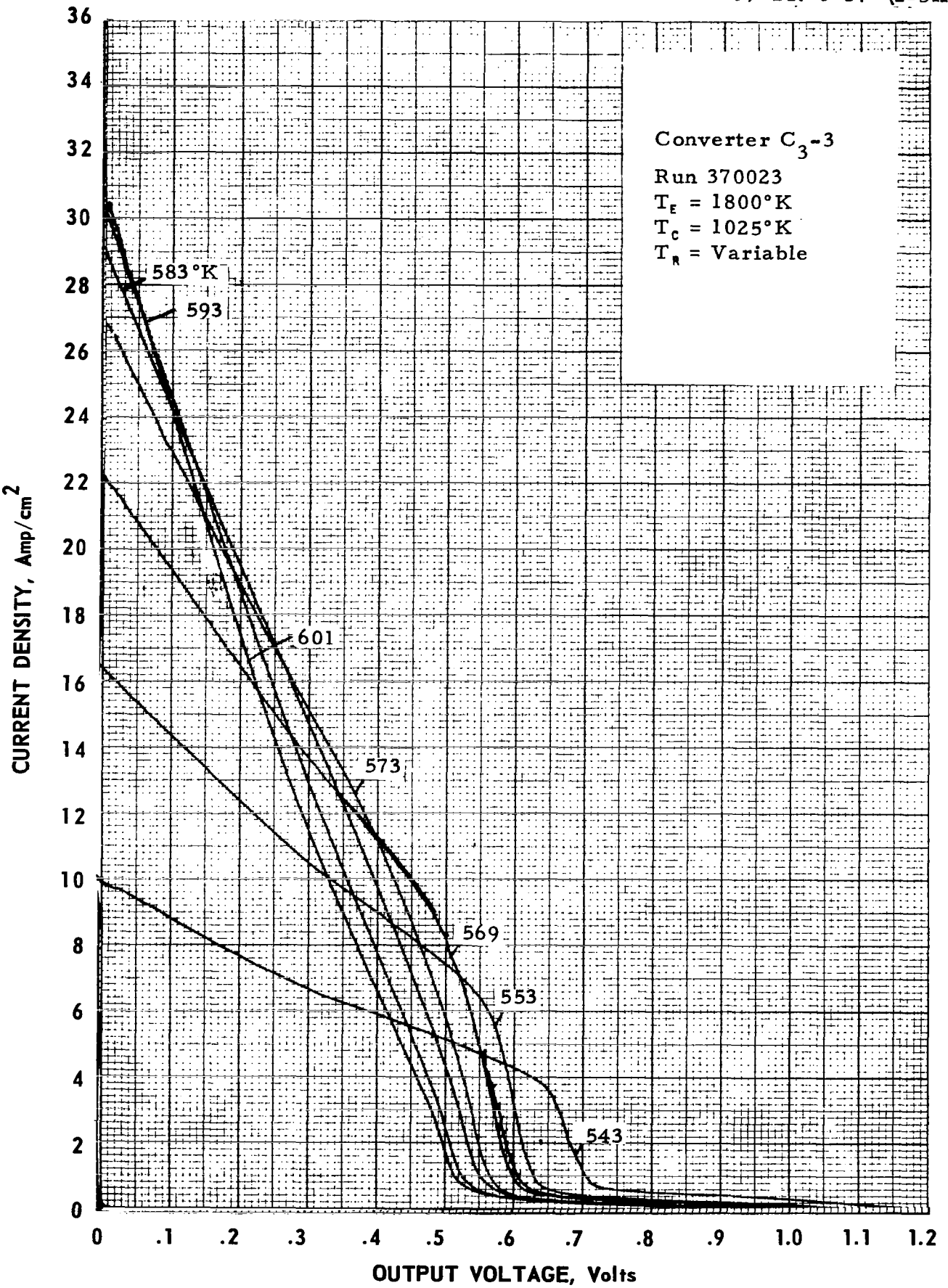

Figure C-17. Cesium Temperature Family of Converter C_3-3 at T_E =1800°K.

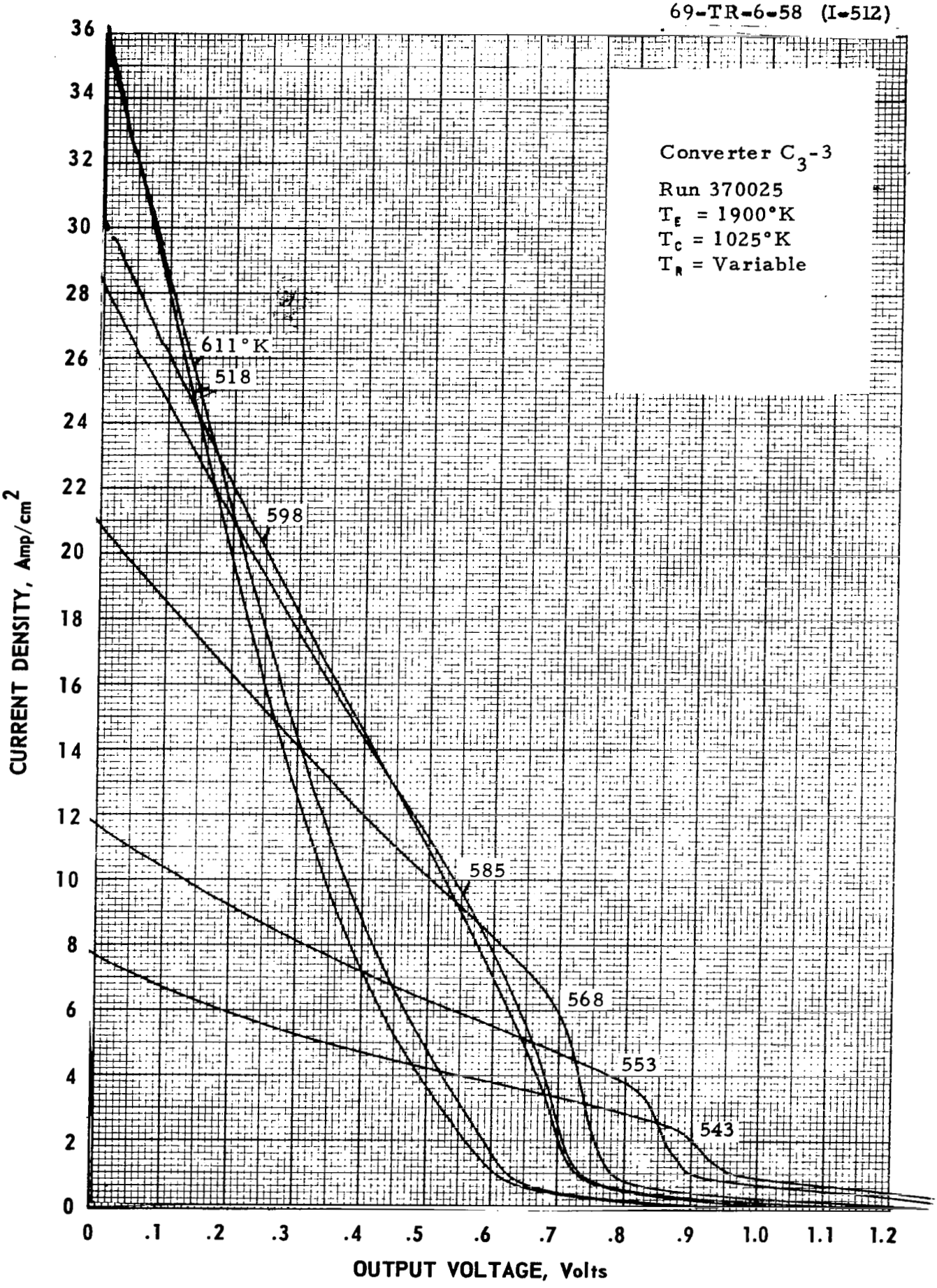

Figure C-18. Cesium Temperature Family of Converter C_3-3 at T_E = 1900°K.

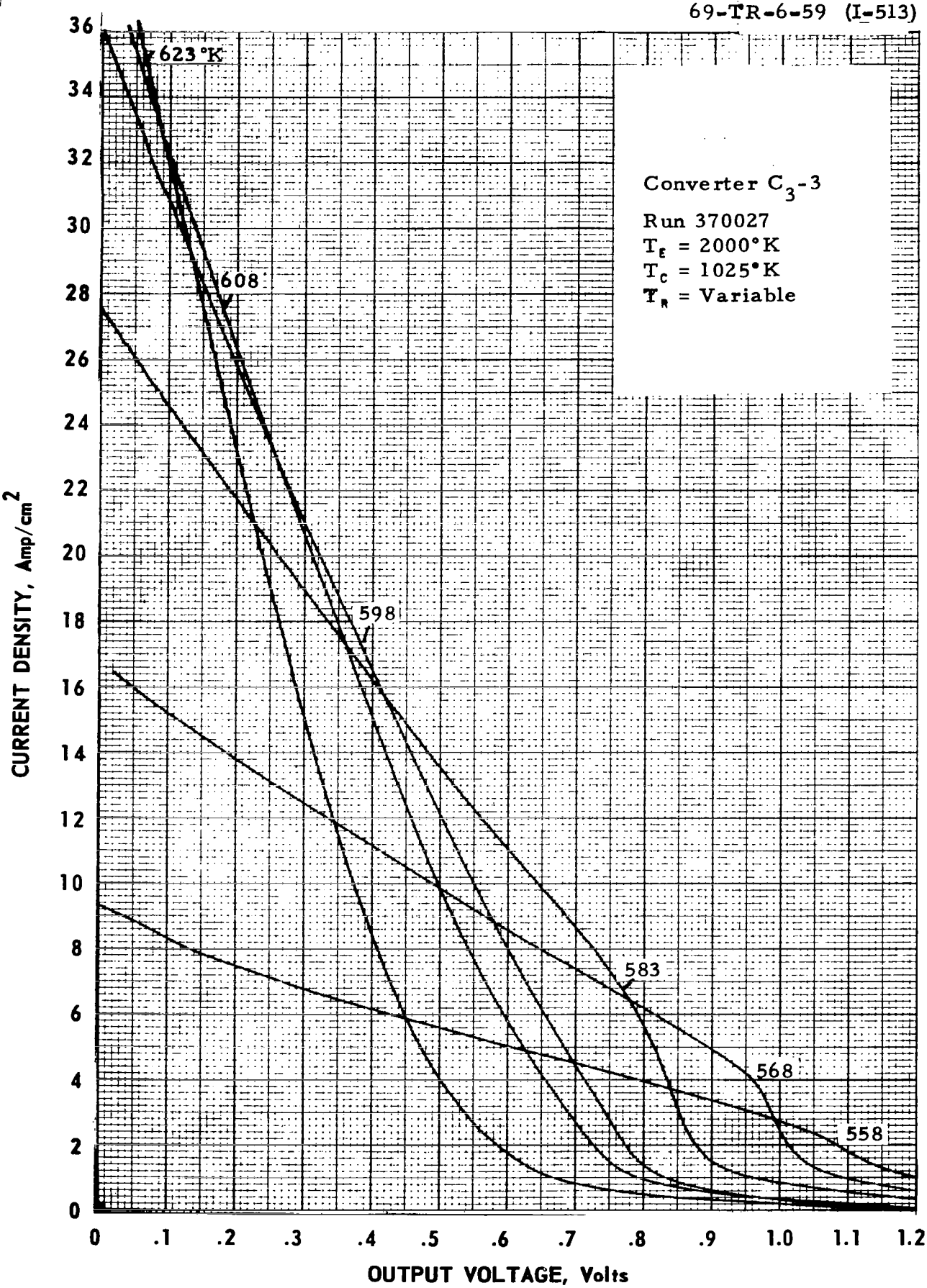

Figure C-19. Cesium Temperature Family of Converter C_3-3 at T_E = 2000°K.